DESIGN AND AUTOMATION OF ETHIOPIAN IRRIGATION SCHEME AND CONTROLLING SOIL MOISTURE INTEGRATING SENSOR WITH MICROCONTROLLER POWERED BY SOLAR ENERGY

A THESIS SUBMITTED TO THE GRADUATE SCHOOL OF APLIED SCIENCES OF NEAR EAST UNIVERSITY

By
TESFAYE ADISU TAREKEGN

In Partial Fulfilment of the Requirements for the Degree of Master of Science in Mechatronics Engineering

NICOSIA, 2019

DESIGN AND AUTOMATION OF ETHIOPIAN IRRIGATION SCHEME AND CONTROLLING SOIL MOISTURE INTEGRATING SENSORS WITH MICROCONTROLLER POWERED BY SOLAR ENERGY

A THESIS SUBMITTED TO THE GRADUATE SCHOOL OF APLIED SCIENCES OF NEAR EAST UNIVERSITY

By
TESFAYE ADISU

In Partial Fulfilment of the Requirements for the Degree of Master of Science in Mechatronics Engineering

NICOSIA, 2019

TESFAYE ADISU TAREKEGN: DESIGN AND AUTOMATION OF ETHIOPIAN IRRIGATION SCHEME AND CONTROLLING SOIL MOISTURE INTEGRATING SENSOR WITH MICROCONTROLLER POWERED BY SOLAR ENERGY

Approval of Director of Graduate School of Applied Sciences

Prof. Dr. Nadire CAVUS

We certify that this thesis is satisfactory for the award of the degree of Master of Science in Mechatronic Engineering

Examining committee in charge:

Prof. Dr. Ahmet Denker	Supervisor, Department Chairman of Mechatronics Engineering, NEU
Prof. Dr. Bulent Bilgehan	Department Chairman of Electrical and Electronics Engineering, NEU
Ass. Prof. Dr. Ali Serener	Department of Electrical and Electronics Engineering, NEU

I hereby declare that, this paper is belonged to me as my own work, which has not submitted for the fulfillment of degree in any other Universities. However all materials not original to this work, used in this paper have been duly acknowledged and cited in accordance with academic rules and ethical conduct..

Name, Last name: Tesfaye Adisu Tarekegn
Signature:
Date: 07/08/2019

To my Parents …

ACKNOWLEDGMENTS

I would like to acknowledge my indebtedness and render my warmest thanks to my supervisor, Prof. Dr. Ahmet Denker, for his guidance, encouragement and advice he has provided me throughout each time. His expert advice has been invaluable throughout stages of the work. I would also like to express my gratitude to Prof. Dr. Bullent Bilgehan for his academic and upkeep advice he has been giving me in reference to the department. Once again, I dedicate ungreedily special feelings of gratitude to Prof. Dr. Ahmet Denker and Prof. Dr. Bullent Bilgehan. I would also like to thank all the members of staff at Near East University who directly and indirectly helped me.

There are a number of people, without whom this thesis might be unthinkable whom I am greatly indebted. I give distinctive gratitude be to my mother Gemede Gerema, without whom I could not have been ever here. I am grateful for her unwavering patronage, encouragement and patience she has been showing. Especially I would not have been here overcoming that dark nights and wilderness if she would not cod-extended. May she be awarded much bless.

I also devote thanks to my brothers and friends whom their togetherness strengthen me to push the wall without being tedious throughout the time. I will always appreciate those who dropped even a value in my pots during my efforts. All beloved! Once at all, I have big respect to you all and miss you all beyond words.

ABSTRACT

Preserving soil moisture conditions is a crucial for optimal yield production. Water is the vital elements for suitable cropping at optimum level; however, its excessiveness must be control, so that the field is neither over-irrigated nor under-irrigated. This thesis identified an inefficient irrigation system was under operation due to unaffordability of water monitoring technologies and labor-intensive affecting productivity in Ethiopia. The intention of the thesis was occupying elimination of such factors by designing and simulating automatic embedded system via integrating sensor with microcontroller. The proposed embedded system is entirely energized by solar energy. In this paper, moisture sensor, microcontroller and dc motor were the major components while modelling the system using Proteus, IDE and Mat lab Simulink software. Moisture sensor was integrated with the intended microcontroller. This sensor submerged into the soil and sensed moisture level persistently of the irrigated land and then reported to the microcontroller for necessary monitoring execution. Thus, when the measured moisture level became less than the desired moisture intervals, the microcontroller decision has been triggering signals automatically without labor intervention to the pumping motor automatically turned ON and pumped water until optimum value of soil moisture was attained. Unless the motor turned OFF. This simulated moisture-controlling automatic irrigation scheme mainly used to reduce labor intervention, water resource inefficiency, soil moisture misalignment causing over and under irrigation difficulties. The paper also presented closed loop servomechanism designation method and resulted in stable and zero-overshoot system.

Keywords: Automatic irrigation; microcontroller; control system; photovoltaic; sensor

ÖZET

Toprağın nem koşullarını korumak, optimum verim üretimi için çok önemlidir. Su, optimum seviyede uygun kırpılma için hayati unsurlardır; bununla birlikte, fazlalığı kontrol altında olmalıdır, böylece alan ne aşırı sulanır ne de az sulanır. Bu tez, Etiyopya'da üretkenliği etkileyen su izleme teknolojilerinin yetersizliği ve emek yoğun olduğu için verimsiz bir sulama sisteminin çalışmakta olduğunu tespit etti. Tezin amacı, algılayıcıyı mikrodenetleyici ile entegre ederek otomatik gömülü sistemi tasarlayıp simüle ederek bu faktörlerin ortadan kaldırılmasını sağlamaktı. Önerilen gömülü sistem tamamen güneş enerjisi ile çalışıyor. Bu yazıda, Proteus, IDE ve Mat lab Simulink yazılımı kullanılarak yapılan sistemin modellenmesinde nem sensörü, mikrodenetleyici ve dc motor ana bileşenlerdir. Nem sensörü amaçlanan mikrodenetleyici ile entegre edildi. Bu sensör toprağa daldırılmış ve sulanan arazinin ısrarla nem seviyesini sürekli olarak algılamış ve daha sonra gerekli izleme uygulaması için mikro denetleyiciye rapor vermiştir. Böylece, ölçülen nem seviyesi istenen nem aralıklarının altına düştüğünde, mikrodenetleyici kararı, pompalama motoruna otomatik olarak AÇIK konuma getirilmiş ve toprağın nemi en uygun değerine ulaşana kadar pompalanan suyu emek müdahalesi olmadan otomatik olarak sinyalleri tetiklemektedir. Motor KAPALI değilse. Bu simüle edilmiş nem kontrol eden otomatik sulama şeması, esas olarak emek müdahalesini, su kaynağı verimsizliğini, sulamanın zorlaşmasına neden olan toprak yanlış hizalamasını azaltmak için kullanılır. Bu makale ayrıca, sistemi değerlendirmek için mikrodenetleyici tabanlı veri toplama sistemi kullanarak kontrollü dc servomekanizma koşullarını analiz etmek için kapalı döngü tanımlama yöntemini sundu.

Anahtar Kelimeler: Otomatik sulama; kontrol sistemi; mikrokontrolör; fotovoltaik; sensörü

TABLE OF CONTENTS

LIST OF TABLES

LIST OF FIGURES

LISTS OF ABBREVIATIONS

GDP:	Gross Domestic Product
MoWIE	Ministry of Water, Irrigation and Electricity
MoA:	Ministry of Agriculture
GTP-II:	Growth and Transformation Plan -II
SSI:	Small-scale irrigation
LSI:	Large-scale irrigation
IDP:	Irrigation development plan
IDE	Integrated Development Environment
USB:	Universal Serial Bus
MCU:	Microcontroller
VLSI:	Very Large Scale Integrated
PC:	personnel computer
CLCS	Closed loop control system
ADC:	Analog into Digital Converter
DAC:	Digital to Analog Converter
LCD:	Liquid Crystal Display
LED:	Light Emitting Diode
TF:	Transfer Function
TFCLCS:	Transfer Function of Closed Loop Control System
TFOLCS:	Transfer Function of Open Loop Control System
PIC:	Peripheral Interface Controller
VDC:	Volt Direct Current
VAC:	Volt Alternative Current
LVR:	Linear Voltage Regulator

CHAPTER 1
INTRODUCTION

1.1 Background

Ethiopia is a noncoastal East African country, with a total area of 1.104×10^6 Km^2, whereas categorically, Land constitutes 1.0 million square kilometer and water body covers 0.104 million square kilometer. Ethiopia is geographically sited in-between longitudes of 35°E & 45°E and latitudes of 5°N &15°N,(D. Alemu & Effort, 2017). Ethiopia fenced by 6-countries; Somalia lies in the Eastern, Kenya in the South, Djibouti in the Northern-East, Eritrea in the Northern, Sudan in the Northern-West and South Sudan lies along Southern-West and Western and edges. According to (World Meters, 2018) its population estimated to be 104.96 million and the second Populous African Country following Nigeria, (Seleshi.B.Awlachew et al., 2016). Agriculture holds the country's economy; engaging 85% of Ethiopian population, accounting about 47% of GDP, 80% and 84% of employment and exports respectively, (Haile, G.G., Kasa, 2017).

Although Ethiopia said to be the water tower of Africa, the unavailability of sustained technological based and inconsequential knowledge leant schemes caused the agriculture sector to be less productive with respect to irrigation. According to (Haile, 2015) (MoWIE, 2018), Ethiopian irrigable land is extended to 5.1 mha that shows 5.1 percent of Ethiopia's total land is irrigable. Out of this (World Bank, 2006); (Makombe et al., 2009) only 0.16mha has been irrigated while (H. Tilahun et al. , 2011) identified only 0.165mha has been irrigated in Ethiopia. While (Cherre, 2017) 0.197mha of the irrigable land is under operation, which majorly monopolized only by Awash Valley. All data showed that out of irrigable farmland only about 3.8% is under operation,(Tilahun, Teklu, Michael, Fitsum, & Awulachew, 2016).

Realizing an embedded system entirely automating irrigation processes help in reduction of water wastages, costs and excess labor-intervention, (Tanujabai & Krupesh, 2017). In a country alike Ethiopia where agriculture is the economy's backbone, the manual irrigation operation were reducing productivity. Therefore, in this research, I planned to rectify these problems via deploying automated irrigation scheme using sensors integrated with

microcontroller entirely energized by solar energy for effective water management, whereas it simultaneously eliminate the main problems of over and/or under irrigation difficulties.

1.2 Paper Framework

The overall framework of the paper was designed as follows. section one entails introduction and it subclass, section two describes about the related researchers' overviews concerning irrigation schemes, and vital role of Arduino Microcontroller, section three concerns about the Methodology and components required to shape the final output of this research, section four entails about Ethiopian Agro-Ecological Zone Selection. Then section five is about the proposed embedded system's design and assembly, section six is result analysis, section seven entails conclusion and recommendation while I addressed finally the reference.

1.3 Problem Statement

As per the second Ethiopian 5-year growth and transformational plan (GTP-II) concord, (MoFED, 2016),(Haile G.G & Kasa, 2017), which covers the time interval (2015-2020), the government has decided as agriculture should be remain as the chief driver of this national inclusive economic growth. In our agriculture, besides leveraging food security and productivity promotion, there are also high value crops, export commodities and industrial inputs expected from this strategic national plan. Inclusively, in order to attain this agricultural based strategic transformation plan, uttermost emphasis and priority is given to modern technological oriented irrigational agriculture, (MoFED, 2016).

However, according to MoWIE (S.B.Awulachew, 2017) many challenges both technical and knowledge gaps have been tackling Ethiopian Irrigation sector, which still are in operation. These are; water wastages, manual and labor-intensive, over and under irrigation difficulties, unavailability of water saving irrigation technologies, which deposited under and over irrigation difficulties in irrigation. Due to these challenges, conventional irrigation has been subjectively deploying with poor productivity in Ethiopia, which its effort and cost is much bigger than its beneficence. Therefore, my research is to be occupy in order to eliminate such problems and maximize by designing and automating the traditional small-scale irrigation farm via integrating sensor with microcontroller, powered by photovoltaic solar energy.

1.4 Objectives of the Research

1.4.1 General objective

The development of irrigational cultivation and water management grasps significant and potential role to improve its productivity and promote economy. Ethiopia has abundant enough irrigable land and water capitals however less performance. The agricultural system did not yet mechanized and benefited due lack of technology-based irrigation promotion and water mismanagement. The major Ethiopian population (>85%) has been persisting as agrarian however there is a huge access limitation to agricultural irrigational advancement due to modern technological disintegration and ineffective advisory supervision on irrigation automation system. Nowadays, including NGOs and local firms who have been participating in Ethiopian agricultures, especially in irrigation schemes, they do not have any considerations regarding modern irrigational expertise and technological implementation that are castoff to transform the sectors as per the required strategic plan. Therefore, this paper intended with a general objective to monitor watering system and reduce labour intervention by designing and simulating automatic irrigation system for SSI-class, which will perform a fundamental role in transforming the scheme.

1.4.2 Specific Objectives

- To eliminate the present ineffective traditional irrigation schemes
- To design and Simulate automated irrigation systems powered over solar energy
- To develop automatic water pumping irrigation Scheme

1.5 The Research Justification

The rapid global population growth, which is leading the exponential increment of basic needs demand is undoubtedly touching Ethiopia. Additionally, the alterations of climate conditions frequently affecting rainfall seasonal rotations, and causing drought. Due to food demand loom and drought pattern increment, irrigation has been remaining as the available solution for supplementary crop productions. To overcome these lifelong problems, we must develop our agricultural resources through optimized technological injection and sustainable management.

However, with strange land size irrigation is under plan in Ethiopia, there are gaps instead of practical application and optimal water use. As gratified in the introduction above almost all the present Ethiopian irrigation system were operating manually that is highly costing Ethiopia with less productivity. In other way, manual irrigation consumes much time and labor-intensive, however automatic irrigation system capable to overcome such problems via frequent monitoring irrigation parameters. Therefore, this research thought as to eliminate manual irrigation schemes, high human intervention and water wastages.

Nowadays, the revolution of electronics like microcontrollers have been starting to monitor the physical quantities (moisture, temperature, humidity, etc.) of the environment by reading their supply in the form of electrical signal. Self-monitoring sensor based irrigation is one kind. This kind of integrated automatic irrigation scheme paves crops' production, optimizes fertilizers and water usage with low costs. This helps to overcome easily the alteration of unreliable climate patterns and shortages of water and food insecurity.

Besides, this research output will provide necessary information for the owner to know the real variables alike moisture content control and watering time during crop irrigation. The automated irrigation scheme permits farmers to proceed with the right volumetric content of water at the accurate time. So, it minimizes significantly unnecessary labour forces on irrigation. Therefore, the research will make Ethiopian Irrigation stakeholders such as Small-scale, Medium-scale & Large-Scale irrigation farmers, investors and Government.

1.6 Significance of the Study

Ethiopia is leading as the second Populated African Country, and Agriculture is its national main actor in the economy. Climate pattern change generally hit developing countries much harder than developed countries due to monitoring performance (Belay Zerga & Getaneh Gebeyehu, 2016). Developing countries were less proficient in mitigating these fluctuations due to economical poverty and environment-dependent for their subsistence. Consequently, this climate changes hitting Ethiopia affects her annual season rainfall, which frequently distressing rain-fed agriculture. Although agriculture is the main role player of national economy in Ethiopia, we do not reinforced mechanized technologies yet henceforth our agricultural stakeholders' productivity is unexpected low. Among this agricultural

disintegrated operational system, our irrigation system and its water misuse led by its manual process and unavailability of technical expertise are exemplary.

However, since all its variables are monitored automatically, controlled Irrigation scheme is more climate change independent and productive than rain-fed agriculture. Hence, I initiate to reduce these challenges by automating Ethiopian Irrigation system by designing and simulating automatic microcontroller integrated system. Therefore, this study is highly significant in transforming the sector from manual to automatic operation, which can reduces resources wastages like unplanned water misuse and labour intensification.

1.7 Scope of the Research

My research will be concerned about designing and simulating automatic and self-controlled irrigation system. Specifically, the paper is scoped with designing and simulating automatic system for small-scale irrigation schemes. In this project, moisture sensor is the main input, Microcontroller is the entire system executor and water-pumping motor is the expected output. Soil moisture sensor will be used to monitor the moisture level and the irrigated soil respectively. They will be set also to report results frequently to the microcontroller for execution.

CHAPTER 2
IRRIGATION AND AUTOMATIC IRRIGATION SYSTEMS

2.1 Agricultural Irrigation Overviews

Irrigation is artificial consumption of water to allowing crops growth in areas where there is shortage of rainfall or unavailable water reservoir for supplementary crop production, (Kotaiah Swamy et al., 2013). The irrigation practice has been passing through numerous enhancements over years, (Abdurrahman, Mehari, Tsigabu, & Bezabih, 2015). Predominantly in evolving countries nowadays, the present irrigation system, has limitations like, poor mechanization, erosion due uncontrollable flooding during watering, escape of soil nutrients, losses due to over and under irrigation, water wastage due to poor knowledge and technological based irrigation systems which caused scarcity of water in drought areas and production of unhealthy yields, (Umeh Maryrose et al., 2015). However, with low cost microcontroller based irrigation can avoid these limitations, (Kumbhar & Ghatule, 2013).

The water's volumetric content, in the irrigation soil determines moisture of that soil and crop productivity. Land type and climate conditions (dry, rainy or hot tropical region) are other variables that define soil moisture level, (U.S. Environmental Protection Agency, 2013). Present days, the advancement of technologies using in agriculture are providing dynamic shifting on agriculture's phase. Consequently, traditional irrigation method user wastes huge amount of water, up-to 50-60% and dripping irrigation method reduces this percentage of lost (Hussain, 2015). An automatic irrigational system with different sensors like humidity, temperature, and soil moisture which sense soil parameters via Arduino microcontroller, can monitor the irrigation environment productive by OFF/ON of the entire system (Kumbhar & Ghatule, 2013). The sensed eternal irrigation parameters and internal monitoring devices are interlinked through simulation program and wires, (Naik, 2017), including Arduino microcontroller, relay units, switching devices, actuators like servo motor/dc motor, and water pump. This automatic irrigation schemes are used for reducing over-labor intervention and creating self-controlling productive agricultural unit, (M. A. Abdurrahman et al, 2015), (Kaluse & Sanjeev, 2017).

2.2 Ethiopian Irrigation Schemes Overviews

Since 1950s, nearly updated irrigation was introduced at the rift Valley basin for commercial's crops production of. To grow irrigation systems, Government, NGOs and donors are investing especially in small-scale farm irrigations, (Haile G.G & Kasa, 2015). However, its contribution to the national economy is insignificant due to poor mechanization and lack of automation system and spontaneous supervision,(Y. Alemu et al., 2016). Ethiopian's have started Agricultural irrigation in 1960s for fabricating industrial crops especially sugar and cotton on large-scale basis,(Taddese, Sonder, & Peden, 2004). Local farmers had been practicing irregular irrigation by diverting water from their canal attributes in the dry seasons for the farm of survival food crops by using cans, bamboo, and hollow plant. Consequently, the Ethiopian agricultural sector is now unable to provide the basic prerequisite to the farmers. Traditionalistic irrigational farming system, environmental degradation, lack of external agro-inputs, population pressure, and recurrent drought effect were together cemented foodstuff insecurity. This implies the need of initiating irrigation project development, that can escalating crop yields, refining life standard (Tilahun et al., 2011),(Y. Alemu et al., 2016).

Ethiopia population (Tilahun et al., 2011) estimated to be 104.96 million, which annually increases by 2.7 percent about, among the accelerated population growth countries. Agriculture contributes 46% to the GDP and 85 percent to the national export beneficence. However, agriculture depends on the highly unseasonably fluctuating rainfall. Accentuated with the land degradation, rainfall seasonal variation due to global sub-warming strictly impedes agricultural productivities (Tilahun et al., 2011).

In Ethiopia, (Tajebe, 2017) (Bekele et al., 2012) traditional irrigation was started practicing before centuries. Different authors; (*Ethiopian Water Resources Management Policy.pdf*, n.d.) (Hagos et al., 2007); (Bacha et al., 2011) stressed that supplementary irrigation types has been experienced by small-scale farm holder of Ethiopia for a century to strike their livelihood challenges. Nowadays, Ethiopian irrigation system is being practiced under Large, medium and small scales farming. Authors including (Tilahun et al., 2011); (Hagos et al., 2009); were used national government irrigation structures classification grades for their descriptive studies. Accordingly, (MoWIE, 2002), irrigation clustering system in

Ethiopia is occurred as per the irrigable land size area; i.e. are 3, (Haile G.G & Kasa, 2015) (D. Alemu & Effort, 2017).

- Small-scale irrigation system less than 50 hectare; (SSI)
- Medium- scale irrigation system (50-3000ha); MSI
- Large- scale irrigation system greater than 3000hectare; LSI.

In this irrigation stakeholders' category, about 46% of them are bracketed in the small-scale irrigation system, (M, 2018), which shows that Ethiopia has left back (Awulachew, 2010). But also, in the growth & transformation (GTP-II), Ethiopian government currently, gives weight to advance the segment to tap fully upto its potentials by assisting and supporting farmers and shareholders to advance irrigation practices, promote the modern irrigation system and resources management (MoFED, 2015). Currently irrigated agriculture is yielding $< 4\%$ of total food production capacity of the country, which is much less than expected plan. The only tangible irrigation at Large Scale Irrigation (LSI) deployment is state oriented enterprises, mainly focused on industrial crops like sugar cane and cotton. However, SSI deployment started in 1970s under the supervision of MoA in reaction to major droughts impacts that has caused spread of consequent starvation and crop yields failure. While the thought on SSI sub-irrigation in Ethiopia was only to minimize survival risks associated with food crop failures. Any emphasis did not given for its improvement except only local farmers were struggling subjectively for their interest without any standardization,(D. Alemu & Effort, 2017).

However, the new era of irrigation development plan (IDP) in Ethiopia providing big emphasis on beginning Small-scale irrigation system via capacity building in designing, researching and implementing agricultural irrigation projects. Therefore, MoA, 2011a Ethiopia has planned to irrigate more than half of the irrigable land (about 5.1Mha) at the end of GTP-II. Additionally, irrigation safety also considered, (Abraham et al., 2011).

2.3 Irrigation Methods and Hindering Factors

Human beings have not separated from irrigation activities in order to harvest supplementary food since centuries ago. Although there was time-to-time irrigation system transformation, not all of them served peoples equally with respect to their yielding capability. This is due

the availability of several factors that hinders irrigation design. However, it does not meant that all irrigation methods are either equally useful or ineffective. Knowing-how of these irrigation methods and their hindrances will results productiveness. Having this in mind, soil type, topography, water resources, climate conditions, environment, government policies are the major hindering factors for irrigation design and methods selection, (T.R. Dhakal, et al , 2018), (Jamal, 2017).

In other case, although Irrigation is the submission of water to the planted soil in areas where there is water scarcity and frequent drought may expected for extra food production/ environmental greening via various tools and methods. Three main techniques regarding water-pumping usage majorly in use, these are; Drip irrigation, surface irrigation and overhead irrigation are among majors, (African, n.d.). Bearing this point in mind, three irrigation (drip, sprinkler surface and overhead irrigation) methods and their hindering factors are summarized in the following table.

Table 2.1: Type of automatic irrigation techniques and comparison

Function	**Types of irrigation** **Drip**	**Surface/sprinkler**	**Overhead**
Water use η(%)	90%	55	75
Water delivery/ distribution	controllable & uniform	controllable & uniform	can be patchy
	suitable to limited water climate, where windy evaporation is high	better for less windy areas and unlimited water	better for less windy areas and unlimited water
Geographical land shape	any field shape	any field shape	depends on sprinkler type
land erosion effect	minimum	vulnerable soil to erosion & floods	depend on water pulling up capacity
Weeds	low due water targets specifically crop	occur as much as the crop get water	occur as much as the crop get water
Costs	lower labor& power costs. high investment& replacement costs.	lowest cost and labor-intensive	relatively high labor-intensive, high investment costs& energy costs to maintain

The moisture exists in the irrigation soil depends on soil type and weather conditions (arid, windy, semi-arid, and tropical hot regions).

2.4 The Implication of Microelectronics based Intelligent Irrigation

Micro irrigation is a non-natural watering of plant substance, (Dumic, 2017). Irrigation types have been using to support in the budding of wild and domestic crops, maintenance of land sceneries, and re-vegetation of disturbed soils during inadequate rainfall. The ancient irrigational operational trends majorly used manual scheme. In this case, water loss, huge effort and crop yields catastrophe had happened, (A. Rajpal et al., 2011), at a time which needs extra improvement to eliminate these wastages. An automated irrigation schemes need to be installed to optimize crops and manageable water use for irrigational agriculture. Therefore, an intelligent automatic irrigation system has to have all the components that autonomously monitored without any failures and human interventions. Its main functions are; continuously monitoring the content of water exists to the plants in the soil, determine and inform if watering is required for plants, enable supplying the true required amount, and cease every supply after the compulsory amount delivered. Saving money, conservation of water and optimized supply chain are the foremost advantages of automatic irrigation outlines, (Mahzabin, Taziz, Amina, Gloria, & Zishan, 2016a).

A self-controlled, automatic irrigation plays a pillar role in safe guarding crop production and food security via promoting crops yields. If it properly programmed and installed, intelligent irrigation scheme can save cost outflow and aid water conservation. Watering manually with cans or hose oscillator wastes resources. Automatic irrigation schemes can be designed to discharge precisely required amounts of water, labour costs and promote crop productivity (Mahzabin, Taziz, Amina, Gloria, & Zishan, 2016b).

2.5 Automatic Irrigation System Components and Functions

2.5.1 Microcontroller category and their application

Microcontroller is a small chipboard, which is a small circuit that contains a whole computer functions. Microcontroller is also called embedded system controller, which is fabricated with a very hefty scale integration system in order to monitor varies tasks in mechatronic fields; Such like in robotics, space shuttle, military gadgets and so on, (Kumbhar & Ghatule,

2013). Although capacities and architectural design differ, all types of Microcontrollers have common basic features such as; The interrupts, Clock Oscillator, Timers,, Input/ Output pins, Peripherals (PWM outputs, DAC outputs and ADC inputs) etc., (Louis, 2016a).

They're available in different processing capacities such like of 4-bit, 8-bit, 16-bit, 32-bit, 64-bit and 128-bit employed for devices look for control, (Kizito et al., 2008). These Microcontrollers' categorization based on their architectural design, bits size, memory and their Instruction capability as summarized in figure below.

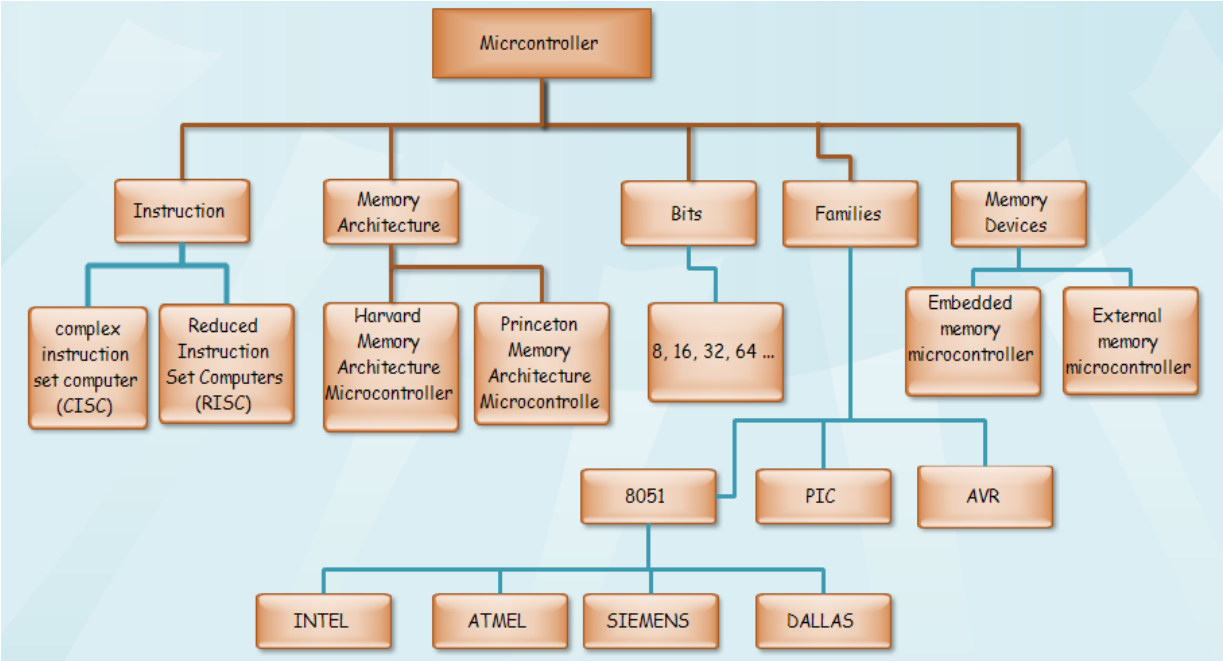

Figure 2.1: Classifications of microcontroller

A Microcontroller comprises various peripherals such as EEPROM, ROM, RAM, Timers, Ports and Pins etc., vital in automation design and control to accomplish predefined activities, (Banzi & Shiloh, 2009) (Applications & Arduino, 2014).

2.5.2 Arduino Uno and embedded systems

It is microcontroller board, which based on Atmega328p chips incorporation. It contains 6-Analog and 14- digital pins uses I/O channels, which 6 of them uses as PWM, a power and USB sockets, a button (reset) and ICSP file header, a 16MHz quartz crystal for running

system timing clock. Therefore, Arduino contains crucial components required for microcontroller for easing programming and processing capacity. Uno was innate of Italian language, which means ‘one’ to express the initial birth of the Arduino Uno board. In case, of program incorporation and powering, simple USB cable connection is enough to start function. Atmega328P is a 32Kb flash memory, 8-bit microcontroller chips family fixed on Arduino Uno boards.

Arduino is inexpensive free source microcontroller, which simply be programmed, erased & then reprogrammed. The Arduino platform designed to create, monitor and control embedded environment that cooperate with its atmosphere using both sensors and actuators through IDE based C/C++ languages. Arduino is (Amit Saha, 2012) a device for developing integrated cooperative objects by receiving inputs from devices such like sensors, switches and controlling outputs of different LEDs, motors and etc (Choudhary, Kumar, Dwivedi, & Tiwary, 2017).

An embedded system (ES) is defined a merged peripherals of computer system that performs a pre-defined programs used within a different size scale of electrical or mechanical system. Embedded systems are most of the time used complex devices due they are set for special purpose. Nowadays, embedded system crucial player; microcontrollers are divided into three classes. Small, medium and large microcontrollers. For example, 4-bit microcontrollers needed in TV remote. $8-16$-bit microcontrollers are medium size system, while >32 above are needed for high performance scale computer systems such as industrial/plant monitoring system, (Barua, Hoque, & Akter, 2014).

In general, ESs are circuit devices designed to accomplish any pre-defined functions that must meet any real time constraint. The difference of single computer and embedded IC system is that, a computer is deployed used to perform multiple tasks defined by the user. While ES is deployed to perform a specific pre-defined task by the builders. In this interpretation, meeting all the entire real time intended constraints is the main characteristic of ES, (Barua et al., 2014).

2.5.3 Sensor unit

A. Moisture Sensor

The sensor units are electrical devices that convert physical stimuli into electrical signal, (Peters, 2016). A soil moisture-gauging sensor used to investigate the volumetric content of water available in the irrigation soil. Exact soil moisture measurement is vital for estimating water balances and for investigation biological and chemical processes around planting ecosystem. The more advanced techniques based on the conductivity and dielectric resistivity moisture in an irrigation soil can be monitored by using TDR (time domain reflectometry), ERT (dc electrical resistivity tomography) sensors, (Kizito et al., 2008)(Peters, 2016) ,(Liu & Xu, 2018).

Therefore, the irrigation system easily read the volumetric content of the irrigable soil based on the displayed resistance values. Therefore, moisture sensors set with microcontroller help to water agricultural plants automatically without any lag of pumping and excessive labor intervention. The higher the volumetric moisture in the soil, the lower resistance against the current flow across the intended circuit. Irrigation soil's resistance based sensors are available both in the digital and analog (higher accuracy) form. They are electrically shielded with synthetic insulation for reducing environmental magnetism risks against their lifespan.

Figure 2.2: Soil moisture sensor

Nowadays, sensor such as electrically soil resistance sensor and capacitance sensor are practically using in measuring soil moisture. The first one (soil resistance measuring oriented sensor) is selected in my project, (Peters, 2016).

Table 2.2: Moisture sensor specification

Assembly name	specifications
Signal output voltage	0-5v
Digital o/ps	1 or 0
Vcc power supply	3.3-5volts
Ground	connect to ground
Analog	r (resistance) in ohm
Panel area dimension	up-to 3*2 cm
Probe length dimension	up-to 6*3.5cm

Therefore, excessive compaction and any air gaps around the sensor probes taken into attention. In automatic irrigation design up-to hardware installation the following soil Moisture Sensor, specifications are recommended to the designer, (Peters, 2016).

B. Temperature Sensor

The uneven climate conditions' change such like temperature fluctuations affect agricultural land crop productivity (IFRC, 2009, 2014). Temperature is the key impacting factor of plant growth rate. The extreme temperature pattern occurred with weather change impacts land fertility and crop productivity. (Jerry L. Hatfield n, 2015). The 5V source LM35 temperature sensor interfaced to the microcontroller board is common.

This sensor has 3-linear terminals, which are used to easily interface in automatic temperature sensing circuit. The two terminals are power pins (i.e. GND and source), while the middle is the main analog output voltage signal pin. It is excited since operated under the supplied source of 3.3-5Volt, while its temperature measuring capacity extends in-between -55 to 155 ºC.

Even though LM35 is a linear temperature, the measuring sensor's output is analog signal therefore it needed to convert to digital signal in order the microcontroller to receive the result directly as its input for the next execution. Unlike older microcontroller like 8051, modern Arduino Microcontrollers including Arduino Uno ATmega328P naturally manufactured with an internal analog-to-digital converter, no need of using external ADC

integration (Banzi & Shiloh, 2009). Arduino Uno has 10-bit inbuilt six analog into digital converter (ADC_0 to ADC_5).

In order, the ATmega328P equipped Arduino Uno Microcontroller enable to read the soil temperature conditions, (Ramos, 2017) (National.Semiconductor, 2017). This generated output potential by sensor is be converted to temperature (ºC) range by;

$$1°\mathrm{C} = 10\mathrm{mV} \qquad (2.1)$$

While LM35 temperature sensor was being under operation, it was supplied this converted, values to be stored in the ADC_1 pin so that the controller read this supplied voltage to measure temperature rise. In my project, equation 5.7 tells us, the microcontroller read as the irrigation field temperature risen by $1°C$, when the microcontroller accurately being supplied 0.01-volt.

2.5.4 Liquid crystal working principle

It's screen panel function, which never emit light straightly; rather than using as reflector or a backlight to yield the images in mono/multi-chrome (single color) form. It is called 'Liquid Crystal Display' because the compounds' mixtures have different crystalline structure of particles, and they flow like fluids in ICs control system. Many more available nowadays in the world, i.e. the $16x2$type. For instance, 16X2 alphanumeric LCD means, it displays up to 16 characters/numerals per line while 2 is total number of lines, (Barua et al., 2014). When an 8-bit configuration, all 8-pins (DB0-DB7) are used while only 4 Data pins (DB0-DB4) are used in a 4-bit.

Table 2.3: Alphanumeric LCD pins configuration

Pin num.	name	Pin type	Function	Pin connection. connected to;
1	Ground	Source pin	Ground-(0V)	the ground of MCU or power source
2	Vcc	powering pin	Supply Voltage	Source
3	V0/ VEE	Cont pin	Contrast regulation through a variable R (potentiometer)	POT source 0-5V
4	Register selct	Cont pin	Select cmd register when LOW; and Data register when HIGH	a MCU pin& gets either 1/0. 0-> Cmd Mode, & 1-> Data Mode
5	Read or write	Cont pin	Low to write to the register; HIGH to read from the register	a MCU pin& gets either 0 or 1. 0-> Write operation, 1-> Read Operation
6	Enable	Control pin	Sends Data to the data pins when a HIGH to LOW (PWM?) is given	MCU& always held HIGH
7-14	Data Bits (D0-7)	Data/Cmd pin	Are (data/command) pins	Four pins Only (0-3) are connected to MCU. In 8-wire Mode: all 8 pins(0-7) are connected to MCU
15	LED +ve	LED pin	Backlight Vcc (5V)	+5V
16	LED -ve	LED pin	Backlight ground (0V)	To ground

2.6 Microcontroller Based Irrigation Trends Reviews

The Arduino based irrigation is a novel system that the moisture sensor sense the condition of dryness of soil at different places on the field feed the signal to Arduino system will take the inputs from sensor and based on that it will decide how much water should be supplied. This system will continue to take the inputs from the sensors until there is sufficient moisture

amount in soil and then it will automatically turn the pump off. This irrigation system will reduce the hardship of farmers, (Choudhary et al., 2017).

Therefore, if the measured value by the sensor is between 1023 to 300 the motor will turn on automatically and initiates supply of water to the crops. However, if the measured value is less than 300 it implies that the soil is wet and hence the motor remains off and no water is sprayed abandoned to crops, (Choudhary et al., 2017). In this project a computerized moisture control and irrigation farm and by using moist sensor to Arduino & L293D module. This automatic system intellects the moisture volumetric of the soil & automatically buttons off the pump while the power wastes.(Anitua, 2016) (Kumar & Magesh, 2017).In previous studies, considering automated soil watering practices, is when the Arduino Uno based sensor has utilized for planting system. An Arduino oriented Automatic Watering plant System was developed in (Lozoya, Mendoza, Aguilar, Román, & Castelló, 2016) which the authors integrated Arduino Uno to control bi-functional components; moisture-sensor & the pumping motor to automatically watering the plant, (Shifa, 2018).

In (Agrawal & Singhal, 2015), a smart drip irrigation system using Arduino was proposed for farm automation-system. A drip irrigation system intensifies EUW where the water gradually dropped to the roots of the plants through narrow tubes and valves. The system can be distantly controlled through email. The study was aimed to change farmer's viewpoint on agricultural progress via contributing modern agriculture. Measuring humidity, moisture & sunlight are all important in agriculture in helping farmers monitor their crops effectively (Zaragoza & Kim, 2017). In (Shifa, 2018) this automatic crop watering project system entailed Arduino Uno, L293D IC, soil moisture sensor, & DC motor are the IC. The code is written and programmed the system as for sensing moisture content of crops at particular illustration of time, if it is less than predefined threshold then desired volume of water is pumped till it ranges threshold.

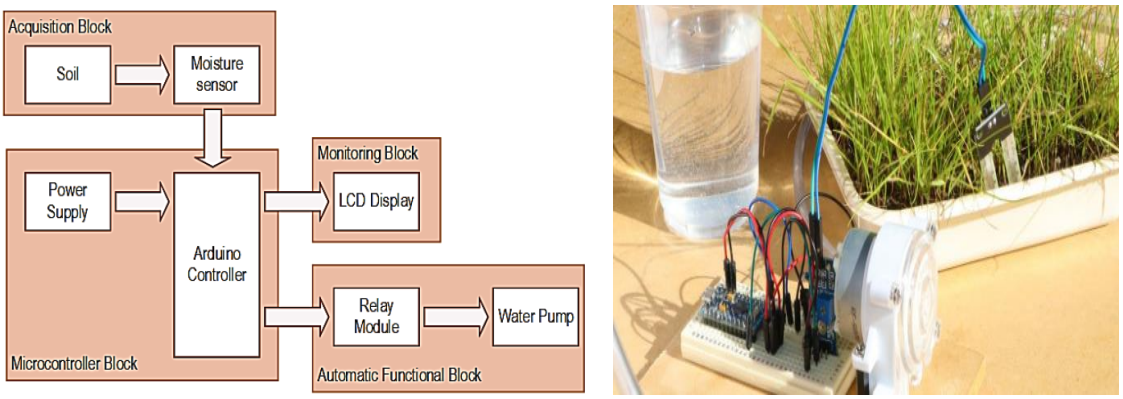

Figure 2. 3: Embedded diagram of automatic plant watering system (Shifa, 2018)

In daily farming, operations watering very vital cultural practice and the utmost labor-intensive task. Consequently, disregarding weathers conditions; one can control water-spraying amount to reach plants' need via this automation when the crops only need it.

CHAPTER 3
METHODOLOGY AND MATERIALS

3.1 Data and Information Gathering Methods

3.1.1 Data collecting techniques

I will have gained informational sources for my thesis. After I have finalized the thesis project design, I handled secondary data gathering and collection methods. A secondary data source is a data composed by somebody else before for different purpose, (Hayter, n.d.). In this case, I have used secondary data collection techniques followed by self-administered telephone call and email. Published & unpublished data resources were also applied.

3.1.2 The sources of the data

Through secondary data collection methods, contacted organizations were;

- Ministry of Water, Irrigation & Electricity
- Ministry of Agriculture
- DebrieZeit Agricultural Research Center and
- Internet for published and unpublished document access.

3.2 Required Components and Methods

In this paper Proteus 8.6 software, Arduino IDE programmer and Mat lab software were, mainly used for designing, programming and analysing system results. The key components considered while designing the embedded system; different conditions are considered; Soil moisture and Temperature range. In another case, in order to settle the problem statement and provide agricultural irrigation widespread, this project mainly used the following electrical components to construct efficient and low cost automatic irrigational system hardware design. These are;

- ATmega328P Arduino Microcontroller
- F-28 Soil Moisture sensor
- Namkici RK377CR dc-Motor

- 16*2 Liquid Crystal Display
- Photovoltaic Panel
- H-bridge driver

Arduino Microcontroller: was developed with determination to provide professionals in order to physique devices interacting with their atmosphere using actuators and sensors(Louis, 2016b). It is less cost, simple and versatile (Louis, 2016b) board processor of my embedded system to process predefined tasks. It consists I/O ports & 8-bit 2D pins per each port to receive instructions and transmit commands to the peripheral devices in the circuit connection,(Shifa, 2018). The selected Arduino Uno equipped with ATmega328P microcontroller is a 16MHz, 32kb flash memory, high performance and lower power consumption while processing tasks. It has six channels of ten-bit ADC. These channels converted and stored the analog data been received from sensor into digital data as the microcontroller only understand digital bits. Therefore, these digital data actively executed so that the processor automatically decided either to ON/OFF the water pumping motor.

H-bridge Driver (L293D): mostly used for electromechanically monitored device. Here in order to drive the pumping actuator I integrated L293D bridge driver, which can drive from 12-38VDC motor based on the requirement of current magnitude. This driver type is current amplifier (V.Kawde& N.Jambhale, 2014), which receipts a low-current gesture from the Arduino and gives out a proportionally upper current signal to drive the motor. Turning a motor ON/OFF entails only one switch.

Soil moisture sensor: it is a capacitive soil contact moisture (Peters, 2016). It is a sensor type, which measures soil's volumetric water content via some indirect methods. It has one probe that which will be dipped inside the soil. The circuit chunk of the sensor contains four pins; V_{in}, GND, analog output, and digital output. The sensor delivers the converted an analog output to the microcontroller. The soil sensor measures moisture content in an irrigation site by determining resistance of current flow between the metallic probes. Each probe acts as sensor elements that can register moisture range and transform it into triggering signal value as output. It further processed into information by an electronic display.

Liquid Crystal Displayer (LCD) Screen: is to demonstrate every running process in the entire system, from initializing to the monitoring up to pumping water. It is a unit where all

information supplied from the sensors will displayed. It assists the system's user to know the status of the irrigation environment.

Embedded IDE software: used to sketch programming for my embedded system automation. It contains script editor for lettering system-integrating code in the embedded 'C' language, text console, and message zone, toolbar having buttons. Therefore, after I successfully sketched the irrigation system program, it will be uploaded to the microcontroller board assembled to my solid hardware system. In such software, diverse tools are included; where to write the code for the ES (editor), converting the source code be understandable by the computer (compiler), converting a code written in assembly verbal language into formal machine language (assembler), and testing whether the written code is free of error (debugger).

3.3 Proposed Model and Working Principles of the System

As I described in chapter one, although the opportunities for agricultural irrigation is too wide, almost all Ethiopia's irrigation farming schemes are traditional, which is less productive and labour intensive. Thus, I proposed sensor based irrigation network as to inspect the circumstances of irrigation. Because of irregularity of rainfalls, soils and weather circumstances in the environment are not easy to farmers, which always challenge them in understanding the present moisture content and then crop watering time. In Ethiopia, due the unavailability time oriented weather prediction system and ideal standard irrigation method, nearly most farmers were suffering financial loss and becoming less productive with respect to irrigation works.

The proposed system will be sustainable solution with low cost to improve Ethiopian resource use efficiency (RUE). To provide the efficient irrigation system, sensors with determined land area will be scattered throughout the irrigable land. The scattered sensors, senses the moisture content (water level) in the land/reservoir. Then, it reports the recorded value to the Arduino Uno ATmega328P controller. After the controller will receive the reports, it determine either the value is less/greater than the value set in the simulation. Then, based on that identified report's values, for example if the recorded value will be less than the simulation values, the controller transfers command to the motor pump through the L293D-driver to open the valve ON to pump out the required volumetric water amount and

vice versa. This system doesn't only reduce extra water wastages but also allows supplying only the required volumetric water amount but also reduces human interventions too.

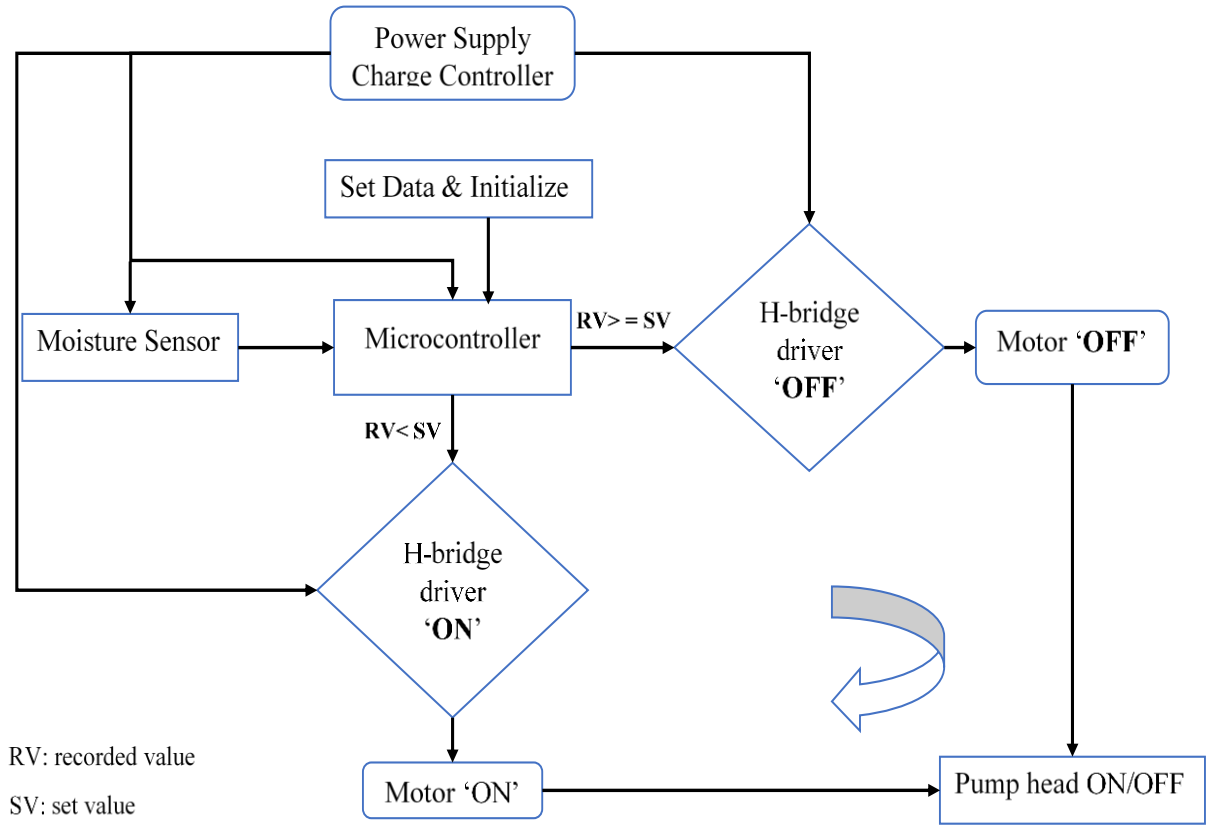

Figure 3.1: The system block diagram flow overview

The sensors buried in the field senses the crop moist then reports consecutively to the microcontroller to execute the irrigation system. The Sensors connected to Arduino Uno ATmega328P Microcontroller are where the irrigation owner will get the analysed actual time data regarding moisture and temperature ranges of the irrigation field, (Dukes, Shedd, & Cardenas-Lailhacar, 2012). This Arduino-centred automatic irrigation system was set, to monitor uninterruptedly irrigation ecosystem. In the proposed research work, I have propagated the entire system communication programming without human intervention, and as power supply, I designed an 18/24V photovoltaic panel based charger controller to energize the system by remedying it into 12-volt and then 5-volt dc source.

3.4 Closed Loop Identification Method

Closed loop system are fundamentally used to monitor the error occurred in system plant using the feedback control which used to avoid undesirable output (Mandloi & Shah, 2015).

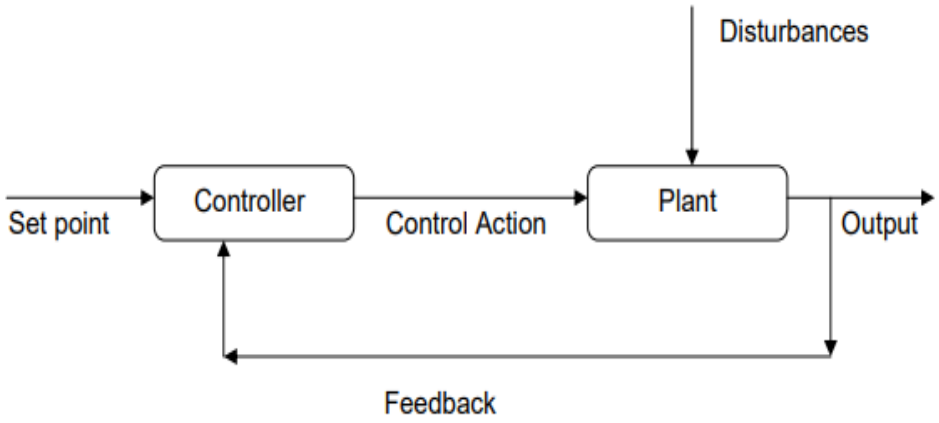

Figure 3.2: Closed loop identification method

The system structure shown above with feedback is allied with plant and controller workout to designate the kin between the input & output of the system (Mandloi & Shah, 2015).

3.5 Simulation

The system's integrated system design energized via soar energy will be done by using Proteus professional 8.6 and Arduino IDE for its simulation. The simulation will be performed as how the moisture sensing and pumping motor will be practically operate during irrigation system. The project simulation will contain spontaneous reading of the doped sensors inside the soil then based on that readings the microcontroller decide either the water pump motor be ON/OFF. Based on the sensor reports, the microcontroller sends signal towards dc motor connected to it accordingly to switch off/on the water pump in the water reservoir.

CHAPTER 4
AGRO-ECOLOGICAL DATA COLLECTION

4.1 Soil Moisture Data

In Ethiopian highlands, for the objective of productivity promotion and systems developments Ethiopian Agricultural Research Center under the Ministry of Agriculture were doing better day and night along with different topologies. Debrie-Zeit Agriculture Research Center is one of the foremost institute (D. Alemu & Effort, 2017) to measure and research Ethiopian agricultures. Based on the agro-ecological weather classifications displayed in table 4.2 and the measured soil moisture analysis, this automatic irrigation system's site affecting factors will be determined. However, out of the bulky data, I have gathered from the center, I selected data of only during the critical dry season (25^{th} march-to-5^{th} may, 2018) in Ethiopia as the data is cascaded table 4.1 below.

Table 4.1 : [1]Soil Moisture data (%) of DebrieZeit Toposequence

Ethiopian Critical Dry season	Date	Minimum Moisture Level (%)	Maximum Moisture Level (%)
25th March To 5th May/ 2018	3/25/2018	18.5	31
	3/26/2018	19	43
	3/27/2018	21.5	49
	3/28/2018	31	45
	3/29/2018	16.5	32
	3/30/2018	14	18
	4/1/2018	18	37.5
	4/2/2018	6	40
	4/3/2018	25.5	44.5
	4/4/2018	30.5	46
	4/5/2018	32	36
	4/6/2018	26	40
	4/7/2018	19.5	47
	4/8/2018	10	48.5
	4/9/2018	34	52
	4/10/2018	33	50
	4/11/2018	34.5	45
	4/12/2018	30	45
	4/13/2018	17.5	39
	4/14/2018	8.5	38
	4/15/2018	21	47
	4/16/2018	28	47
	4/17/2018	34	45
	4/18/2018	39	50
	4/19/2018	9.5	49
	4/20/2018	16	54
	4/21/2018	21	50.5
	4/22/2018	18	51
	4/23/2018	38	52
	4/24/2018	44.5	53
	4/25/2018	12.5	39
	4/26/2018	18.5	31
	4/27/2018	19	43
	4/28/2018	21.5	51.5
	4/29/2018	31	45
	4/30/2018	16.5	32
	5/1/2018	14	18
	5/2/2018	18	37.5
	5/3/2018	9.5	40
	5/4/2018	25.5	44.5
	5/5/2018	30.5	46

4.2 Ethiopian Weather Conditions Roadmap (2015 -2020)

Ethiopia has abundant climate variety from wet to dry, with numerous topography. It is very necessary to know and investigate characters of weather patterns of any areas where water and soil conserving technologies are going to be implement for the purpose of productivity promotion, (K.Hurni et al, 2015). According to (Osman & Sauerborn, 2001), (MoA, 2016) the Ethiopian agro-ecology is categorized into 15 agro zones, which three of them one in the

[1] DebrieZeit Agricultural Research Center, Ethiopia 2018

extreme lowlands, two in the extreme highlands are categorized as life threatening and few production zones,(Girma & Awulachew, 2007), (MoA, 2016).

I have taken an ecological sample size between Dry Dega and Wet kolla, which cover altitude in-between 500 -3200m in order to regulate soil moisture and temperature average as the design input. Because the majorities of Ethiopian food crops and economic factors are produced in these zones. In another case, three main zones; Wurch, High-dega and berha are excluded. Because, first in case of Ethiopia, none of these zones directly and indirectly affects living standards with respect to irrigational agriculture products.

Including types of crops, key characteristics and weather conditions of each zones are given, however I myself summarized only the necessary variables required for my embedded system design as in Table 4.1. Therefore, before designing & implementing this kind of automatic irrigational system, I decided, as it is essential to identify and fix characteristic of zonal weather conditions. So I have cascaded the nationally measured moisture intervals for the system design as tabulated below, (Dhabi & Derbew, 2013), (Long-term Agro-climatic and Hydro-sediment Observatory Report Long-term Agro-climatic and Hydro-sediment Observatory Report, 2017).

Table 4.2: Ethiopian agro-ecology and their weather conditions[2]

Ecology name	Sub-ecological Name	Altitude Range (m)	Average Temperature (ºC)
High Dega	Moist High Dega	3200–3700	7-12
	Wet-high dega	3200-3700	7-12
Dega	Dry Dega	2300–3200	12–18
	Moist Dega	2300–3200	12–18
	Wet Dega	2300–3200	12–18
Weyna Dega	Dry-Weyna Dega	1500–2300	18–25
	Moist-Weyna Dega	1500–2300	18–25
	Wet-Weyna Dega	1500–2300	18–25
Kolla	Dry Kolla	500–1500	Over 25
	Moist Kolla	500–1500	Over 25
	Wet kolla	500–1500	Over 25
Berha	Moist Berha	Below 500 m	Over 30
	Dry Berha	Below 500m	30-40

The embedded system requires initially predefined threshold values as described in my methodology to which they incline relatively while they are in operation in the field. Therefore, all these data (in Table 4.1 & 4.2) will be integrated and analyzed later in chapter five and six, to determine the threshold values and impacting factors of the automatic irrigation system designed in this thesis.

[2] Ethiopian agro ecological Road Map 2016

CHAPTER 5
DESIGN AND ASSEMBLY OF PROPOSED SYSTEM COMPONENT

5.1 The Integrated System Component Analysis and Hardware Design

Before outlining systematical designing& assembling the parts is crucial, so that the entire proposed embedded hardware components were analyzed and assembled as follows.

5.1.1 Arduino Uno microcontroller

It's a processor board, conjugated by ATmega328p processing unit to execute my embedded system as per predefined tasks. It is a 16MHz, 32kb flash memory, high performance and lower power consumption used to, while entirely monitoring this irrigation handling tasks. It has about 20 + 2 hidden pins. Out of them, 14-digital I/O, while 6 out of the 14 digital are used as PWM output, 6 are analog inputs and the hidden 2 pins are power supply pins. The six ADCs convert and store the analog data been received from sensor into digital data as the microcontroller only understand digital values. it has the following tabulated Specification.

Table 5.1: Arduino Uno atmega328P specification[3]

Microcontroller:	**ATmega328p**
Analog Pins:	6
Input Supply Voltage:	7V -to-12V (recommended)
Operating Supply Voltage:	5V
$\mathbf{V_{input}}$ (limits):	6-20Volt
DC Current for Source power 3.3V Pin:	50 mA
Flash Memory:	32 KB (ATmega328p)
DC Current per pin (I/O):	40 mA
Clock Speed:	16 MHz

5.1.2 Liquid crystal display interfaced with microcontroller

[3] Arduino Uno R3 Microcontroller Datasheet

In this project the 16*2 LCD without backlight was used to display the required data on the screen commencing the tri intra-communication (System-human-irrigation variables) environment. Vdd and Vss are power and ground pins respectively, while (VEE) pin created to monitor the LCD's light contrast, whereas to the second VEE pin end, a variable resistor of 10K ohm was linked to regulate contrast of light. However, this variable resistor of the VEE pin is linked to ground and 5V on its extra two side for better contrasting. Also using 10kΩ variable resister is possible, by connecting its two sides to the VEE pin and the 2nd terminal to the 5-volt source. During interfacing the two component, telling the board as which pin of the microcontroller ought to connect to which LCD's pin is the main task for Liquid Crystal Displayer programming.

The 14 Pins of the LCD discarding the two positive and negative pins has been used because there is no backlight in this embedded design system. Consequently, out of 14 pins in my embedded system, 8 pins (7-14 or D7-D0), the two power supply (1-2VSS and VDD or Gnd & +5V), and display style contrasting pin (VEE) and control pins (RS, RW and E) are boldly considered as in Figure 5.1 below.

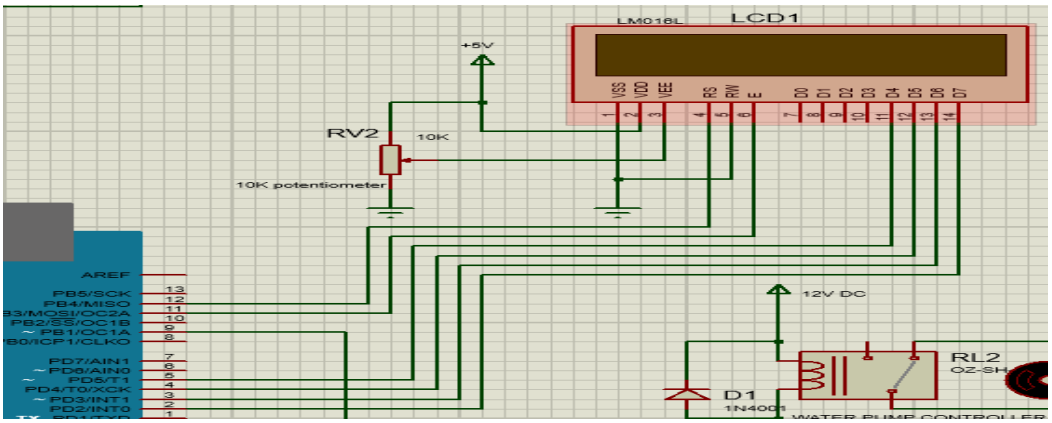

Figure 5.1: LCD interfaced to microcontroller

In the embedded system drawn in Figure 5.1, three of the control pins to provide system flexibility were taken when one pin (RW) linked to the ground to make the LCD in read mode. The read/write pin in addition to contrasting pin through potentiometer are shortened

to the ground. This helped me to make the liquid crystal displayer be into a better contrast read style. RS and enable (E) pins were needed to send data and characters to be showed accordingly. Therefore based on the description above the adjoining mode between the Atmega328P and the LCD in case of my embed circuit system is done as per in appendix. 3.

Consequently, as the IDE software allows the designer using the LCD in four (4) and eight (8)-bit mode possibly, lower limit (i.e. layout places, pins, and wires) were used considering resource's considerations. In this case, <LiqiudCrystal.h> header and the instruction code created without constraint.

5.1.3 Power supply

Photovoltaic solar-based charge controller has been applied over dc motor or simple dc battery as power source of this project. Because of photovoltaic solar power source is reliable, greenhouse gas emission less and pollution free (Gilbert.M.Masters, 2004). It is easy to access by the farmers so that it reduces dependence of the farmers on electricity and foreign oils, (Tamrakar, Gupta, & Sawle, 2015).

Using simple dc battery in a such sensitive circuit is eventually drain out and loose its potential power over short period of time, whereas photovoltaic solar panel is renewable energy overtime so advantageous than using simple direct battery or dc motor as power source for sensitive embedded circuit.

5.1.3.1 Photovoltaic solar panel as power supply

In general, (EEPCO, 2013) access to basic energy services is unswervingly related to country's economic performance. Ethiopia (Dhabi & Derbew, 2013) (OECD/IEA, 2017) is among countries of lowest access rate to advanced energy services highly reliant on traditional power sources. According to (OECD/IEA, 2017) bioenergy source shared 92% followed by oil (6.2%), and then followed by hydropower (1.7%) and geothermal (0.5%) (Dhabi & Derbew, 2013)(Guta, Damte, & Rede, 2015).

In other case, Ethiopia obtained average solar irradiation in-between 5-6KWh/m2 based on season and regional location, to adapt abundant potential for using solar energy compared to oil-based/hydropower source accessibility. Solar irradiation varied seasonally, has been attained 4200Wh/m2/day in country's lowlands while it measured 6150Wh/m2/day in the

northern hemisphere of Ethiopia (GTZ, 2016). Whereas the average irradiation was almost uniform with around 5200Wh/m2/day, (EEPCo, 2014).

Photovoltaic panel is a semiconductor cell structure used to convert sun light into direct electrical current. It is a combination of solar cell structures, mounted with the aim of converting sun radiations into a valuable energy via integrated circuit. (Gilbert.M.Masters, 2004) PV structure captures the sun‘s energy using solar photovoltaic cells. Taking the challenges of modern electricity access in Ethiopia especially field irrigation, which electricity supply is more uncommon, An 18-to-24volt photovoltaic solar panel was used as a power supply to energize the designed system. Consequently, in this project beyond efficient automatic system building, this renewable energy boost to agricultural irrigation is another benefit to overcome one of the main challenges in Ethiopia, especially which have not yet considered to access renewable electricity for agricultural related activities.

To characterize the manners of PV module composed of current, resistor, diode (M. Azzouzi, et al, 2016), I considered the two mainly known conditions (Gilbert.M.Masters, 2004). The first is short circuited current, that means, the current flow in the circuit terminal is shorted together and is equal to short circuited current (I_{SC}) nearly no current loss since voltage across diode is zero ($V_d = 0$). The second condition is open circuit, which potential across open terminals V_{OC} of the PV panel is shorten, the current through diode become zero (I_d=0) so that, ($V = V_{OC}$).

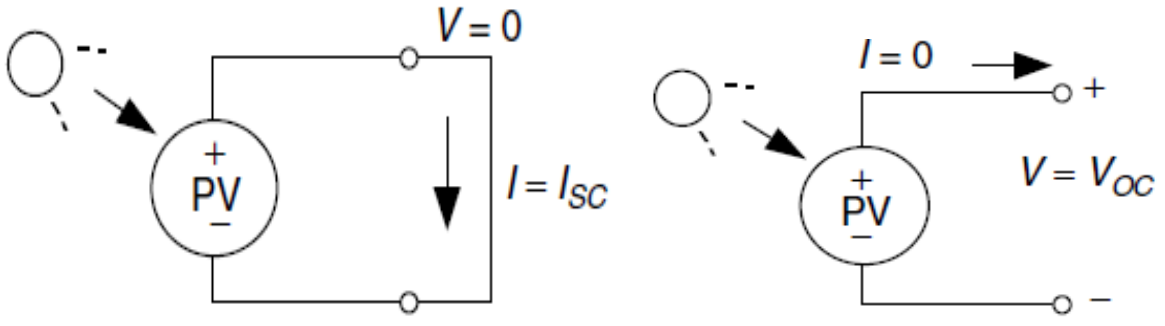

Figure 5.2: a/ Short circuit b/ Open circuit

5.1.3.2 Components analysis

A/ Solar panel plate is formed when its cells are combined together. Their electric energy generation output depends on their own area, solar irradiation performance that can hit each cells, weather conditions and geographical positions. The principle in which semiconductor panel interacts to do works is photovoltaic effect to produce current then voltage by the time sun photons absorbed by the panels,(Uddin et al., 2012). Open circuit voltage of in-between 18-to-24volt solar panel has been used taking the required voltage magnitude for system consumption and the available drop across terminals into consideration. It was aimed to charge a 7.2Ah, 12-volt, battery with the help of solar charge controller. a lead (Pb) Acid battery with 12volt was designated, 6Ah capacity, which can deliver a maximum voltage 12-14volt (Masters, 2013).

B. Diode (1N4001): in this potential regulating circuit, 1N4001 diode was applied to aid current flow only in a solitary direction from anode to cathode. However, diode can behave as opened circuit in case if current flows ensued from cathode to anode. In my project, 1n4001 diode was integrated to allow the current flow only from photovoltaic panel to chargeable battery and no to the vice-versa to prevent my battery from damage. There is no backward biased due to current does not flow backward. So the 1N4001 diode inserted to allow one direction current flow from anode to cathode or from photovoltaic module to the selected battery. However, in Si-made diode there is a constant voltage drop across the forward biased diode, which is about 0.7volt, while almost negligible in ideal diode in comparison (Diode Application, 2014).

C/ LM317 Voltage regulator: as its name implies it was applied to adjust voltage supply, which can intake input DC voltage between of 2.5–to-40 volt and more than 1.5A values from rectifiers or smoothing circuits. Based on the required output voltage, the regulator needs only two external resistors. therefore, two external resistors; R_1, R_2, were added which were needed targeting the required magnitude of output voltage from output Stocky resistor matrix.

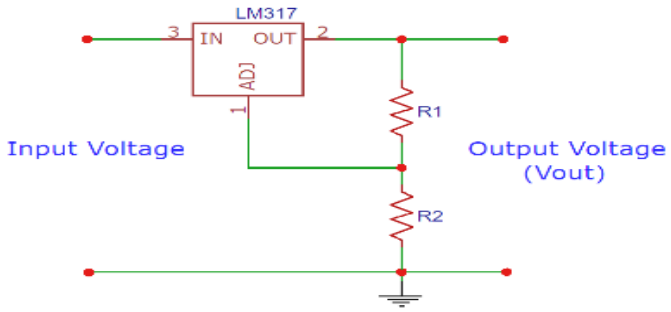

Figure 5. 3: LM317 Adjustable regulator schematic circuit diagram

For independent represented schematic circuit the value of resistor R_1 is 240-ohm, so based on the given Vout, R2 is found from equation 5.1 below.

$$Vout = V_{ref}\left(\frac{R_1+R_2}{R_1}\right) \quad (5.1)$$

Another factor called reference voltage (V_{ref}) and adjusting current (I_{adj}) use to set extra drops found between output and adjusting pin terminals of LM317 regulator, needed to be concern during interfaced with the entire IC. Whereas reference voltage (V_{ref}) value is remain constantly 1.25V and the maximum adjusting current drop is < 100mA. Due to this principle does not work when the regulator is interfaced with other circuit components, the value of resistor R1 also changes, which must be between 0.3<R_1<120-ohm (it is R_5 in in Figure 5.6). Therefore, I have selected the maximum interval $R_1 = 120\ ohm$ to maximum limit voltage. Then calculateR_2 , as the required output voltage must attain the minimum battery's charging requirement, which 12-volt to power motor without disturbance.

$$Vout = V_{ref}\left(\frac{R_1+R_2}{R_1}\right) + I_{adj}R_2 \quad (5.2)$$

However, in this 18-24 volt photovoltaic panel, to provide the 12-V lead battery be recharged, LM317 regulator was selected from its manufacturing datasheet due its less energy dissipation occurred at 120ohm and 470ohm.

D/ BC848 transistor: is a general-purpose bipolar, npn silicon applied to use for switching and amplification purposes. The peak gaining of its dc current is up to 800. The series family

of this transistor are BC548c, BC548b, and BC548, which are created variedly in their current gaining performance and extra characteristics. The bc584 transistor requires from its nature bias to be operate in the desired region for instance a fixed voltage is one. this transistor was chosen to be used in a configuration of common emitter to amplifier. The BC848A in the circuit is used as switch in order to regulate the voltage and leaf current. It has high current gain (800), with parameters, (Guta et al., 2015) in Table 5.2.

Table 5.2: NPN general-purpose silicon transistor

Parameter	ß	V_{CB}	V_{CEO}	V_{EBO}
Value	800	30V	30V	5V

$$\frac{I_C}{I_B} = Current\ gain = 800 \qquad (5.3)$$

While, $I_C = \frac{V_{ref}}{R_1}, which\ is\ I_{C=}\ \frac{1.25volt}{120} = 10.42mA$. Inserting the value into equation 5.3, $I_B = 13\mu A$, and $I_e = I_b + I_C = 0.010433 = 10.433mA$. Therefore, dissipated voltage of the regulator along while the transistor is acts as switch; the

$$V_{drop} = I_C R_1 + R_b I_b + I_e R_e$$

$$= 0.01042 * 120\ ohm + 0.000013 * 100ohm + 0.010433 * 10$$

$$= 0.01042 * 120\ ohm + 0.000013 * 100ohm + 0.010433 * 10$$

$$= 1.2517 + 0.10433 = 1.3563volt.$$

The battery imposed to discharge through the photovoltaic solar circuit obviously need 12-volt regulated voltage. Therefore, using equation 5.2, determine the impacts of external resistor R_2 considering as the output voltage across that terminals must be 12V. In some design cases the I_{adj} is negligible since it is an error must be controlled less than 100µA, however it was considered due to its potential drawn across resistorR_2. The adjusting current $I_{adj} = \frac{V_{ref}}{R_b} = \frac{1.25V}{100o\ hm} = 12.5mA$ replacing the values into equation 5.2.

$$Vout = V_{ref}\left(\frac{R_1+R_2}{R_1}\right) + I_{adj}R_2$$

$$12volt = 1.25(\frac{120 + R_2}{120}) + 12.5mA * R_2,$$

$$120 * [12volt = 1.25(\frac{120 + R_2}{120}) + 0.0125A * R_2],$$

$$1440VR = 1.25(\frac{120 + R_2}{120}) + 1.5AV * R_2],$$

$$1440VVohm = 1.25(120 + R_2) + 1.5AV * R_2],$$

$$1440VR = 150Vohm + 1.25VR_2 + 1.5AV * R_2,$$

$$1440VR - 150Vohm = 1.25VR_2 + 1.5AV * R_2,$$

$$1290Vohm = 1.25VR_2 + 1.5AV * R_2,$$

$1290Vohm = 1.75VR_2$, rearranging and inserting into Mat lab, to calculate for R2 as follows;

```
% define the variables
% let j = Vref reference voltage in volt
%     k = Iadj, linear voltage adjusting current
%     l = Vout, output voltage for the solar power supply circuit
%     Rb = 100, is base resistor in ohm
%     R1, R2 regulating resistor for LM317T voltage regulator in ohms
%     Using Equation 5.2 to calculate R2
Ib = base current; R1 and R2 are adjusting resistors for LM317T voltage regulator

R1 = 120                    j = 1.25;                    Rb = 100;
```

l = 12;	n = m*R1	Rb = 100
Rb = 100	o = j+k*R1	k = 0.0125
k = j/Rb	R2 = n/o	m = 10.7500
m = l-j	R1 = 120	
n = 1290	o = 2.7500	

R2 = 469.0909.

Therefore, in order to the output terminal of the voltage regulator yield a constant voltage of 12volt the load R2 must be 470-ohm. These two external resistors values ($R_2 = 470\ ohm, R_2 = 120\ ohm$) were used to yield the 12volt regulated output voltage as per the battery's requirement. Additionally LM317 potential regulator sometimes a little bit varying its regulated output voltage, while the battery used here requiring a constant output voltage that is 12-Volt. Therefore, in order to address voltage division regulation, 2.4k potentiometer is set in the circuit as shown below in fig: 5.6.

E/Resistor (120, and 470 ohms): in this case, each design resistors are used to resist or monitor extra voltage flow across circuit from photovoltaic panel specifically after LM317 regulator. It allows the transportation of only the required amount of current and voltage towards output voltage terminals. However, this fixed resistors values can be affected slightly with operating voltage or time, temperature, which the potentiometer used to monitor these variation in case of my design timely. This characterizes of variable resistor is used for sensing electrical components such as humidity, force, temperature force, light, or any physical quantity. In my project various resistors; 5, 100, 120, and 470 ohms were applied, when the two 120 and 470 ohm are external resistors needed by LM317 adjustable regulator via the circuit. The motive behind the 10-ohm resistor is to prevent the storage battery from damage while 100 ohm is of base resistor, which used to monitor current entrance into base juncture f bipolar transistor.

G. Capacitor: In this paper, a larger filter capacitor value is little bit be considered to reduce the input requirements. Capacitor mainly settled for power factor correction. A capacitor consists equal to/more than two parallel semi conductive plates, separated against each other

by insulating material (called dielectric insulation). Therefore, from the LM317T datasheet for the required supplied power of 3 to 37 input voltage, ceramic capacitors C_{in} 1050µf and as well as, for the output voltage in-between 6-to-28volt, at the stability region, the output capacitance of ceramic capacitance reads 21.65uF, (Gilbert.M.Masters, 2004) (InfineonTechnology, 2014). Therefore, 1050µf as input capacitor and 22µf capacitors were used in line with the input and output terminals of LM317T voltage regulators. C_{in} is used to reduce input ripple of voltage, while C_{out} is to reduce ripple voltage at the output terminal. For open voltage circuit, the across capacitor voltage (V_c) as time function is given by; Using equation 5.4 I analyzed the time to charge the battery as in table 5.4

$$V_{Cap} = V_{in}(1 - e^{\frac{-t}{RC}}) \qquad (5.4)$$

Table 5.3: Charging-discharging capacitor and time

V_{in}	RC	Time (t, S)	t/RC	voltage across capacitor $V_{Cap} = V_{in}(1 - e^{\frac{-t}{RC}})$	Voltage Used for charging(%) at each constant time out of 18V $\left(V_{Cap}(\%) = \frac{V_{Cap} * 100}{V_{in}}\right)$
18	1	1	1	11.37817006	63.21205588
18	1	2	2	15.5639649	86.46647168
18	1	3	3	17.10383277	95.02129316
18	1	4	4	17.6703185	98.16843611
18	1	5	5	17.87871695	99.3262053
18	1	6	6	17.95538246	99.75212478
18	1	7	7	17.98358612	99.9088118
18	1	8	8	17.99396167	99.96645374
18	1	9	9	17.99777862	99.98765902
18	1	10	10	17.9991828	99.99546001

In this case taking two significant digit close to a 100, within the shortest time at which the capacitor is fully charged is 8 second. When designing capacitors for charging/discharging batteries via regulators, determining capacitors at the input/output terminals of the regulators is crucial tasks (Gilbert.M.Masters, 2004). Electrical performance, transient, load transient amplitude, voltage deviation, capacitor impedance, and distance are the key factors. The aim of (input C_{in} capacitor) is to reduce voltage ripple found at an input of interfaced photovoltaic module(s). Ceramic capacitor has been inserted since they have low enough ESR, which is required to shrink the ripple voltage. This capacitor ought to be located close to input pin of the regulators as much as possible to be efficient. Assuming the two parallel capacitor by the voltage divider rule to find the voltage across the two capacitors are;

$$V_{C1} = \left(\frac{C_{in}}{C_{in} + C_{out}}\right) V_{in}$$

$$V_{C1} = \left(\frac{1050uF}{1050uF + 22uF}\right) 18V$$

$$V_{C1} = \left(\frac{1050 * 10^{-6}F}{1050 * 10^{-6}F + 22 * 10^{-6}F}\right) 18V$$

$$V_{C1} = \left(\frac{1050 * 10^{-6}F}{1050 * 10^{-6}F + 22 * 10^{-6}F}\right) 18V$$

$$V_{C1} = \left(\frac{1050 * 10^{-6}F}{1050 * 10^{-6}F + 22 * 10^{-6}F}\right) 18V$$

$$V_{C1} = \left(\frac{1050 * 10^{-6}F}{1072 * 10^{-6}F}\right) 18V$$

$$V_{C1} = \left(\frac{1050 * 10^{-6}F}{1072 * 10^{-6}F}\right) 18V$$

$$V_{C1} = 17.63V$$

Therefore, while filtering input voltage in order to prevent the battery from immediate damage during charging this potential will be stored in the charge form in C_{in}. The charge that can be stored in the input capacitor can be up to;

$$Q = C_{in}V_{C1}$$

$$Q = 1050uF * 17.63V$$
$$Q = 1050uF * 17.63V$$
$$Q = 18511uC$$

While the output capacitor used to reduce ripple voltage across the output capacitor, can store up to;

$$V_{C2} = \left(\frac{C_{out}}{C_{in} + C_{out}}\right) V_{in}$$
$$V_{C2} = \left(\frac{22uF}{1050uF + 22uF}\right) 12V$$
$$V_{C2} = \left(\frac{22 * 10^{-6}F}{1050 * 10^{-6}F + 22 * 10^{-6}F}\right) 12V$$
$$V_{C2} = \left(\frac{22 * 10^{-6}F}{1072 * 10^{-6}F}\right) 12V$$
$$V_{C2} = 0.25v$$

While the charge that can be stored in the output capacitor can be up to while used to filter the output voltage;

$$Q = C_{out} V_{C2}$$
$$Q = 22uF * 0.25V$$
$$Q = 5.5uC$$

Using Kirchhoff voltage rule in the second loop of the entire circuit;

$$V_{C1} - V_{cc} - R_b I_b - V_{EB} + V_{CB-} V_{CEO} = 0;\ V_{cc} = V_{ref}$$

$$17.63V - 1.25V - 100I_b - 5V - 30V + 30V = 0$$
$$17.63V - 6.25V - 100I_b = 0$$
$$11.38V - 100I_b = 0$$
$$11.38V = 100I_b$$
$$\frac{11.38V}{100ohm} = I_b$$
$$I_b = \frac{11.38V}{100ohm}$$
$$I_b = 0.1138A$$

Through the charge controller, the LM317 LVR ensures that the voltage between the output and adjusting terminal be kept 1.25volt.So the divider While the constant current () through R_1 used to recharge the battery is pot

$$I_{R1} = \frac{V_{out}}{R_1} + \left(1 + \frac{xR3}{R_2}\right) I_{R7}$$

The x denotes fraction of wiper position of the potentiometer from 0 to 1. Considering the higher wiper (x = 1);

$$I_{R1} = \frac{12V}{120} + \left(1 + \frac{xR3}{R_2}\right) * \sqrt{\frac{5W}{5ohm}}$$

$$I_{R1} = \frac{12}{120} + \left(1 + \frac{2400}{470}\right) * \sqrt{1A}$$

$$I_{R1} = 0.1 + (6.1063) * 1A$$

$$I_{R1} = 6.2063A$$

This is the required current due to the constant regulated voltage across the load to recharge the battery and the transistor cut off the current flow when the base current be greater than 0.1138A and the potential difference between emitter and base larger than the reference voltage.

H/ Rechargeable Batteries (12V): are device used to fabricate electrical energy repeatedly from chemical reaction. Rechargeable battery uses for both energy storage and direct DC electricity production via electrochemical redox method,(Hassan & Kamran, 2018). Lead-Acid Battery was selected among other rechargeable batteries due to two main reasons, first despite other forms of recharging batteries, still it is very common application and so it is accessible, second it dissipates very little energy compared other rechargeable types of battery. A Lead Acid Battery type class of AT12-7.4, which means 12-volt and 7.4Ah battery is used.

I/ Linear Voltage 7805 regulator: is a commonly used linear power regulator (class-7805) is applied. Specifically, 7805 is DC-to-DC source regulator that produces linearly a fixed 5V as required to Arduino since this is the optimum voltage that the connected pin can adopt.

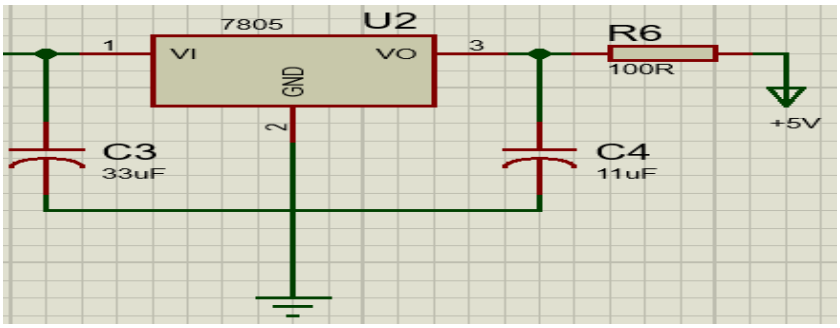

Figure 5.4: Linear voltage regulator

In this project, the 7805 regulator capable to filter constantly 5volt and 1A by taking the input source in-between 8-15 voltages. The supply voltage in this project's circuit design is 12V from LM317T voltage regulator through 12-volt battery. Thus, this regulator regulated the 5-volt power supply into five volt. While, extra supplied voltages above the 5volt evaporates as heat. To prevent the embedded system from being damaged due to the heat two heat sinker capacitors from its standard datasheet for clean 5volt drop were selected; for a distance between source filter and regulator of up to 2.3m $C_{\text{in}} = 33\mu\text{F}$ and C_{out}= 11µF) used (InfineonTechnology, 2014). These capacitance values coupled for stabilizing output source of the regulator however, during implementation distance of between power source filter and regulator must considered.

However, U_6-7805 voltage regulator has standard output current of 1A, which the Arduino Microcontroller cannot acclimatize more than 5v and a maximum of input/output pin current of 50mA. Therefore, based on the values that the board need, the 1A is going to be diminished into a maximum limit of 50mA as follows as shown in circuit fig 5.5 to diminish the 1 ampere output current to 50mA as follow some load need to be signified in series to the output terminal of the regulator.

$$V_{Out} = I_{max} R_s$$

$$R_6 = R_s = \frac{V_{out}}{I_{max}}$$

$$R_s = \frac{5V}{50mA}$$

$$R_s = 100ohm$$

To regulate the required maximum current by the Microcontroller; 100ohm load need to be aligned in series with the output terminal of the 7805 linear voltage regulator. Thus, the following power supply circuit has been developed collecting and putting all the analyzed variables under section 5.1.3 for photovoltaic power supply based charge controller used in the embedded system of this project as displayed in fig 5.6 below.

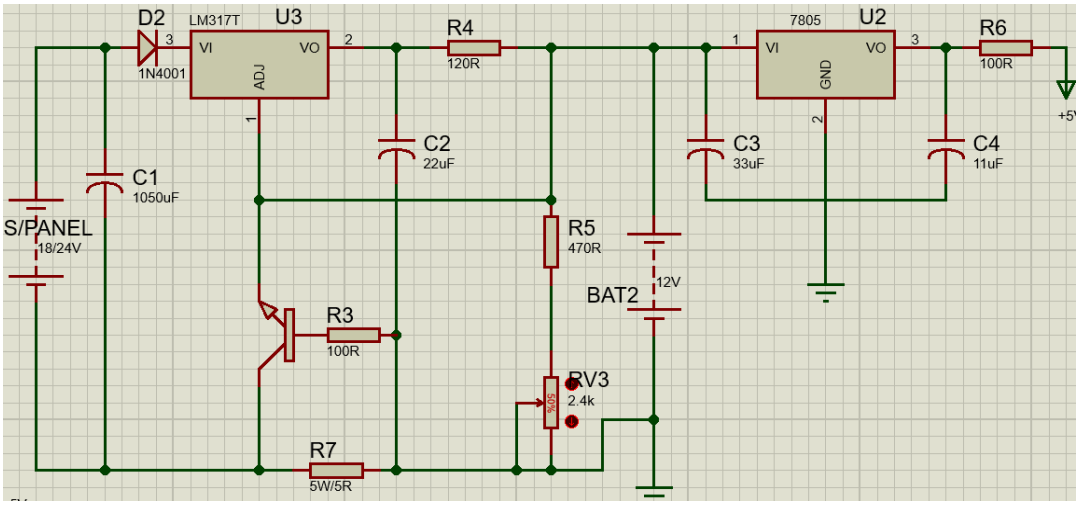

Figure 5.5: Solar photovoltaic IC schematic charge controller

5.1.3.3 Working principle of solar panel power circuit

By the time solar irradiation rays directly hits the solar panel, then it frequently absorbed light energy (photons) to generate electricity. In my system, the 1N4001 a series diode with solar panel was used to direct the current flowing in only one direction which means the current flow out from the solar modules and towards the storage battery but not vice versa. The interfaced LM317 IC is used to receive a clear not DC voltage from the rectifiers or solar panel to adjust regulate the voltage into more clear dc voltage. In this case, a capacitor is used to filter a ripple. The motive behind the 10 ohm is to prevent the storage battery from damage. A 2.4kΩ-potentiometer was used to condition voltage as per the requirement via which the battery has to been charging. Additionally, since the microcontroller specifically need only 5-volt, a 7805 is used to give a supply of 5volt by clearly regulating the 12-volt output voltage of LM317 IC. In this project to adjusting an output voltage of LM317 as 12

while the last adjustment been 5volt as per the Arduino microcontroller maximum limit supply. In this power supply system, a BC848/548 BJT transistor used to monitor the current flown from photovoltaic solar irradiation to electric energy.

5.1.4 Soil moisture sensor

In this study FC-28 moisture sensor is among the main component used in order to measure the volumetric moisture conditions of the irrigation soil alongside variable voltage. It set by measuring the frequent volumetric moisture of the irrigation soil and report it to the Arduino microcontroller for execution. The working principles of all types of moisture sensors are nearly the same, (Microcontrollers Lab, 2013). They work on through the principle of changing in the resistance (ΔR) accordingly the higher the moisture, the lower the resistance and the lower the moisture, the higher the resistance, since the increment of the moisture intensifies conductivity of the metal probes in soil and vice versa.

Soil moisture content sensor was connected to analog ADC_2 jot of the Arduino Uno ATmega328P microcontroller board, thus it set to convert the sensor's analog output value to be transform into digital signal value in order to execute and by pass the main executor. The analog output result of the soil moisture sensor values are sequentially converted in the intervals of analog into digital convertor (ADC) values, which is in-between 0-to-1023.

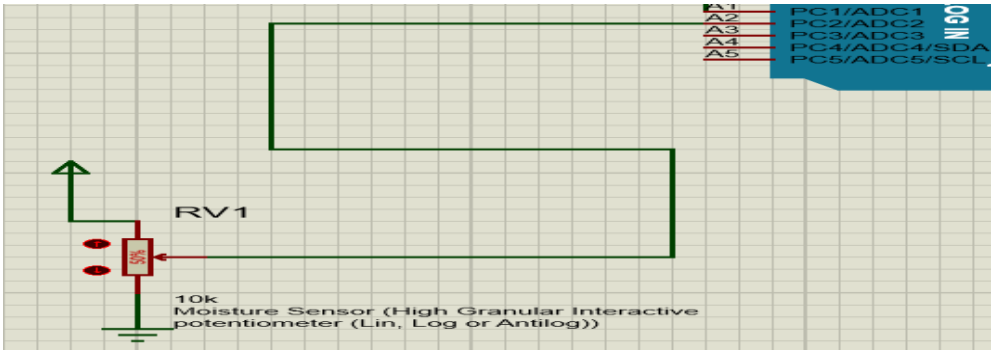

Figure 5.6: Moisture sensor potentiometer

Accordingly, the maximum ADC value $(ADC = 1023)$ yields zero value of soil moisture content, while minimum $(ADC = 0)$ value yields maximum (~100%) moisture content.

Arduino Uno Microcontroller was employed to monitor the change in soil resistance of moisture sensor so that this alteration in resistance pushed to turn off/on water pumping motor.

A. The embedded system Analog into digital converter analysis

Regarding analog voltage reading of Arduino Uno in this project, I discussed applications and techniques of how to use ADC channels. Since Arduino Atmega328P microcontroller is mini-computer, which never understand analog values to accomplish its tasks rather every microelectronic system deals with 1's or 0's digital binary. Arduino Microcontroller use ADC to understand and read analog values from interfaced sensors (Shifa, 2018).

ATmega328p microcontroller do not understand analog (variable) voltage, for the seek of microcontroller understanding these variable voltages; output of interfaced sensors must be stored until changed into digital in analog (ADC) pins read sensors. It converts these readings into digital in-between 0 & 1023. The ADC of Arduino Uno ATmega328p Microcontroller is a 10-bit, which means that it has the ability to detect ($2^{10} = 1024$) discrete analog values. Several microcontrollers contain 8-bit (2^8 to be in-between 0 & 256), while some have 16-bit (2^{16} to be in-between 0 & 65536) discrete size level.

The ADC pin reports its reading from sensor in ratio-metric factor form. It means that, the ADC of Arduino Microcontroller assumed that 5-volt is 1023, with this limits, any value less than 5volt supplied to the microcontroller become a ratio (x) in-between 5 and 1023. Therefore, sensor's variable voltage (0-to-5V) (Kumbhar & Ghatule, 2013) is equivalent with digital readings (0-to-1023) is calculated using the following formulae (Banzi & Shiloh, 2009);

$$\frac{\text{Resolution of the ADC}}{\text{System Voltage}} = \frac{\text{ADC Reading}}{\text{Ananlog Voltage Measured}} \qquad (5.5)$$

Whereas;

Resolution of the ADC = 1023

System Voltage = 5 volt

Analog Voltage Measured =	sensor's Output Value in-between 0-5volt
ADC reading =	Interval between (0-to-1023) found after changing Analog Voltage Measured into digital. i.e. this is what the microcontroller reports for necessary activities

Irrigation field location, weather condition and soil type are the main factors of this automatic irrigation scheme, which then mainly affected ADC outputs to the microcontroller while this embedded system played crucial role to been productive in variable climatic conditions through adjusting the variables. The analog such as A_1, A_2 pins specifically were interfaced in my embedded system supplied their output, which is in-between 0-5Volt that is under the interval of the power source supplied to system. This Arduino ATmega328P microcontroller only received these stored Values in ADC1 and ADC2. Uttermost these values ought to converted into the binary digits (i.e. in-between 0-1023), in order to understood and executed it.

Arduino Uno ATmega328P microcontroller in this project has used only analogRead and analogWrite functions to interpret the analog voltage inputs of interfaced environment to digital number. The AnalogRead State is used the microcontroller to read the analog voltage while analogWrite used to display values on the interfaced LCD or run the motor ON/OFF.

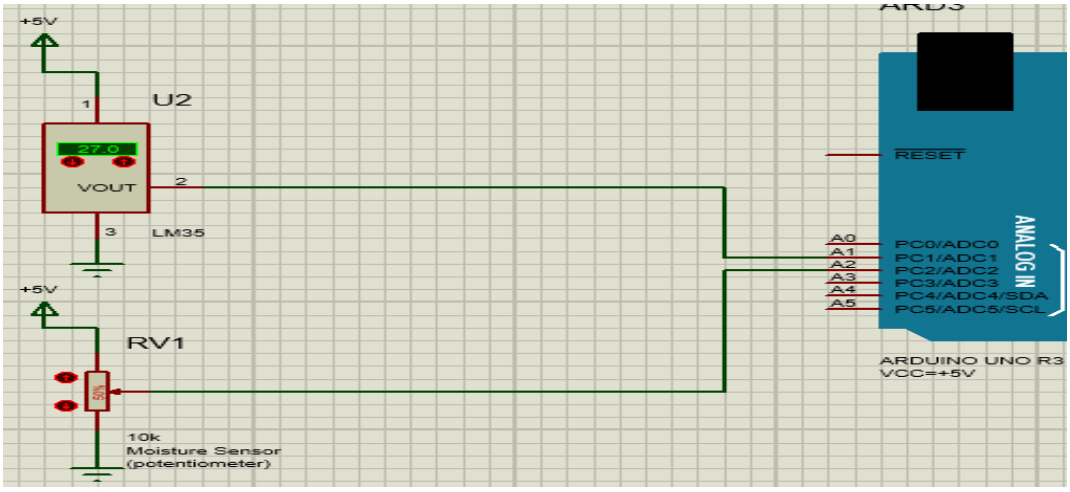

Figure 5.7: Arduino Uno atmega328P microcontroller

In this project, moisture sensor through variable resistor and temperature sensor, which both were of output voltage, adjoined to ADC_1 and ADC_2 of Microcontroller as shown above in figure: 5:8, respectively. They also connected to 5volts and ground on their other ends. Thus, the microcontroller ON the water pump motor, when their voltage become in-between 2.24volts and the microcontroller via the driver off the motor when the voltage used to move current inside the soil circuit became zero volt.

To identify the output soil moisture (%) detected by the moisture sensor in the form of digital values, I have to identified the analog reading of the moisture sensor pin via rearrangement of equation 5.6 as follows;

$$ADC\ Reading = \frac{Resolution\ of\ the\ ADC * Analog\ Measured}{System\ Voltage}$$

(5.6)

```
%      x = ADC readings
%      y = resolution of ADC=1023
%      w = analog sensor voltage
%      z = system voltage (5V)

y = 1023;
w = 0:0.25:5;
z = 5;
m = y*w;
n = m/z; so using equation 5 .7 in mat lab to calculate the
```
microcontroller's ADC readings as follows

```
>> y = 1023

y =    1023

>> w = 0:0.25:5

w =
  Columns 1 through 11
```

```
    0    0.2500    0.5000    0.7500    1.0000    1.2500    1.5000    1.7500    2.0000    2.2500
2.5000

  Columns 12 through 21

    2.7500    3.0000    3.2500    3.5000    3.7500    4.0000    4.2500    4.5000    4.7500    5.0000

>> z = 5

z =     5
>> y*w

Ans =
   1.0e+03 *

  Columns 1 through 11

    0    0.2557    0.5115    0.7672    1.0230    1.2788    1.5345    1.7902    2.0460    2.3018
2.5575

  Columns 12 through 21

    2.8133    3.0690    3.3247    3.5805    3.8363    4.0920    4.3477    4.6035    4.8593    5.1150

>> y*w/z

Ans =
   1.0e+03 *

  Columns 1 through 11

    0    0.0512    0.1023    0.1534    0.2046    0.2557    0.3069    0.3581    0.4092    0.4604
0.5115

  Columns 12 through 21

    0.5626    0.6138    0.6650    0.7161    0.7672    0.8184    0.8695    0.9207    0.9718    1.0230
```

Therefore, for the moisture sensor buried in the irrigated soil, the microcontroller read the values in digital outputs. From the above result, for supplied analog sensor voltage to the microcontroller in between 0-5volt, the microcontroller can read the moisture level in digital

score form in between 0-1023. Therefore, for the sensed 0V, the microcontroller received 0 percent moisture level while for the sensed 5V values the microcontroller received 100 percent moisture. Thus from analyzed moisture level of figure 5;3, the lower and upper optimum percentage values (i.e. 22.9020, 43.8039) must be changed into digital scores for the purpose of that the microcontroller can only understand digital scores for decision making. Therefore, from the above mat lab result, the equivalent ADC readings for the analyzed threshold values became 236.86 and 451.37 which were bold in the following table;

Table 5.4: Analog into digital moisture sensor analyzed values

System voltage (V)	**Resolution of ADC**	**Analog Measured voltage (1-5V)**	**ADC reading (0 - 1023)**	**Moisture Percentage**	**Remarks**
5	1023	0	0	0	
5	1023	0.5	102.3	10	
5	1023	1	204.6	20	
5	**1023**	**1.16**	**228.2**	**22.3**	**lower threshold value**
		1.25	255.75	25	
5	1023	1.5	306.9	30	
	1023	1.75	358.05	35	
5	1023	2	409.2	40	
5	**1023**	**2.24**	**448**	**43.8**	**upper threshold value**
5	1023	2.25	460.4	45	
5	1023	2.5	511.5	50	
5	1023	2.75	562.6	55	
5	1023	3	613.8	60	
5	1023	3.25	664.95	65	
5	1023	3.5	716.1	70	
5	1023	3.75	767.25	75	
5	1023	4	818.4	80	
5	1023	4.25	869.55	85	
5	1023	4.5	920.7	90	
5	1023	4.75	971.8	95	
5	1023	5	1023	100	

Additionally the upper and lower mean moisture level result was calculated in mat lab as follows.

% Calculate the Lower and Upper Threshold values for the threshold values of the embedded system programming

% Therefore, the lower threshold Level of the Minimum Moisture level (%) is;
x = [18.5 19 21.5 31 16.5 14 18 6 25.5 30.5 32 26 19.5 10 34 33 34.5 30 17.5 8.5 21 28 34 39 9.5 16 21 18 38 44 5 12.5 18.5 19 21.5 31 16.5 14 18 9.5 25.5 30.5];

$$\text{Mean(x)} = \frac{\sum_1^{\text{N}} \text{Minimum Moisture Level}}{\text{N}}$$

% Therefore, the lower threshold Level of the Minimum Moisture level (%)is;
y = [31 43 49 45 32 18 37.5 40 44.5 46 36 40 47 48.5 52 50 45 45 39 38 47 47 45 50 49 54 50.5 51 52 53 39 31 43 51.5 45 32 18 37.5 40 44.5 46];

$$\text{Mean(y)} = \frac{\sum_1^{\text{N}} \text{Maximum Moisture Level}}{\text{N}}$$

M = mean(x) = 22.3
N = mean(y) = 43.8

In conclusion, the Microcontroller's ADC readings of the soil moisture sensor is 0 percent for 0 digital response soil response and 100 percent for 1023. Therefore, entire my system should monitor the moisture level be in between $234 \leq MoistureLevel \leq 448$ digital score. Accoring to the analsysis of equation 5.6 and table 5.5 result, the micrcontroler monitored the sensor-to-motor interconnection, through converting the measured voltage of the sensor into binary digital (Banzi & Shiloh, 2009). The Micrcontroller cannot understand the soil physical quantity (analog voltage) and to communicate with its environemnt like the pumping motor. So that, it must be converted immediately into digital values. This conversion uttermost used the micrcontroller to monitor the enntire system. This digital read has a linear relationship (Manimaran & Arfath, 2016) with the moisture sensor output as displayed in Figure 6.3 below.

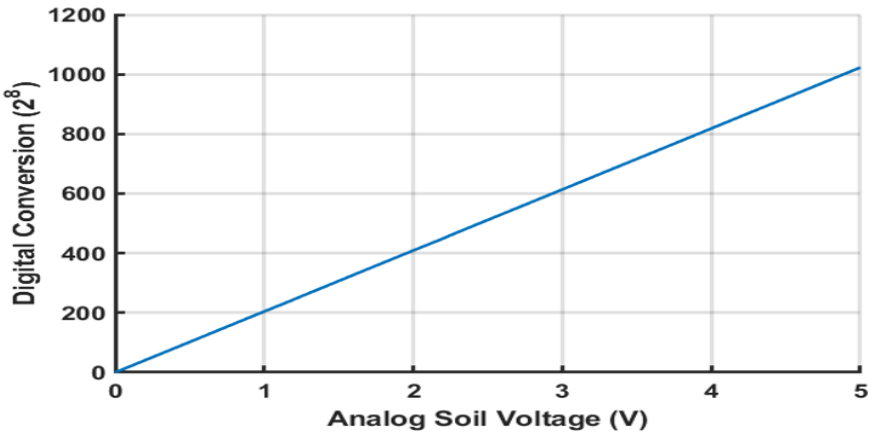

Figure 5.8: Analog to digital conversion result of the microcontroller

Therefore, collecting all the analyzed components assembly and variables above in this chapter, embedded automatic irrigation system was designed as laid out below in figure 5.10 below.

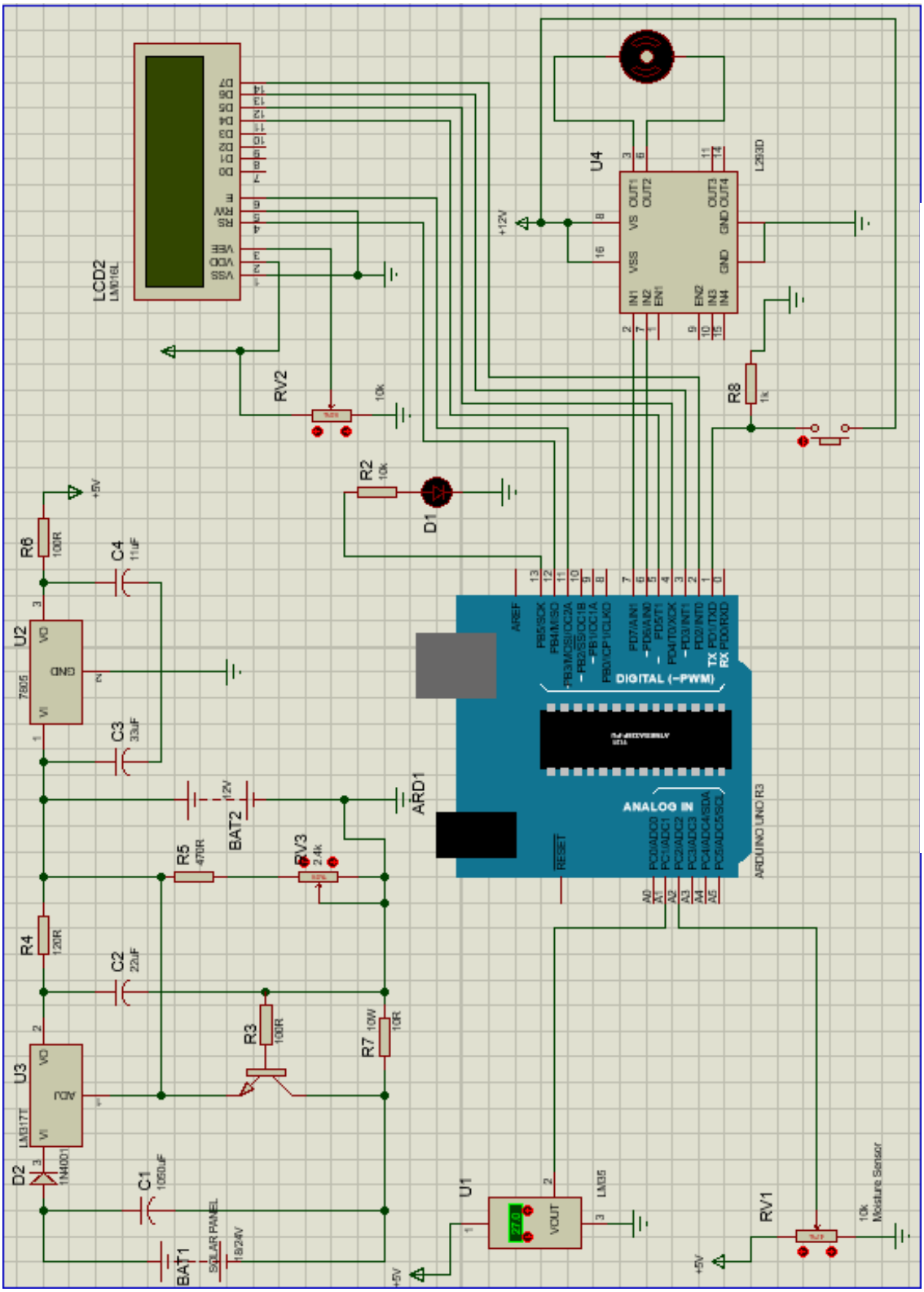

Figure 5.9: Entire Designed Embedded System

CHAPTER 6
SIMULATION AND RESULT DISCUSSION

6.1 Soil Moisture Threshold Result Discussion

As cascaded and determined in chapter 5 above, maximum and minimum moisture content (%) were measured and analysed for the selected site. This soil moisture identification was objectively determined the lower limit and upper limit leading values of the soil moisture that the automated embedded system preliminary monitored watering system of the irrigation. Accordingly, based on the measured data of Table 4.1 the maximum and minimum moisture content (%) per date's graphical representation using mat lab was plotted in Figure 6.1.

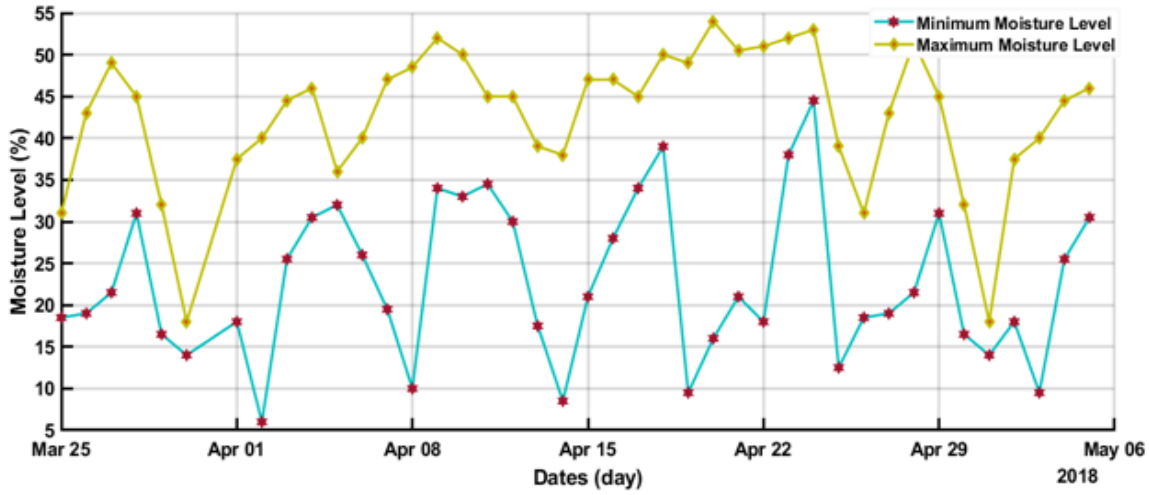

Figure 6.1: Maximum and minimum soil moisture mat lab result

While the mat lab oriented optimized mean results of maximum and minimum soil, moisture (%) of the selected site was plotted in Figure 6.2 below. It was used to identify the mean values of each moisture scores (upper and lower intermediate) limit. Here the two-dashed straight lines were the intermediate values of the result, which the automated irrigation

system has been implementing to monitor the soil moisture to be in between these dashed lines.

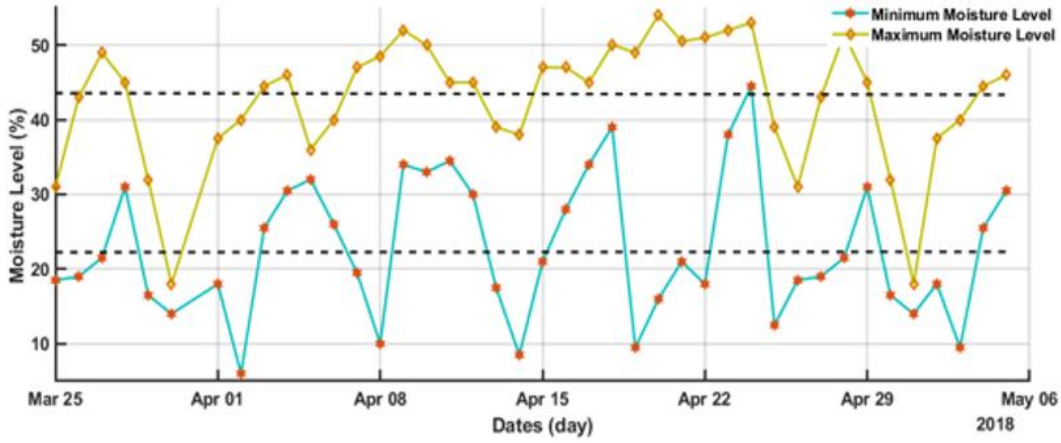

Figure 6.2: Lower and upper moisture boundary mat lab result

Based on the mat lab result presented in figure 6.2 above, the automatic embedded system should monitor the irrigated land moisture interval be in-between 22.3 (1.14v) < Optimum Moisture Region ≤ 43.8(2.24v). As a result, the values from graph between the two dashed horizontal lines shows threshold moisture region of the system. In the other case, the values below 22.3 describes that the irrigated soil was too much dry so called most dry region while for the values above the 43.8 percent moisture describes to much wet so called most wet region. It meant, when the entire system realized in DebrieZeit within selected irrigation site, the mechanized system must kept soil moisture level in between $22.3 < \text{moisture} \leq 43.8\%$). Based on these results, the designed embedded system was evaluated and simulated.

This project was designed, based on the farm site's (DebrieZeit) data possessing an altitude coverage of 1851m. Therefore, based on the determined altitude and according to Table 4.1 the site categorized under Ethiopia's Agro-ecology weather classification of Wayne-Dega.

On the other hand, based on the converted digital values, microcontroller was going to monitor water pumping motor state. Therefore, based on the Analog into Digital converting techniques of Arduino's result in Table 5.5 shown that, 0 and 5volt are the reference interval. As a result graph has revealed below, that the irrigation soil attained full moisture (100%)

when the moisture sensor measured 5volt while the soil is totally dry or 0% moist when the sensor read zero-volt as publicized in Figure :6.3.

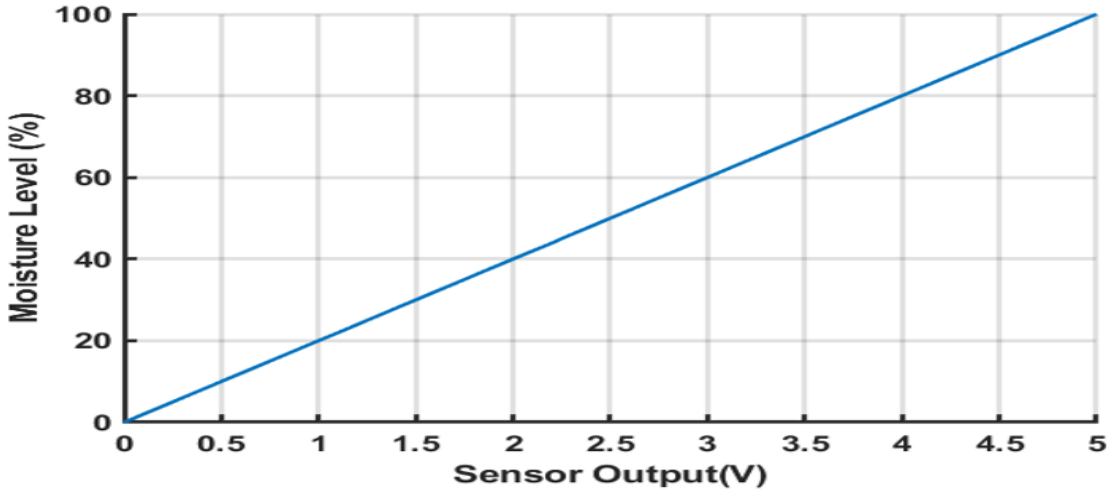

Figure 6.3: Moisture sensor readings

Thus combining the result found in table 5.5 as well as the moisture (%) and sensor reading (V) relationship depicted in figure 5.9, the determined moisture level that the simulated automatic irrigation system was working dwell in between 1.16 and 2.24volt (22.3 and 43.8 percent moisture level respectively). Therefore, the following figure shown the result that the irrigation soil was at optimum moisture for the voltage readings of between 1.16 and 2.24volts. while the irrigation soil dry when the sensor read for signal voltage of less than or equal to 1.16 volt and wet when a sensor read above 2.24volt as resulted by the thicker hidden below.

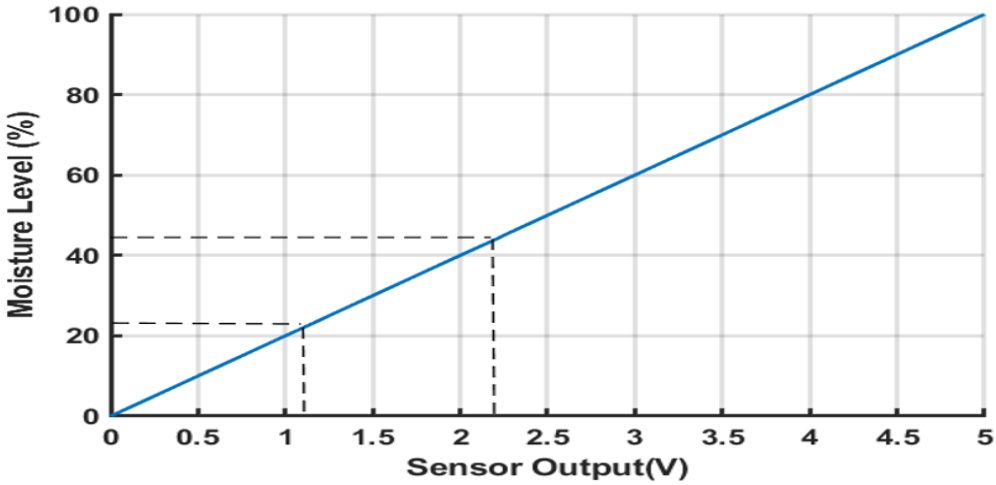

Figure 6.4: Optimized Sensor voltage

6.2 The Block Diagram and System Control Result Evaluation

Mathematical and numerical modelling is the course of representing a system plant (Aloo, Kihato, & Kamau, 2016) using numeric and logic mathematical equations. Therefore, to identify designing model and operational norm of the plant I investigated two; mechanical & electrical characteristics of the system. In this paper, parameter of angular speed response controlled servomechanism identification method was presented with controller algorithm used for a constant input voltage to determine the signal response. In this paper, a 12DVC namki motor with a metal gearbox, which has integrated quadrature encoder, was used to measure the interfaced motor activities (Abd El-Hamid, 2012) like speed and velocity of the motor shaft is used.

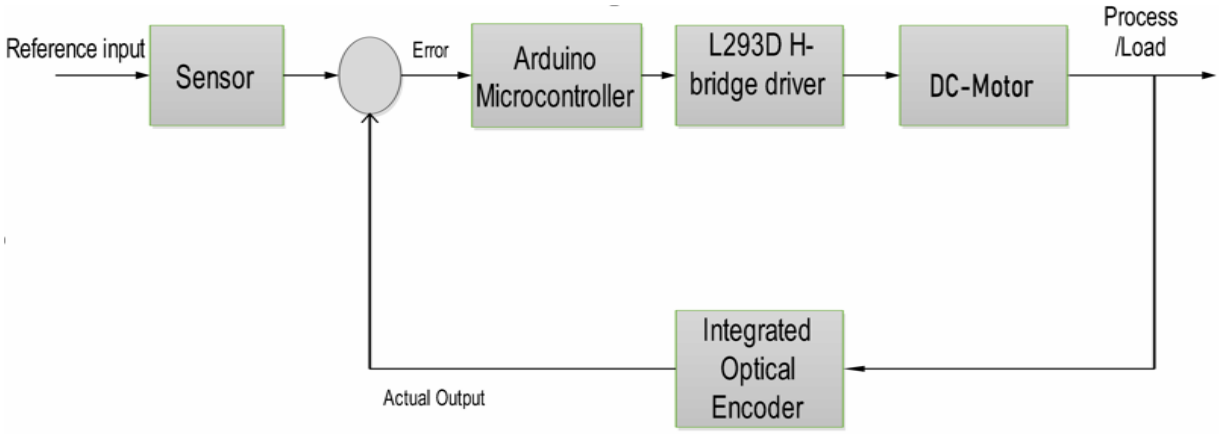

Figure 6.5: Schematic embedded diagram of the dumping DC-motor

For application purpose, this servomechanism approach supplied motor shaft speed measuring optical encoder that the DC motor is naturally integrated. The current amplifier loop (up to the H-bridge driver) lets current controlling and minimizes electrical time constant (Soria, Garrido, & Concha, 2010) making it much faster than mechanical constant time. From (C. R. Phillips & Nagle, 2012),(Ogata, 2002) most of simple closed loop control systems often modelled as using zero order system when hold and sampling.

Additionally, the following assumptions were considered while analysis and modelling the control system. The H-bridge driver used as power amplifier (Shebani & Iqbal, 2017) (Choudhary et al., 2017) since the mini-computer cannot drive the motor. The following are the anatomized variables to drive equations and analysis controlling system of the water pumping DC motor and the entire system. In addition, the Arduino pwm as per coded in the program interface drive (Soria et al., 2010) the dc motor through the driver.

MV: input motor voltage (V)

Ia: the DC motor armature current (A)

Kemf=emf ((V/rev)/s)

ω: Angular position of the shaft (rev/s)

Ra: armature resistance (Ω)

La: armature inductance (H)

τ : torque (Nm)

s: Laplace transform variable

B: Viscous friction coefficient (Nms)

Ki: Optical encoder sensor gain,

J: motor and load inertia (kgKgm^2/m^2)

K_H: H-bridge driver gain

Km: motor torque constant (Nm/A)

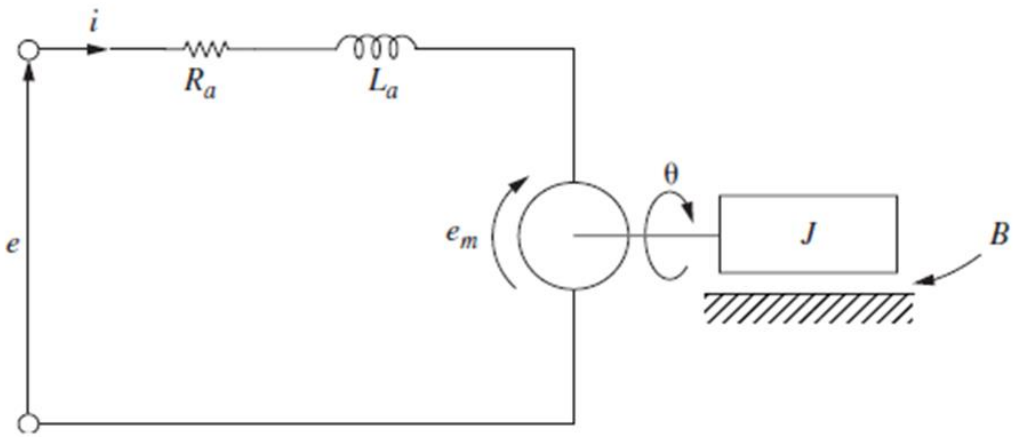

Figure 6.6: Servomotor system parameter assignment

The following table is the manufacturing design and variables of the 12 DVC namki armature controlled motor with a metal gearbox. To analysis and describe the control system of the water pumping DC motor and the entire system simulation in this paper this values were deployed,(C. L. Phillips, Nagle, & Chakrabortty, 2014), (Wu, 2012).

Table 6.1: A 12 DVC namki RK377CR armature controlled parameters

Parameter	**Unit**	**Symbol**	**Value**
Back emf constant	(V/rev/s)	k_{emf}	1.706± 34%
Motor load gain	rad/Nms	k_m	0.9048±49%
H-bridge driver gain	(Nm/A)	K_H	1.6
Viscous friction coefficient	(Nms/rad)	B	0.0124±3%
Motor armature resistance	(Ω)	R_a	18-20
Integrated Optical sensor gain	(N.ms/V)	K_i	1.61±12%
Motor& load Moment of inertia	(KNms/rad^2)	J	0.06198

In case of my embedded system; continuous and discrete time subsystem were entailed. The Arduino microcontroller has analog input and digital output. Thus, before proceeding analysis of the system, in order to the entire analog system work continuously the digital output means discrete control system must be transformed into analog system or discrete system into continues control system.

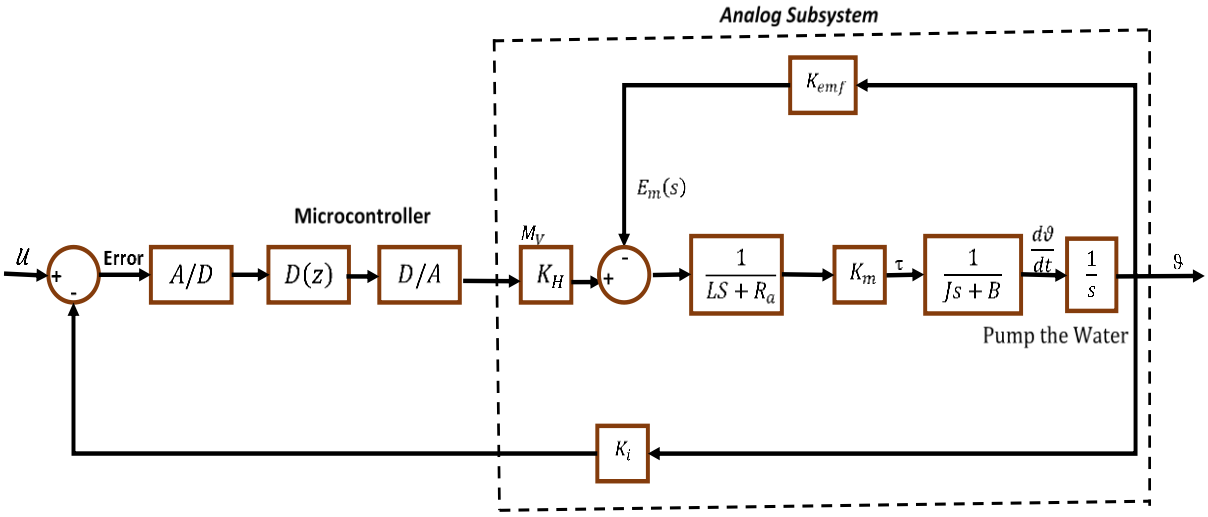

Figure 6.7: Block diagram of the water pumping control system

Accordingly, following equations were derived and applying Laplace transform as the water pumping system contains DAC, and analog subsystem using electrical & mechanical components dynamic analysis.

6.2.1 Modelling electrical characteristics of the system

The torque produced due to electrical characterization of angular dc motor control system, whose currents are i_f and i_a is;

$$\tau(t) = ki_f(\mathrm{t})i_a(\mathrm{t}) \qquad (6.1)$$

$where\ k_t = ki_f(\mathrm{t})(\mathrm{Nm/A})$ is constant. In this water pumping actuator control case, since the input voltage directly applied to the armature thus i_f is remain constant. The created torque uses to drive the water pumping centrifugal head load through rotating. Considering

the viscous coefficient b between bearing and rotating shaft and total inertia J of load, rotor and motor shaft. The applied input voltage to motor can be proportionate to the H-bridge driver gain (Soria et al., 2010). as; M_V α K_H, so

$$m_V(t) = K_H u(t)$$

The fixed magnetic field induces back electromotive, EMF, $e_a(t)$. Applying KVL to the armature circuit so that the armature loop is described

$$e_a(t) = k_{emf} \frac{d\vartheta(t)}{dt} = k_{emf} * \omega$$

Deploying KVL and ohm laws to the electrical dc-loop and the ohm's law respectively;

$$\sum V = V_{in} - V_R - V_L - EMF = 0$$

$$V_{in} - V_R - V_L - EMF = 0$$

$$V_{in} - R_{a*} i_a - L_a \frac{di_a}{dt} - k_{emf} \frac{d\vartheta(t)}{dt} = 0$$

$$V_{in} = R_{a*} i_a + L_a \frac{di_a}{dt} + k_{emf} \frac{d\vartheta(t)}{dt} \quad (6.2)$$

Appling Laplace transform to

$$V_{in}(s) = R_{a*} i_a(s) + sL_a i_a(s) + sk_{emf} * \omega$$

$$V_{in}(s) - sk_{emf} * \omega(s) = R_{a*} i_a(s) + sL_a i_a(s) \quad (6.3)$$

6.2.2 Modelling mechanical characteristics of the system

The generated torque is used to drive the water pumping head through the shaft. Majorly the paper considered here the viscous friction, b, total moment inertia of the pumping head load, J, the shaft and rotor of the moment; let ϑ be angular position of the pump head load and q is the water flow rate to reach the desired level. The rotating shaft of the servomotor used to spray the water consists two mechanical components. The centrifugal pumping head under the input of created motor torque produces angular velocity, $\omega = \frac{d\vartheta(t)}{dt}$, dumping friction, b of the pumping head load and total moment of inertia, J. Considering that, the torques'

disturbance and dynamics of system and depends on dimensions and then shape of the load, the summation of produced torque is equal to zero.

$$\sum \tau = \mathrm{J}\alpha = \mathrm{J}\frac{d^2\vartheta(t)}{dt^2} = 0$$

$$\tau_{in} - \tau_R - \tau_L - EMF = 0$$

The entire mechanical characteristics of the water pumping system is given by;

$$\tau_e + \tau_\omega + \tau_a + \tau_{emf} = 0 \qquad (6.4)$$

Thus, the mechanical components of the system has;

$$k_t i_a(\mathrm{t}) = \tau_a + \tau_\omega + \tau_l + \tau_{emf} \qquad (6.5)$$

Where k_t torque constant and $\tau_a, \tau_f, \tau_L, \tau_\omega$ are torques produced due to acceleration, back EMF, load and velocity respectively. Coulomb's friction law (Salem, Mahfouz, & Aly, 2015) at steady state is found by ;

$$k_t i_a(\mathrm{t}) = \mathrm{b} * \omega = \tau_f \qquad (6.6)$$

Again, the selected centrifugal pump head connected to the dc motor is used for low-to-middle pumping head application. Therefore, from Darcy Weisbach equation, shaft torque generated in this case is driven from the power mandated by this pumping head pressure through the motor shaft (Salem et al., 2015) is;

$$p_{in}(\mathrm{t}) = \frac{\rho.g.h.\mathrm{q}}{\eta} = \tau_m * \frac{d\vartheta}{dt} = \tau_m w \qquad (6.7a)$$

Where p_{in}, η, ρ, h and q are input pressure due to the shaft, pumping head efficiency, pump head and water flow rate respectively. Thus, by applying motor pump power balance principles (Hassan & Kamran, 2018) the above equation become;

$$\rho.g.h.q = \eta\tau_m w$$

$$\tau_m(t) = \frac{q\eta}{\rho.g.h}\frac{d\vartheta}{dt}$$

In this paper, the following parameters are the low-to-middle centrifugal head parameter average values (Hassan & Kamran, 2018) η=85%, ρ_{water} =1000kg/m^3, g = 9.8$^{m}/_{s^2}$, $h = 0.004m$ while q (water spraying rate) is the compulsory variable to attain the required moisture level. Inserting all variables into the equation yields;

$$\tau_m(t) = \frac{Q*0.85}{1000\text{kg}/m^3*9.8^{m}/_{s^2}*0.004m}\frac{d\vartheta}{dt}$$

$$\tau_l(t) = 0.0217q\frac{d\vartheta}{dt} \qquad (6.7b)$$

Henceforth, substituting,$\tau_l = 0.0217q\frac{d\vartheta}{dt}, \tau_e = \tau_m = k_t * i_a,\ \tau_a = \mathrm{J}\frac{d^2\vartheta(t)}{{d_t}^2},\ \tau_\omega = \mathrm{b}\frac{d\vartheta(t)}{\mathrm{dt}}$ with geared water pumping head, made the sum of the produced torques to be zero. Therefore, the mechanical characteristics of the system become;

$$k_t i_a(\mathrm{t}) - \mathrm{J}\frac{d^2\vartheta(t)}{\mathrm{dt}^2} - \mathrm{B}\frac{d\vartheta(t)}{\mathrm{d_t}} - 0.0217q\frac{d\vartheta}{dt} \qquad (6.8)$$

Applying Laplace transform

$$k_t I_a(\mathrm{s}) = \mathrm{J}s^2\Theta(s) + \mathrm{sB}\Theta(s) + 0.0217q \qquad (6.9)$$

At the common junction of this system, the mechanical and electrical characteristics of pumping dc motor along in line with pumping head is coupled by; $\tau_{motor} = k_t i_a(\mathrm{t})$ and eliminating $I_a(\mathrm{s})$ from both equation 6.3 and 6. 9,

$$V_{in}(s) - sk_{emf} * \omega(\mathrm{s}) = R_{a*}I_a(s) + sL_aI_a(s)$$

$$\mathrm{M}_v(s) - sk_{emf}\omega(s) = \mathrm{I}(s)(R_a + \mathrm{sL}_a)$$

Therefore, the water pumping dc motor electrical components transfer function relating input to armature current is given by;

$$\mathrm{I}(s) = \frac{V_{in}(s) - \mathrm{s}k_{emf}\omega(s)}{(R_a + + \mathrm{sL}_a)} \qquad (6.10)$$

While the water pumping dc motor mechanical components transfer function relating input torque to the water pump head load is given by;

$$\frac{\omega(s)}{ki_a(s)-T_L} = \left[\frac{1}{JS+B+0.0217q}\right] \qquad (6.11)$$

In case during unloading the motor, which means while switching off motor while the desired moisture is reach, reduces the equation to $\frac{\omega(s)}{ki_a(s)} = \left[\frac{1}{JS+B}\right]$. Now substituting equation 6.11 into 6.9 instead of $I_a(s)$

$$k_m \frac{1}{(R_a+sL)}\left(M_v(s) - sk_{emf}\Theta(s)\right) = Js^2\omega(s) + sB\omega(s) + 0.0217sq\omega(s)$$

Rearranging this equation and bearing that, the electrical and mechanical characteristics of this water pumping dc motor are coupled by $\tau_{motor} = k_t i_a(t)$. Thus, the transferal function of the loaded shaft coupled input armature voltage to the shaft's output angular speed ϑ or pumping head rotational angle $\vartheta_g(s)$ is given by;

$$\vartheta_g(s = \frac{\vartheta(s)}{V(s)} = \frac{k_t}{s[(R_a+sL_a)(Js+B+0.0217q)+k_m k_{emf}]}$$

$$\leftrightarrow (L_aJs + JR_a + BL_a)s^2 + \left(BR_a + 0.0217q + k_m k_{emf}\right)s \qquad (6.12)$$

This is third order deferential equation. However depending on the poles' dominancy, electrical time constant is far lesser than mechanical time constant. Accordingly, L_a is often set zero in application due it is far smaller than its resistance, which allows the armature torque; $\tau_a = \frac{L}{R}$ to be very small.

$$\vartheta_g(s = \frac{\vartheta(s)}{V(s)} = \frac{n*k_t}{s[JR_as+BR_a+0.0217q+k_m k_{emf}]} \qquad (6.13)$$

This is the desired model for the analog plant of the water pumping system with the load, which, it is the second order equation.

Again move the second summing point of the analog subsystem to the left of the H-bridge motor driver gain k_H and integrated optical encoder sensor gain k_i of figure 6.7 to reduce both constant gains block, using Mason's gain rule, K_H moves to the left of the second summing point and the feedback K_i become feedback of the second summing junction. Assuming the rotational speed ratio remain uniform causes, n constant, therefore, the simplified transfer function ($G_p(s)$) of the analog plant become;

$$G_p(s) = \frac{K_H * \dfrac{k_t}{(\mathrm{J}R_a s^2 + 0.0217qs + \mathrm{s}\mathrm{B}R_a) + \mathrm{s}k_t k_{emf}}}{1 + \dfrac{k_H k_t}{(\mathrm{J}R_a s^2 + 0.0217qs + \mathrm{s}\mathrm{B}R_a) + \mathrm{s}k_p k_{emf}} * \dfrac{K_i}{k_H}}$$

$$G_p(s) = \frac{\dfrac{K_H k_t}{\mathrm{J}R_a s^2 + \mathrm{s}\mathrm{B}R_a + \mathrm{s}k_t k_{emf}}}{1 + \dfrac{K_i k_t}{(\mathrm{J}R_a s^2 + 0.0217q + \mathrm{s}\mathrm{B}R_a) + \mathrm{s}k_t k_{emf}}}$$

$$= \left[\frac{k_t K_H}{(\mathrm{J}R_a s^2 + 0.0217qs + \mathrm{s}\mathrm{B}R_a) + \mathrm{s}k_t k_{emf}}\right] * \left[\frac{(\mathrm{J}R_a s^2 + 0.0217qs + \mathrm{s}\mathrm{B}R_a) + \mathrm{s}k_t k_{emf}}{(\mathrm{J}R_a s^2 + 0.0217sq + \mathrm{s}\mathrm{B}R_a) + \mathrm{s}k_t k_{emf} + k_t K_i}\right]$$

$$G_p(s) = \frac{\vartheta(s)}{\mathrm{V}(s)} = \frac{k_t K_H}{\mathrm{J}R_a s^2 + (\mathrm{B}R_a + 0.0217q + k_m k_{emf})\mathrm{s} + k_t K_e} \qquad (6.14)$$

While the transfer function with n number of rotations to spray q amount of desired moisture is;

$$\vartheta_g(s = \frac{\vartheta(s)}{\mathrm{V}(s)} = \frac{n * k_t}{s\left[(R_a)(\mathrm{J}s + \mathrm{B} + 0.0217q) + k_m k_{emf}\right]}$$

Henceforth based on the mechanical and electrical transfer function of this motor-to-centrifugal pumping head load interconnection, I integrated and determined the analog sub-system.

$$G_p(s) = \frac{\vartheta(s)}{\mathrm{V}(s)} = \frac{\dfrac{n * k_t}{\mathrm{B}R_a + 0.0217q + k_m k_{emf}}}{s\left[\dfrac{\mathrm{J}R_a \mathrm{s}}{\mathrm{B}R_a + 0.0217q + k_m k_{emf}} + \dfrac{\mathrm{B}R_a + k_m k_{emf}}{\mathrm{B}R_a + 0.0217q + k_m k_{emf}}\right]}$$

$$G_p(s) = \frac{\vartheta(s)}{\mathrm{V}(s)} = \frac{\dfrac{n * k_t}{\mathrm{B}R_a + 0.0217q + k_m k_{emf}}}{s\left[\dfrac{\mathrm{J}R_a \mathrm{s}}{\mathrm{B}R_a + 0.0217q + k_m k_{emf}} + \dfrac{\mathrm{B}R_a + k_m k_{emf}}{\mathrm{B}R_a + k_m k_{emf}}\right]}$$

$$\therefore \quad \frac{n * k_t}{\mathrm{B}R_a + 0.0217q + k_m k_{emf}} = k_m : motor\ gain\ constant$$

$$\frac{\mathrm{J}R_a\mathrm{s}}{\mathrm{B}R_a + 0.0217q + k_m k_{emf}} = \ t_m : motor\ time\ constant$$

Thus, equation 6.12 is simplified to

$$G_p(s) = \frac{\vartheta(s)}{\mathrm{V}(s)} = \frac{k_m}{s[t_m+1]} \qquad (6.15a)$$

In another way, for the seek state poles iteration equation 6.12 can be individually reduce as;

$$G_p(s) = \frac{\vartheta(s)}{\mathrm{V}(s)} = \frac{{}^{n*k_t}/_{JR_a}}{s+{}^{B}/_{J}+{}^{0.0217q}/_{J}\ {}^{k_m k_{emf}}/_{JR_a}}$$

$$\frac{\mathrm{B}}{J} + \frac{0.0217q}{J} + \frac{k_m k_{emf}}{JR_a} = a\ and\ \frac{n * k_t}{JR_a} = k_m$$

$$G_p(s) = \frac{\vartheta(s)}{\mathrm{V}(s)} = \frac{k_m}{s[\mathrm{s}+a]} \qquad (6.15b)$$

Therefore, substituting values of Table 6.1 above into equation 6.14 yields the analog plant's numerical transfer function analyzed as follows;

$$G_p(s) = \frac{\frac{k_p K_H}{\mathrm{J}R_a}}{s^2 + \mathrm{s}\left(\frac{\mathrm{B}R_a + k_p k_{emf}}{\mathrm{J}R_a}\right) + \frac{k_p K_i}{\mathrm{J}R_a}}$$

$$G_p(s) = \frac{\frac{1.6 * 2.5}{0.06198 * 20}}{s^2 + \mathrm{s}\left(\frac{.0124 * 20 + 2.5 * 1.706}{0.06198 * 20}\right) + \frac{2.5 * 1.61}{0.06198 * 20}}$$

$$G_p(s) = \frac{\frac{4}{1.2396}}{s^2 + \mathrm{s}\left(\frac{4.513}{1.2396}\right) + \frac{4.025}{1.2396}}$$

$$G_p(s) = \frac{3.227}{s^2+3.64s+3.2448} \qquad (6.16)$$

This is the desired model for the analog plant of the water pumping system with the load, which, it is the second order equation. However If the armature inductance is not ignored due to its very small, the system would have been third order. The ADC, DAC & Analog Subsection cascade block is drawn as follow.

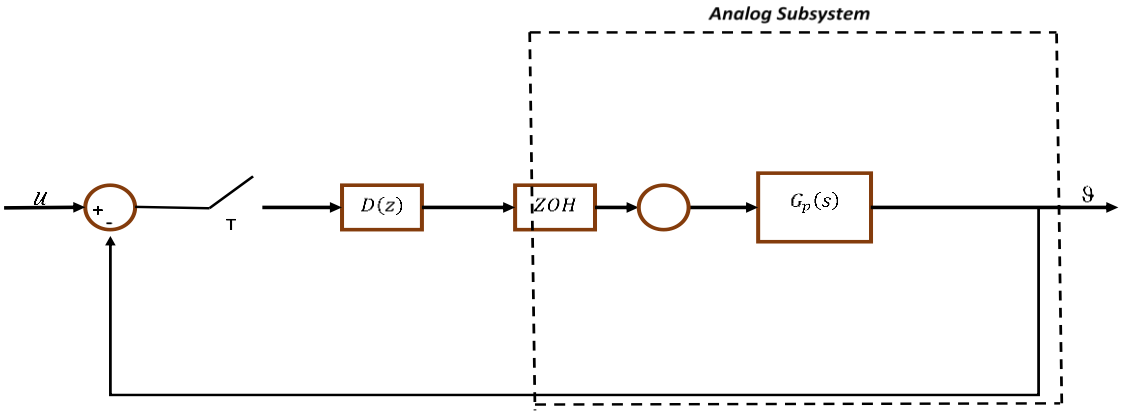

Figure 6.8: ADC, analog subsystem and DAC cascade block

The system was digital control system, although it contained both continuous and discrete time system. To calculate its transferal function and design its model the continuous time system into discrete time system was changed using z-transform as follows. As said before, the system contains DAC, analog subsystem and ADC control system. The system is now cascaded analog plant$G_p(s)$, sampler, and zero order hold.

Zero Order Hold: from (Y. Gholipour et.al, 2014) ZOH is used in reconstruction operator. It's hybrid system (Shebani & Iqbal, 2017) operator with discrete-time input and continuous-time output in DAC user industry. The transfer function for zoh used in this digital input to analog system transformation is;

$$G_{ZOH}(s) = \frac{1-e^{-Ts}}{s} \qquad (6.17)$$

As known, although it is discrete control system, the system covers both discrete, DTS & continuous, CTS subsystems. Assume $D(z) = 1$. To evaluate and model the entire transfer and time response functions of the system in order as the (12V) input voltage command the pumping head to spray Q ($^{m^3}/_{s}$) output amount of water through shaft rotation. Therefore using the DAC model designed in figure 6.9 & analog plant's subsystem TF, $G_p(s)$, the transfer function of is;

$$G_{ZAS}(s) = \mathcal{Z}\Big(G_p(s)G_{ZOH}(s)\Big) * D(z)$$

$$G_{ZAS} = ZOH * \mathcal{Z}\{G_p(s)\}D(z)$$

$$G_{ZAS}(z) = \mathcal{Z}\left\{\left(\frac{1-e^{-Ts}}{s}\right)\left(\frac{3.227}{s^2+3.64s+3.2448}\right)\right\}D(z),$$

$$G_{ZAS}(z) = \mathcal{Z}\left\{\frac{1-e^{-Ts}}{s}\frac{3.227}{s^2+3.64s+3.2448}\right\} \quad (6.18)$$

Using appendix 2 inverse Laplace transform pairs for the bracketed terms

$$G_{ZAS}(z) = 1 * \frac{1-e^{-Ts}}{s} * Z\left\{\frac{3.227}{s^2+3.64s+3.2448}\right\}$$

$$G_{ZAS}(z) = Z\left[1 - e^{-Ts} * \left(\frac{1}{s}\right) * \left\{\frac{3.227}{s^2+3.64s+3.2448}\right\}\right]$$

$$G_{ZAS}(z) = Z\left[(1-e^{-Ts}) * \left(\left(\frac{1}{s}\right)\left(\frac{3.227}{(s++1.56)(s++2.08)}\right)\right)\right]$$

$$G_{ZAS} = Z\left[(1-e^{-Ts}) * \left\{\frac{A}{s} + \frac{B}{s++1.56} + \frac{C}{s++2.08}\right\}\right]$$

Then after taking the partial fraction of $\left(\frac{1}{s}\right)\left(\frac{3.227}{(s+1.56)(s+2.08)}\right)$ part;

$$G_{ZAS} = Z\left[(1-e^{-Ts}) * \left\{\left(\frac{1}{s}\right)\left(\frac{3.227}{(s+1.56))}\right)\left(\frac{1}{(s+2.08))}\right)\right\}\right]$$

$$\left\{\left(\frac{1}{s}\right)\left(\frac{3.227}{(s+1.56)}\right)\left(\frac{1}{(s+2.08)}\right)\right\} = \frac{A}{s} + \frac{B}{s+1.56} + \frac{C}{s+2.08}$$

(6.19)

$$= \frac{A}{s} + \frac{B}{s+1.56} + \frac{C}{s++2.08}$$

$$\rightarrow (A(s+1.56))(s+2.08)) + Bs(s+2.08)) + Cs(s+1.56) = 3.227$$

$$(As^2 + 3.64As + 3.2448A + Bs^2 + 2.08Bs + Cs^2 + 1.56Cs) = 3.227$$

$$0: \ (3.2448A = 3.227); \ A = 0.995 \cong 1 - - - - - - - - i$$

$$1: \quad 3.64A + 2.08B + 1.56C = 0 - - - - - - - - - - - - ii$$

$$2: \qquad A + B + C = 0 - - - - - - - - - - - - - - iii$$

Substituting values of i into ii and simultaneously eliminating ii and iii provides

$$A = 1, \qquad B = -4 \; and \; C = 3$$

The system is digital control system. Thus, discretizing the sub-continuous-time's transfer function using zoh as sampling method can be done as follows. Substituting $A = 1,\ B = -4 \; and \; C = 3$ in equation 6.19 and inverse z-transforming yields;

$$G_{ZAS}(z) = Z\left[(1 - e^{-Ts}) * \left\{\frac{1}{s} + \frac{-4}{s + 1.56} + \frac{3}{s + 2.08}\right\}\right]$$

$$G_{ZAS}(z) = Z\left[(1 - e^{-Ts}) * \left\{\frac{1}{s} - \frac{4}{s + 1.56} + \frac{3}{s + 2.08}\right\}\right]$$

$$G_{ZAS}(z) = Z\left[\left(\frac{1}{\frac{1}{1 - e^{-Ts})}}\right)\left\{\frac{1}{s} - \frac{4}{s + 1.56)} + \frac{3}{s + 2.08)}\right\}\right]$$

$$G_{ZAS}(z) = Z\left[\left(\frac{1}{\frac{1}{1 - e^{-Ts}}}\right) * \left\{\frac{1}{s} - \frac{4}{s + 1.56} + \frac{3}{s + 2.08}\right\}\right]$$

From sampling terminology take $z = e^{sT}$ thus the ZT of $\frac{1}{1-e^{-Ts}}$ is;

$$\left[\frac{1}{1 - \mathrm{e}^{-\mathrm{Ts}})}\right] \overset{z}{\Leftrightarrow} \left[\frac{\mathrm{z}}{\mathrm{z} - 1)}\right]$$

$$G_{ZAS}(\mathrm{z}) = \left(\frac{1}{\frac{\mathrm{z}}{\mathrm{z} - 1)}}\right)\mathrm{Z}\left[\left\{\frac{1}{\mathrm{s} + 0} - \frac{4}{\mathrm{s} + 1.56} + \frac{3}{\mathrm{s} + 2.08}\right\}\right]$$

$$G_{ZAS}(\mathrm{z}) = \left(\frac{1}{\frac{\mathrm{z}}{\mathrm{z} - 1}}\right)\left[\left\{\frac{\mathrm{z}}{\mathrm{z} - 1)} - \frac{4\mathrm{z}}{\mathrm{z} - \mathrm{e}^{-1.56\mathrm{T}})} + \frac{3\mathrm{z}}{\mathrm{z} - \mathrm{e}^{-2.08\mathrm{T}})}\right\}\right], \text{let } \mathrm{T} = 2\mathrm{s}$$

$$G_{ZAS}(\mathrm{z}) = \left(\frac{\mathrm{z} - 1)}{\mathrm{z}}\right)\left[\left\{\frac{\mathrm{z}}{\mathrm{z} - 1)} - \frac{4\mathrm{z}}{\mathrm{z} - \mathrm{e}^{-1.56*2})} + \frac{3\mathrm{z}}{\mathrm{z} - \mathrm{e}^{-2.08*2})}\right\}\right]$$

$$G_{ZAS}(z) = \left(\frac{z - 1)}{z}\right)\left[\left\{\frac{z}{z - 1)} - \frac{4z}{z - e^{-3.12})} + \frac{3z}{z - e^{-4.16})}\right\}\right]$$

$$G_{ZAS}(z) = \left[\left\{1 - \frac{4(z-1)}{z - e^{-3.12}} + \frac{3(z-1)}{z - e^{-4.16}}\right\}\right]$$

$$G_{ZAS}(z) = \left[\left\{1 - \frac{4(z-1)}{z-0.044} + \frac{3(z-1)}{z-0.016}\right\}\right] \quad (6.20)$$

The applied input electrical voltage to the water pumping head via DC-motor shaft was 12V, thus which $R(s) = 12/s$ and its z-transform become $R(s) = \frac{12z}{z-1}$. Thus, inserting into equation 6.19 and then after applying inverse z-transform to equation 6.20

$$\Theta(z) = G_{ZAS}(z)\mathrm{R}(z)$$

$$(z) = \left(\frac{12z}{z-1}\right)\left[1 - \frac{4(z-1)}{z-0.044)} + \frac{3(z-1)}{z-0.016)}\right]$$

$$\Theta(z) = 12\left[\left\{\frac{z}{z-1)} - \frac{4z}{z-0.044)} + \frac{3z}{z-0.016)}\right\}\right] \quad (6.21)$$

$$\Theta(t) = 12\mathcal{Z}^{-1}\left[\left\{\frac{z}{z-1)} - \frac{4z}{z-0.044)} + \frac{3z}{z-0.016)}\right\}\right]$$

$$\Theta(t) = G(t) * R(t) = (12)[\{1 - 4(0.044)^K + 4(0.016)^K\}]$$

$$\Theta(t) = 12[1 - 4(0.044)^K + 4(0.016)^K] \quad (6.22)$$

Let C(t) = $\Theta(t)$. K: kalman stability constant. Therefore, the sampled output response of the intended closed loop system with 12-volt electrical voltage input DC-motor controller, of stability variable K is;

$$\mathrm{C}(kT) = 12[1 - 4(0.044)^K + 3(0.016)^K] \quad (6.23)$$

Since the system is digital controller system, the discrete-time filter transfer function need to be driven of both mixed closed loop continuous and discrete system in Tylor series expansion of z-variable. Thus reducing equation 6.20 into polynomial series yields;

$$G_{ZAS}(z) = \frac{\Theta(z)}{\mathrm{R}(z)} = \frac{12\left[\left\{\frac{z}{z-1} - \frac{4z}{z-0.044} + \frac{3z}{z-0.016}\right\}\right]}{\frac{12z}{z-1}}$$

$$= \left[\left\{1 + \frac{-4(z)}{z-0.044)} + \frac{3(z)}{z-0.016)}\right\}\right]$$

$$= \left\{\frac{(z-0.044)(z-0.016) - 4z(z-0.016) + 3z(z-0.044)}{(z-0.044)(z-0.016)}\right\}$$

$$= \left\{\frac{z^2 - 0.016z - 0.044z + 0.000704 - 4z^2 + 0.064z + 3z^2 - 0.132z}{z^2 - 0.06z + 0.000704}\right\}$$

$$= \left\{\frac{z^2 - 4z^2 + 3z^2 - 0.016z - 0.044z + 0.064z - 0.132z + 0.000704}{z^2 - 0.06z + 0.000704}\right\}$$

$$\therefore \qquad G(z) \quad = \frac{0.1286z + 0.000704}{z^2 - 0.06z + 0.000704}$$

It is a second order filter polynomial. The optical encoder integration is allowing measuring the motor's speed while the controller commands via pulse width modulation. Thus, the motor speed was calculated while pumping irrigation water from encoder sensor position with filter based on determined analysis of $\mathrm{C}(kT) = 12[\,1 - 4(0.044)^K + 3(0.016)^K]$, the output response table is plotted with stability gain variable k varies in-between 0- to-15 below.

Table 6.2: System output response

	System output time response
K	$\Theta(KT) = 12[\,1 - 4(0.044)^K + 3(0.016)^K]$
0	0
1	10.464
2	11.916
3	11.996058
4	11.999822
5	11.99999212
6	11.99999965
7	11.99999998
8	12
9	12
10	12
11	12
12	12
13	12
14	12
15	12

The sampled entire steady state output response of the closed loop system with 12-volt electrical voltage supplied DC-motor controller to move the pumping head, of stability gain, variable K is determined in equation 6.23 and Table 6.2. Accordingly, the output response mat lab simulation for the intended closed loop digital controller model is plotted below;

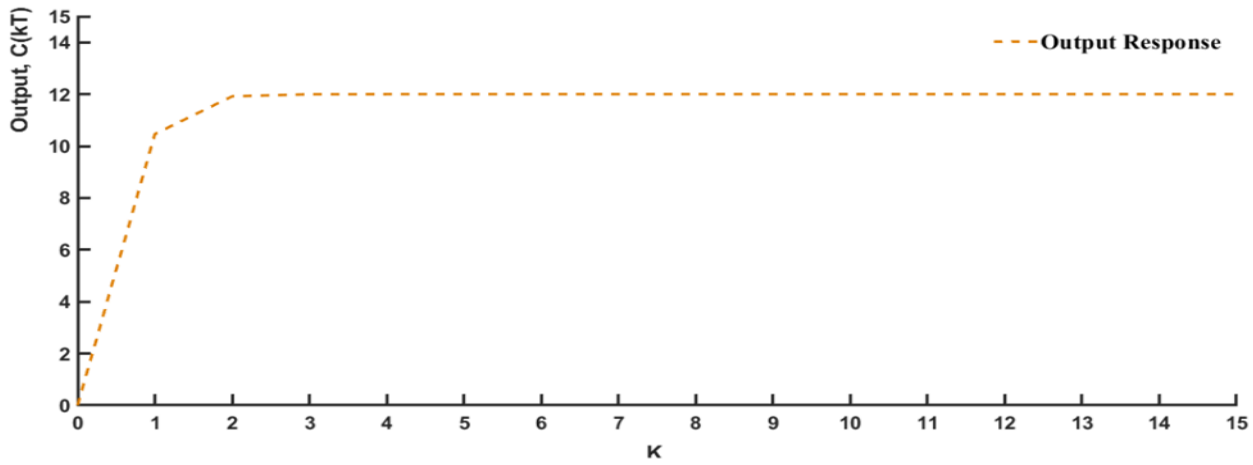

Figure 6.9: Output response of closed loop system

Hence the output response of the identified closed loop water Pumping Dc motor is drawn. As a result, output response is independent of sampled tie T instead digital stability gain k.

Therefore, combining all the transferal function of each mechanical units and electrical units theoretically analyzed under section 6.2 above, the operational characteristics of the entire SSI-irrigation simulation from moisture sensor- via-controller up to centrifugal pumping head was simulated as follows. Here soil moisture, applied voltage and armature current were key inputs while angular speed and generated torque of the pumping head through shaft were output for spraying Q amount of water. Thus, when the sensor measured the soil moist content and became <= 1.16V (228 digital bits), the controller sent an emergent signal to rotate the shaft opening the motor ON to produce torque to pressurize pumping head as shown in Figure 6.11. While the controller holds OFF when the soil moist level become greater or equal to 2.24V (448 digital bits) as shown in Figure 6.12. The inverse relationship between generated torque and angular speed tells us that the increase in water pressurizing load attachment to the shaft decreases the speed of the shaft.

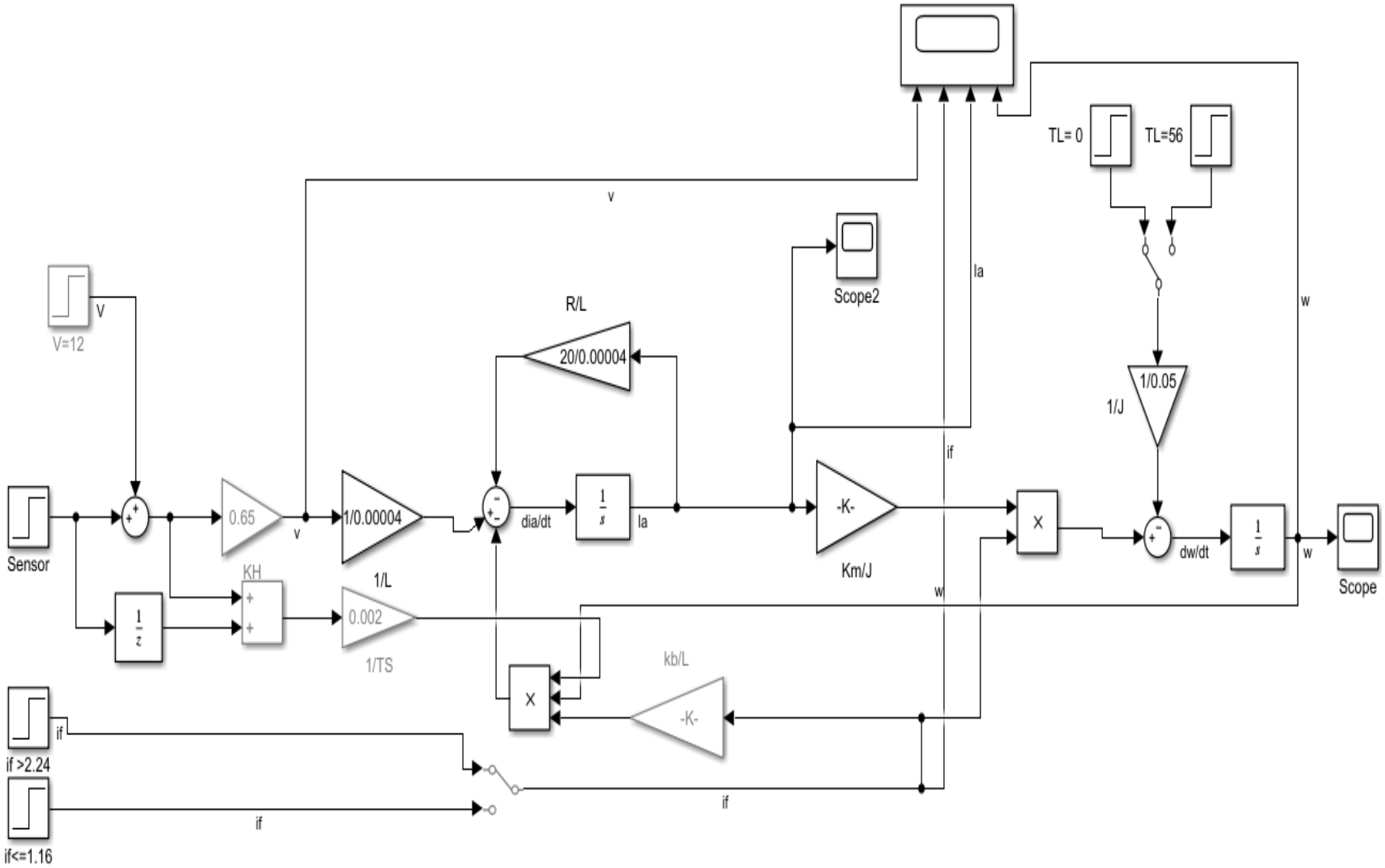

Figure 6.10: Simulation model of full state water pumping system

Based on the above Simulink simulation model, in this paper, the angular and output voltage responses from the Simulink simulation were about 71rps and 11.92V, when the sensor measured the soil moisture and it became less than 1.16V as shown in Figure 6.11, a 12V supplied motor has started pumping water with identified speed. Whereas I_a: armature current, w: angular speed, if: represents the soil moisture conditions in volt and v: is output voltage.

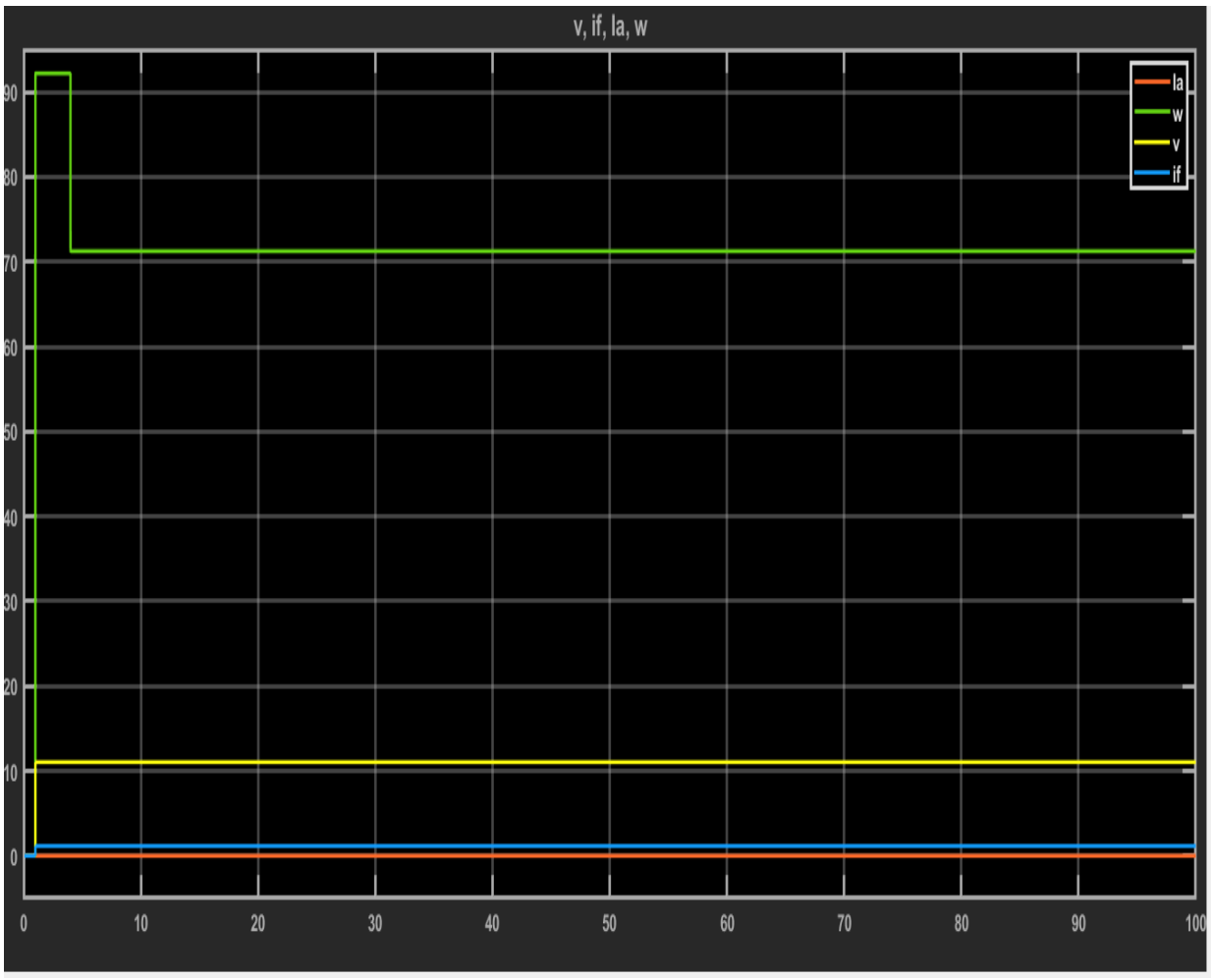

Figure 6.11: Angular speed response of the Motor (ON)

According (Shebani & Iqbal, 2017) closed loop system's stability can be determined via its symmetrical poles site location in the s-plane. The system is said to be stable, its poles

(closed loop) must be either located to the left of the s-plane or at least a single pole must failed on the zero-imaginary axis. Unless and otherwise the system is unstable. In this paper, the poles of the plant transfer function are -1.56 and -2.08, which were located fully on the left of the s-plane and totally found on zero imaginary axis as depicted in Figure 6.13. Thus, the system was completely stable, and has zero overshoot. Accordingly, the stability program & its Mata lab graph are depicted below respectively.

```
% determine poles stability and graph of the system
n = [3.227];
d= [1 3.64 3.2448];
g = tf(n,d)
step(g)
 pGroots = (d)      % poles as root of denominator
pG=pole(g);
pzmap(g)           %shows all poles
grid on
function createhggroup(Parent1, XData1, YData1, XData2, YData2)
%CREATEHGGROUP(Parent1, XData1, YData1, XData2, YData2)
%  PARENT1:  hggroup parent
%  XDATA1:  line xdata
%  YDATA1:  line ydata
%  XDATA2:  line xdata
%  YDATA2:  line ydata

%  Auto-generated by MATLAB on 27-Jul-2019 10:53:07
% Create hggroup
hggroup1 = hggroup('Parent',Parent1,'DisplayName','g');

% Create line
line(XData1,YData1,'Parent',hggroup1,'Tag','PZ_Pole','MarkerSize',13,...
    'Marker','x',...
    'LineWidth',6,...
    'LineStyle','none',...
    'Color',[0 0.447058823529412 0.741176470588235]);

% Create line
line(XData2,YData2,'Parent',hggroup1,'Tag','PZ_Zero','MarkerSize',12,...

 'Marker','o',...
```

```
    'LineWidth',6,...
    'LineStyle','none'...
    'Color',[0 0.447058823529412 0.741176470588235]);
g =
         3.227
  --------------------
  S^2 + 3.64 s + 3.245
```

Transfer function of the system.

```
>> Stability test

g =
         3.227
  --------------------
  S^2 + 3.64 s + 3.245

pGroots =

    2.08         1.56
```

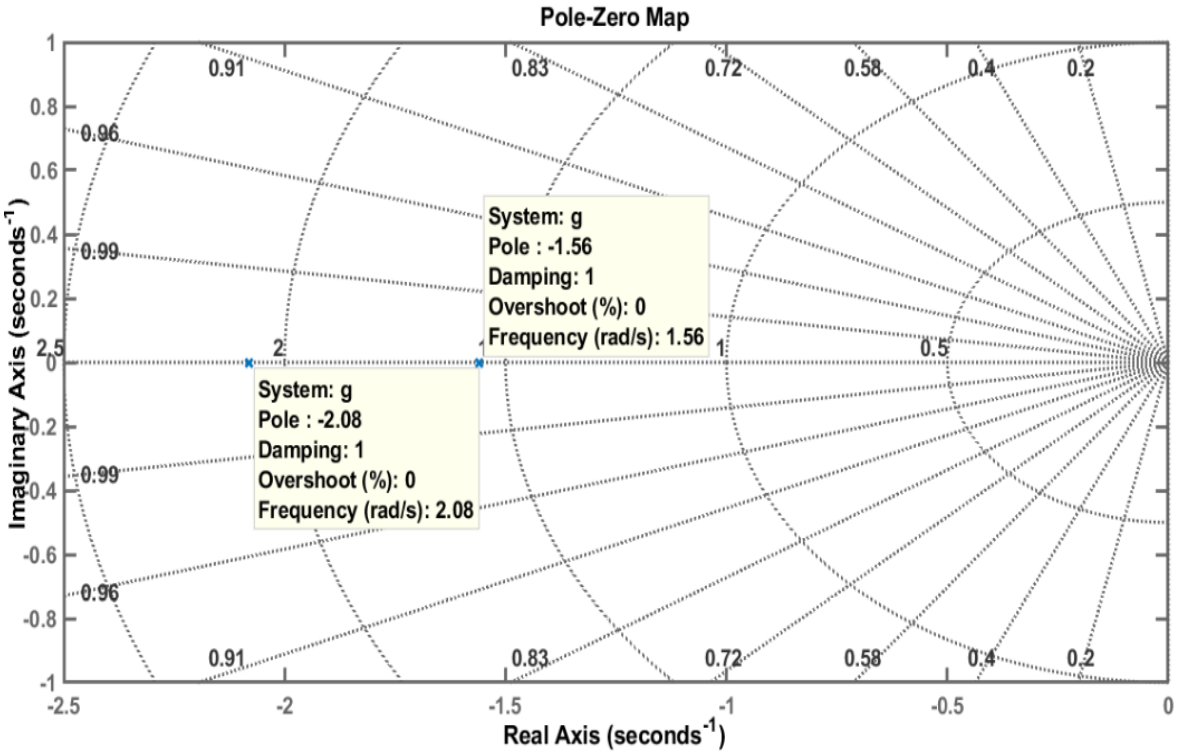

Figure 6.12: System stability response

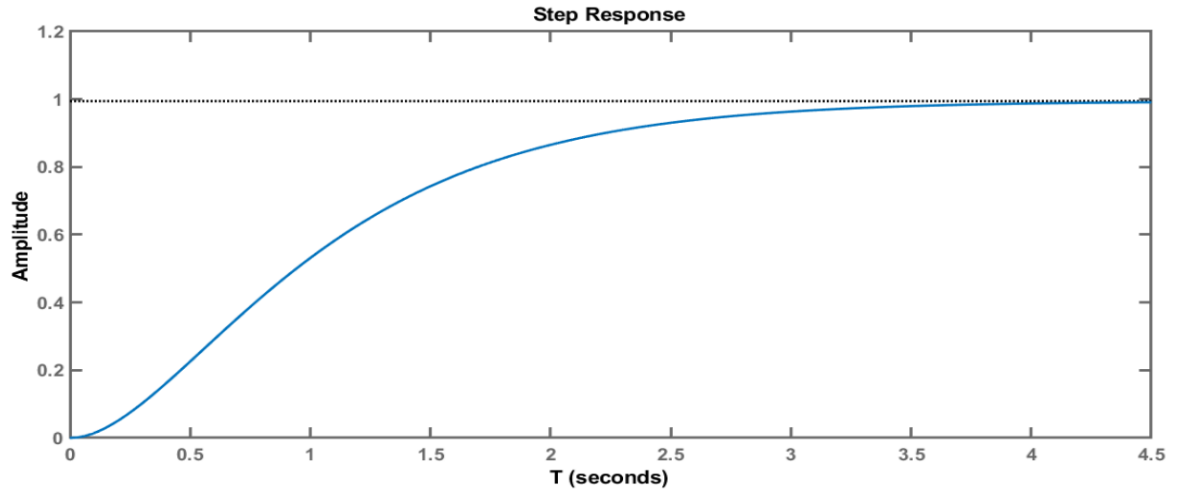

Figure 6.13: Unit step response curve of the system

The system's steady error is determined via applying final value theorem as follows;

$$e^{ss} = \lim_{s\to 0} G_{go}(s) * G_p(s) = \lim_{z\to 1} G_{ZAS}(z)$$

$$\frac{\Theta(z)}{E^*(z)} = \mathcal{Z}\left[G_{go}(s) * G_p(s)\right]$$

$$= \frac{1 - e^{-Ts})}{s}\left\{\frac{3.227}{s^2 + 3.64s + 3.2448}\right\}$$

$$= (1 - e^{-Ts})\left\{\left(\frac{1}{S}\right)\frac{3.227}{s^2 + 3.64s + 3.2448}\right\}$$

$$= \left(\frac{1}{1/_{1 - e^{-Ts}}}\right)\left\{\left(\frac{1}{S}\right)\frac{3.227}{s^2 + 3.64s + 3.2448}\right\}$$

Taking z-transform and simplifying yields;

$$= \frac{1}{\frac{z}{z + (-1)}} * \frac{1}{12} * \left\{\frac{z}{z - 1)} - \frac{4z}{z - e^{-1.56T})} + \frac{3z}{z - e^{-2.08T})}\right\}$$

$$= \lim_{Z\to 1}\left(\frac{1}{12}\left(\frac{z - 1)}{z}\right)\left[\left\{\frac{z}{z - 1)} - \frac{4z}{z - e^{-1.56T})} + \frac{3z}{z - e^{-2.08T})}\right\}\right]\right)$$

$$= \lim_{z\to 1}(z - 1)\left(\frac{1}{12} * \left(\frac{1}{\frac{z}{z - 1)}}\left\{\frac{z}{z - 1)} - \frac{4z}{z - e^{-1.56T})} + \frac{3z}{z - e^{-2.08T})}\right\}\right)\right)$$

$$= \lim_{z\to 1}(z - 1)\left(\frac{1}{12} * \left\{1 - \frac{4(z - 1)}{z - e^{-1.56T}} + \frac{3(z - 1)}{z - e^{-2.08T}}\right\}\right)$$

$$= \frac{1}{12} * \left\{\lim_{z\to 1}(z + (-1)) - \lim_{z\to 1}(z + (-1))\frac{4(z + (-1))}{z + (-e^{-1.56T})} + \lim_{z\to 1}(z + (-1))\frac{3(z + (-1))}{z - e^{-2.08T}}\right\}$$

$$\therefore \mathrm{e^{ss}} = \frac{1}{12}\lim_{z\to 1}(\{1 - 0 + 0\}) = \frac{1}{12} = 0.0833$$

Based on the error signal found the compensated controller's coefficient constants (Soria et al., 2010) in control system, can be selected, often by trial and error or by using look up table in industrial practice, (Dorf, Bishop, & Hall, 2010). Therefore, Figure 6.13 below displays the simulation result of dc motor position controlled analog subsystem for the applied input voltage and operation error signal. The selected design tuned gains k_p and k_i values were 9 and 2.3. So that the positional output response of the system is plotted in Figure 6.13 with

the error signal. The blue colored line is the output response; one can understand that the system has less rising time and 0.083 error values.

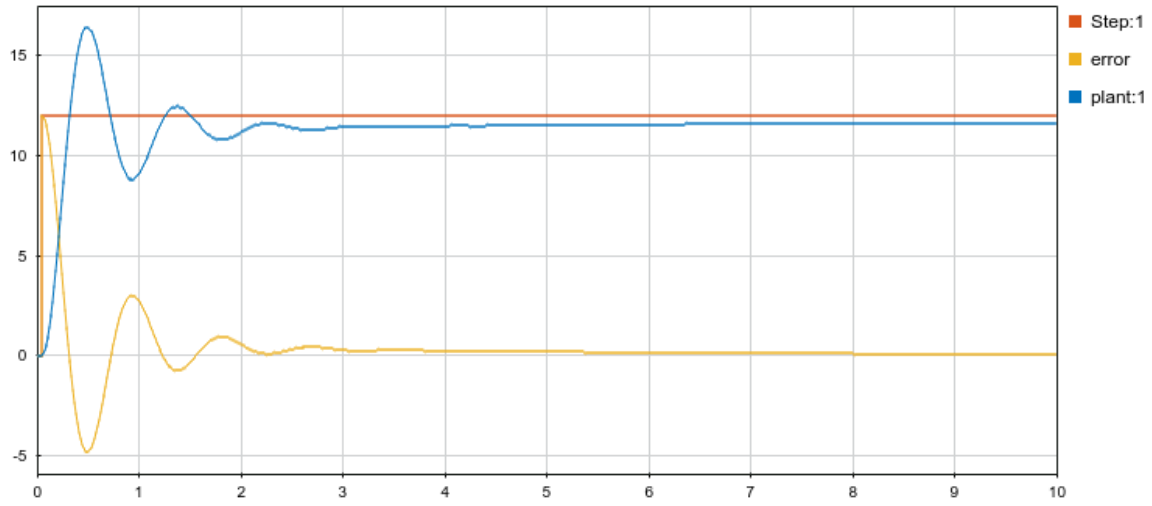

Figure 6.14: Input voltage output response of system

State space modelling of the system: The state variables in-line with input functions casted off in modelling equations determining the dynamic environment of the system provides the sustainable future state performance (Shebani & Iqbal, 2017) of the system. The system state is designated by a first order deferential equation (Choudhary et al., 2017)in terms of the system's state variables. Rearranging equations 6.2 and 6.7, hence the space model for this automatic irrigation system is;

$$\frac{dx}{dt} = Ax + Bu$$

$$\frac{d\omega}{dt} = \frac{k_t * i_a}{J} + \frac{b*\omega}{J} + \frac{\tau_l}{J} \qquad (6.23)$$

$$\frac{dy}{dt} = Cx + Du$$

$$\frac{d\omega}{dt} = \frac{R_a * i_a}{L_a} + \frac{b*\omega}{L_a} + \frac{V_{in}}{L_a} \qquad (6.24)$$

Therefore, taking angular position, $\vartheta(t)$ of the dc-motor as output which in other way it's the input for the pumping head to pump q amount of flow rate and selecting state variables position (ϑ), angular velocity (ω) and armature current (i_a) henceforth substituting these variables into mechanical and electrical components behavioral determiners gives;

$$x_1 = \vartheta,\ \dot{x_1} = \frac{d\vartheta}{dt} = x_2$$

$$x_2 = \frac{d\vartheta}{dt}, \dot{x_2} = \frac{d^2\vartheta}{dt^2} = \frac{d\omega}{dt}$$
$$= \frac{k_t * i_a}{J} + \frac{b*\omega}{J} + \frac{\tau_l}{J}$$

$$x_3 = i_a,\ \dot{x_3} = \frac{di_a}{dt} = -\frac{R_a * i_a}{L_a} - \frac{b*\omega}{L_a} - \frac{\mathrm{V}_{in}}{L_a}$$

$$x_4 = \frac{dq}{dt}$$

Thus; $\dot{x_1} = \frac{d\vartheta}{dt} = x_2$

$$\dot{x_2} = \frac{d^2\vartheta}{dt^2} = \frac{k_t * i_a}{J} + \frac{b*\omega}{J} + \frac{\tau_l}{J}$$

$$\dot{x_3} = \frac{di_a}{dt} = -\frac{R_a * i_a}{L_a} - \frac{b*\omega}{L_a} - \frac{\mathrm{V}_{in}}{L_a}$$

Substituting the state variables and then rearranging gives state space model of;

$$\dot{x_1} = \frac{d\vartheta}{dt} = x_2$$

$$\dot{x_2} = \frac{\mathrm{B}}{J}x_2 + \frac{k_t}{J}x_3 - \tau_l$$

$$\dot{x_3} = \frac{k_b}{L_a}x_2 - \frac{R_a}{L_a}x_2 - \frac{1}{L_a}\mathrm{V}_{in}$$

$$\dot{x_4} = \mathrm{q}/J$$

$$\frac{d}{dt}\begin{bmatrix} q \\ \vartheta \\ \omega \\ i_a \end{bmatrix} = \begin{bmatrix} {}^{q}/_{J} & 0 & 0 & 0 \\ 0 & 1 & -{}^{b}/_{J} & {}^{k_m}/_{\mathrm{J}} \\ 0 & 0 & {}^{k_m}/_{L_a} & {}^{R_a}/_{L_a} \end{bmatrix}\begin{bmatrix} q \\ \vartheta \\ \omega \\ i_a \end{bmatrix} + \begin{bmatrix} 0 \\ 0 \\ 0 \\ {}^{1}/_{L_a} \end{bmatrix} V_{in}$$

$$\frac{d}{dt}\begin{bmatrix} q \\ \vartheta \\ \omega \\ i_a \end{bmatrix} = \begin{bmatrix} {}^{q}/_{J} & 0 & 0 & 0 \\ 0 & 1 & 0 & 0 \\ 0 & 0 & -0.2 & 14.6 \\ 0 & 0 & 18.096 & 1000 \end{bmatrix}\begin{bmatrix} q \\ \vartheta \\ \omega \\ i_a \end{bmatrix} + \begin{bmatrix} 0 \\ 0 \\ 0 \\ 200 \end{bmatrix} V_{in}$$

$$\omega(t) = [0 \;\; 1 \;\; 0 \;\; 0]\begin{bmatrix} q \\ \vartheta \\ \omega \\ i_a \end{bmatrix}$$

In this dynamic model of water pumping dc-motor, the variables to be controlled were predominantly the armature current$i_a(t)$, and mechanical variable of angular velocity$\omega(t)$, which is the output to the pumping head.

6.3 The System Pumping Capacity

In pumping system, the aim of the pump was to provide a comparative sufficient water to moist the irrigation soil feeding the required flow rate (Matthew Milnes, n.d.). The operating system's pressure is a function of flow quantity and some arrangements in terms of pipe size, fittings, and pressure on the water. From Bernoulli's liquid analysis, let us contemplate an incompressible class fluid of density ρ along after the centrifugal pump head is assumed as flowing through an imaginary cylindrical tube, which tells us water particles motion are uniformly in steady flow. However, this paper only concerned and theoretically analyzed up to pump head analysis. So the centrifugal pump head's flowing rate performance is analyzed as follows. Water is incompressible fluid and has steady state flow here. Mathematically from first affinity law "pumping water flow rate is directly proportional to the speed of pumping shaft".

$$Q = \omega \leftrightarrow \frac{Q_1}{Q_2} = \frac{\omega_1}{\omega_2} \qquad (6.25)$$

Where Q is water flow rate (${}^{m^3}/_{S}$), ω speed of the shaft (rpm) and from second law of affinity head pressure is directly proportional to shaft speed square during pumping the water

$$H = \omega^2 \;\leftrightarrow\; \frac{H_1}{H_2} = \frac{(\omega_1)^2}{(\omega_2)^2} \qquad (6.26)$$

The power transported into water via pumping shaft is termed as waterpower. To calculate it, the flow rate and the pump head must be known. The shaft power determines pumping

efficiency. So, the waterpower is determined from the relationship of adjusting all the above iterative equations and calculating the resultant water flow rate across the pumping head of this system, the centrifugal pumping head of the system flow rate as follows;

$$P(w) = \frac{Q*H*g*\rho}{\eta} \quad (6.27)$$

P = Power (W) of the shaft, ρ = Density (Kg/m 3) = 1000 $^{kg}/_{m^3}$ for water, η =Pumping efficiency. However, the work done due the electric power via shaft is done due to the net applied voltage to allow current flow I is;

$$P(w) = V_{app} * I \quad (6.28)$$

Where the net V_{app} is errorless output of the applied voltage to the system and I is applied current to the motor through the battery. Inserting equation 6.28 into 6.27, the flow rate of this irrigation system is calculated as

$$V * I = \frac{Q*H*g*\rho}{\eta} \quad (6.19)$$

Thus the capacity of pumping water per unit time (m^3/sec) of this automatic irrigation system denoted as Q is;

$$Q = \frac{\eta*V_{net}*I}{H*g*\rho} \quad (6.30)$$

From potential dissipation result, of Figure 6.10 the net voltage output applied to shaft is 12v-0.0833 = 11.92V and the current I is the output current from the solar charge controller assuming armature resistance is lied in series ($i.e. 6 - 6A/20\,\Omega = 5.4A$). According to (Branan, 2007); (Thin, Khaing, & Aye, 2008) for the selected centrifugal pumping head, the pumping efficiency lies 75-85% depending on head friction, ρ_{water}= 1000kg/m^3, g = 9.8 $^{m}/_{s^2}$, and the low-to-middle centrifugal head parameter average theoretical (Hassan & Kamran, 2018) head pressure for non-returnable centrifugal head is as H = 1.02m. Thus, inserting these values with intended pumping efficiencies into equation 6.29 yields minimum and maximum flow rate capacity are;

$$Q = \frac{0.75 * 11.92\text{V} * (6 - I_{drop\ across\ armature\ res})\text{A}}{1.02m * \text{g} = 9.8\,{}^{m}/_{s^2} * 1000\text{kg/m}^3}$$

$$Q = \frac{0.75 * 11.92\text{V} * (6 - {}^{12v}/_{20\Omega})\text{A}}{1.02m * \text{g} = 9.8\,{}^{m}/_{s^2} * 1000\text{kg/m}^3}$$

$$Q = \frac{0.75 * 11.92\text{V} * (6 - 0.6)\text{A}}{1.02m * \text{g} = 9.8\,{}^{m}/_{s^2} * 1000\text{kg/m}^3} = \frac{48.276}{9996}$$

$$Q = 4.83 * 10^{-3}\,{}^{m^3}/_{s} = 4.83\,{}^{l}/_{s}$$

While for maximum efficiency, the pumping head capacity is calculated as;

$$Q = \frac{0.85 * 11.92\text{V} * (6 - I_{drop\ across\ armature\ res})\text{A}}{1.02m * \text{g} = 9.8\,{}^{m}/_{s^2} * 1000\text{kg/m}^3}$$

$$Q = \frac{0.85 * 11.92\text{V} * (6 - {}^{12v}/_{20\Omega})\text{A}}{1.02m * \text{g} = 9.8\,{}^{m}/_{s^2} * 1000\text{kg/m}^3}$$

$$Q = \frac{0.85 * 11.92\text{V} * (6 - 0.6)\text{A}}{1.02m * \text{g} = 9.8\,{}^{m}/_{s^2} * 1000\text{kg/m}^3} = \frac{54.71}{9996}$$

$$Q = 5.47 * 10^{-3}\,{}^{m^3}/_{s} = 5.47\,{}^{l}/_{s}$$

Table 6.3: Pumping capacity indicator of the system

C(kT)=12[1-4(0.044)^k+3(0.016)^k]	Min. η	Max. η	I	Vnet*I	Head* ρ*g	Min. Q (l/s)	Max. Q (l/s)
0	0.75	0.85	5.4	0	9996	0	0
10.464	0.75	0.85	5.4	56.5056	9996	4.239615846	4.804897959
11.916	0.75	0.85	5.4	64.3464	9996	4.827911164	5.471632653
11.996058	0.75	0.85	5.4	64.7787132	9996	4.860347629	5.50839398
11.999822	0.75	0.85	5.4	64.7990388	9996	4.861872659	5.510122347
11.99999212	0.75	0.85	5.4	64.79995745	9996	4.861941585	5.510200463
11.99999965	0.75	0.85	5.4	64.79999811	9996	4.861944636	5.510203921
11.99999998	0.75	0.85	5.4	64.79999989	9996	4.86194477	5.510204072
12	0.75	0.85	5.4		9996	4.861944778	5.510204082

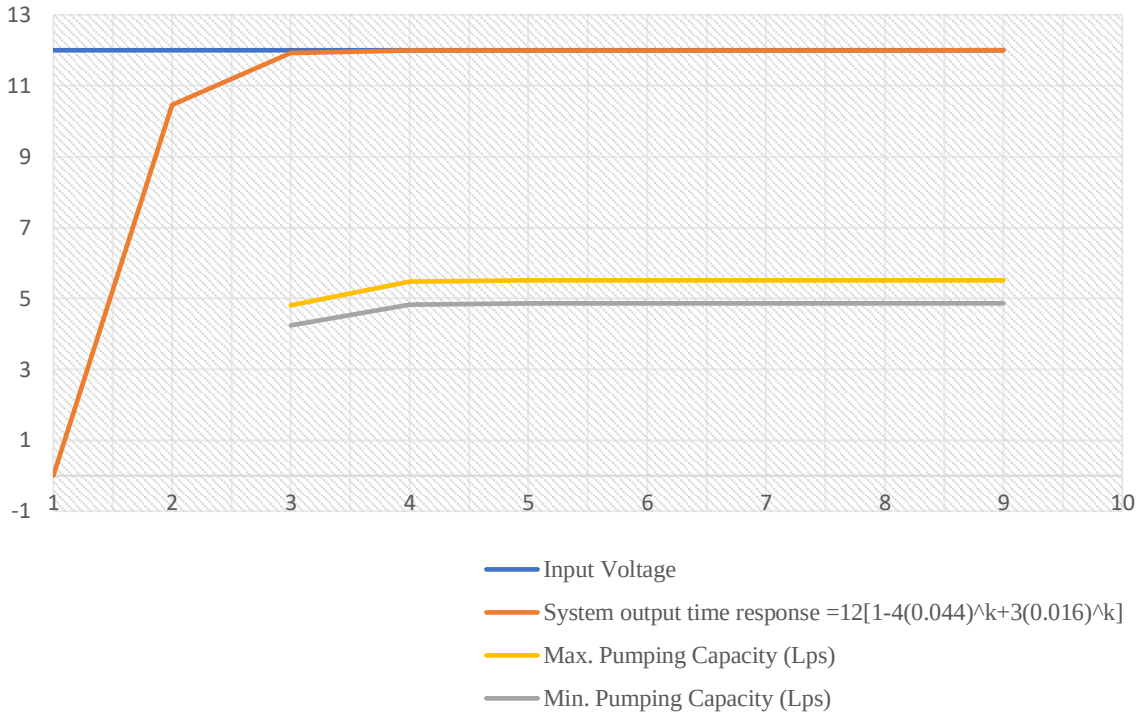

Figure 6.15: Pumping performance indicator of the system

From the analysis, at initial conditions this automatic irrigation system water pumping average capacity was in-between 4.83 and 5.47lps. Thus, from Table 6.3 and Figure 6.14 of result, the pumping capacity of system depends on the output response of the input voltage.

6.4 Result Summary

The system objectively moved to automate Ethiopian SSI for the purpose of productivity promotion. Thus, embedded system construction and simulation was entirely taken place. The system to be operated timely, the study predefined threshold intervals in terms of percent and digital bits of the moisture content of the irrigated land. After I designed and interfaced every embedded system components, mechanical and electrical entire system control evaluation has been determined for its operational continuity. From the electrical and mechanical control system evaluation analyses, it's clear that the system has zero overshot, very small almost zero error and according to stability (Mandloi & Shah, 2015) rules, this mechanized irrigation system was stable with all poles lied on zero imaginary axis to left of the system's s-plane.

In this paper beyond automation, how to quantitatively monitor irrigation water was crucial. Therefore, from pumping performance analysis, this designed controller based automatic system through the intended shaft can pressure out in-between 4.83 and 5.47lps. From the result, however the pumping performance of the system depends on the output response of the input voltage.

Henceforth I sketched programming language using, C^{++} oriented IDE software in order that to simulate and automate the entire embedded irrigation system. Thus, after assembling all the design components, I sketched and uploaded the run automation program on the controller, the result fixed that the entire system accomplished the SSI irrigation automatically within the predefined tasks without manual interventions as follows.

A. **Pumps Water Automatically for Dry Soil**: when the moisture level measured by the respective sensor, and then displayed lesser moist values than the least predefined moisture (threshold i.e. 228.2 digital bits read by analog convertor) the controller send command signal to the actuator. When this was occurred the irrigated soil productivity of the site become visibly under irrigated, therefore the embedded system automatically open the water pumping motor and pumps automatically until it realized the optimum moisture value.

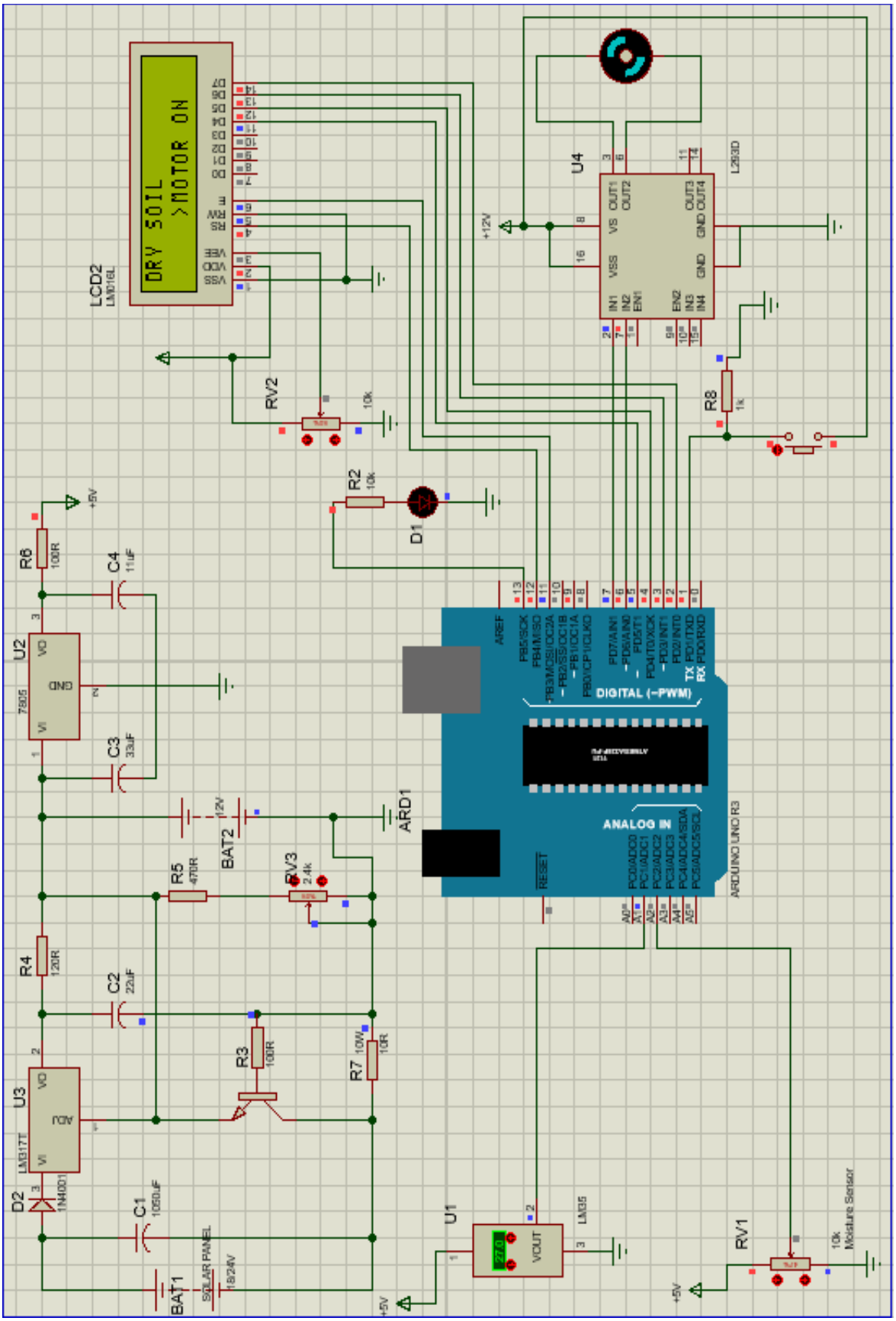

Figure 6.16: Pumps water automatically for irrigated dry soil

B. Close water pump automatically for excess wet soil: when the irrigated land soil moisture become greater than 448 ADC bit resolution (equivalent to 43.8percent), the system reported as the soil moisture became excess wet, which may causes over irrigation. Next to under irrigation due to less moisture in Ethiopian irrigation farm, over irrigation farm is the other main irrigation delinquent. Therefore, the designed automatic embedded system and simulated in this thesis holds off watering until the irrigated soil moisture level drops less than the limited value. Therefore, this designed automatic irrigation system, assists the users/farmers to monitor volumetric moisture content without labor intervention.

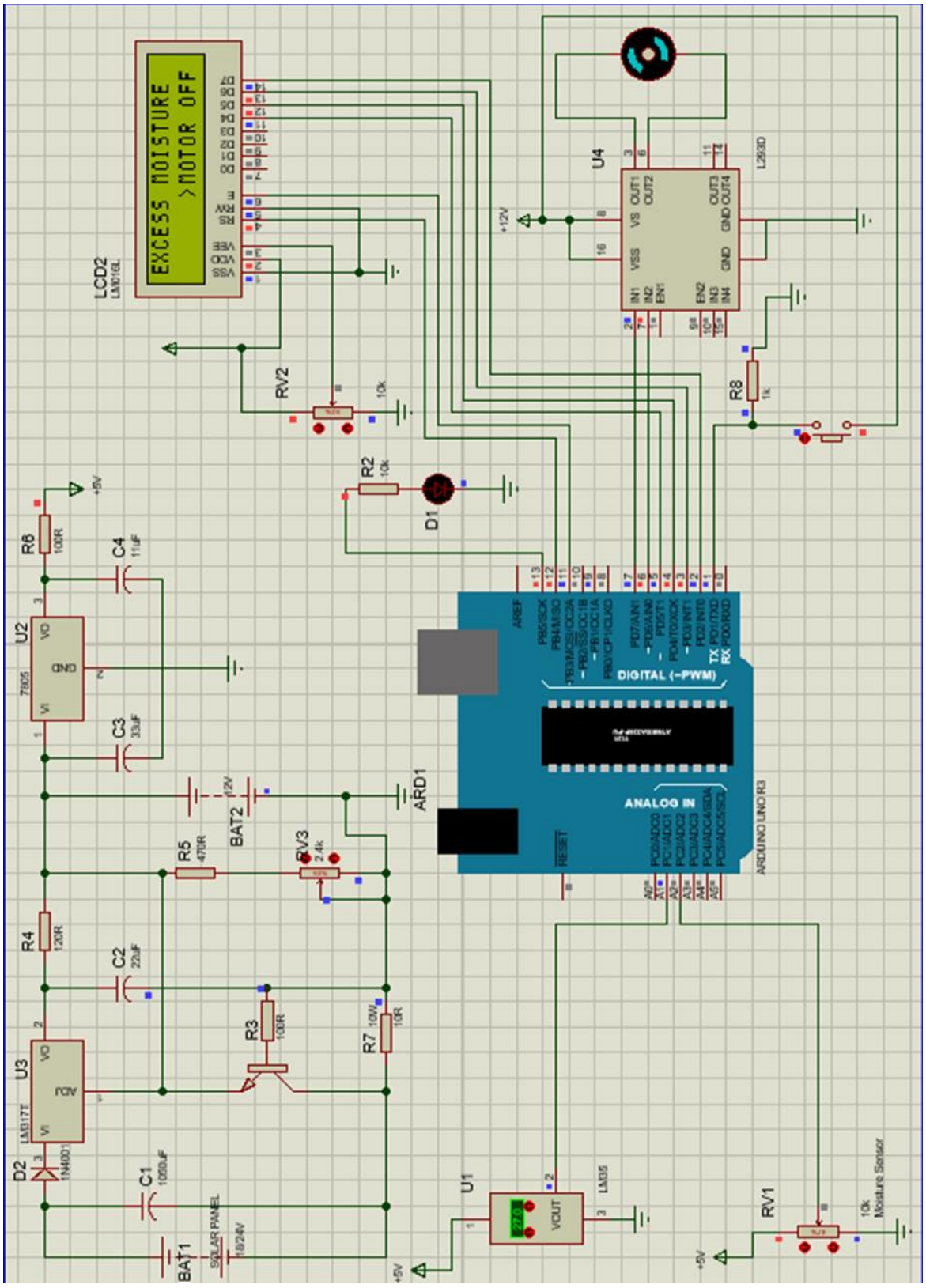

Figure 6.17: Close water pump automatically for excess wet soil

CHAPTER 7
CONCLUSION AND FUTURE WORKS

7.1 Conclusion

This paper demonstrated the determination of a sensor response based small-scale irrigation monitoring scheme in DebrieZeit. Mainly FC-28 moisture sensor was deployed along with Arduino Uno and Namkci DC-motor to consecutively monitor soil moisture contents of the irrigation field. The integrated sensors to ATmega328P equipped Arduino Uno Microcontroller based reflexive irrigation system has designed and simulated automatically. Based on simulation result, when the sensed soil moisture became less than the preset threshold value, the microcontroller sent signals to the driver that trigger the water pumping dc motor to turn ON pumping head through shaft until it achieved the desired moisture.

This paper was entailed design and automation of Ethiopian small-scale irrigation system entirely energized by photovoltaic energy. Proteus 8.6, Arduino IDE programming and mat lab Simulink were used to design, assembly and automate the system. Thus, theoretical execution of this entire embedded system has been functional thoroughly and it will be enabled the farmers easily to monitor under and over irrigation difficulties via watering only the real required amount and dewatering without labor intensity.

Moreover, after every mechanical and electrical system control evaluation using a simple loop closed system identification method has been theoretically determined. From this control system evaluation analyses, the system has no overshot, small rise time, almost zero error and stabled with all poles lied on imaginary axis.

Beyond SSI irrigation automation, the paper also identified the pumping performance limits of the interconnected centrifugal pumping head through the shaft as in-between 4.83 and 5.47lps. The system's pumping performance depends on the output response of the input voltage.

Alternatively, the price for these system's components including the quadrature encoder, microcontroller, solar, namki RK377CR dc-motor, H-bridge driver, and the LCD is about

319 USD. This price is plentifully too low compared to the minimum labor based generator user (Y. Alemu et al., 2016) for lower-scale irrigation system which is 514 USD in Ethiopia. Thus, this proposed system enactment will be a reasonable substitute.

7.2 Future Works

In order to practically improve and implement the effectiveness of this entire automatic irrigation scheme and controlling soil moisture integrating sensors with microcontroller powered by photovoltaic energy, the following recommendations must be put into future considerations:

- Most SSI operation in Ethiopia is cost-ineffective and moisture level misalignment, due lacks of resources managing technological integration, so that the concerned stakeholders must facilitate the enactment of this low cost alternative technology with more research concerning volume of the water to be pumped vs. area coverage performance.

- In Ethiopia, there is huge amount of energy deficiency while this project site is mainly occurred in villages, where is too hard to access electricity. So that, this paper proposed solar based energy to power the entire embedded system components while operating the irrigation works. Thus, solar harvesting capacity of each irrigation sites must be investigate in detail with their all-powering characteristics before this project will be widely implement.

- Additionally, as explained in the paper, there are different irrigation performances size wise in Ethiopia, from small-scale to large-scale clusters, which were operating under inefficient farm. Thus, researchers shall give a more research priority in deploying upto 128-bit microcontroller breading for large-scale automatic irrigation.

REFERENCES

Abdurrahman, M. A., Mehari, G., Tsigabu, G. &, & Bezabih, T. (2015). Sensor Based Automatic Irrigation Management System. *International Journal of Computer and Information Technology*, 04(03), 2279–2764. Retrieved from www.ijcit.com

Alemu, D., & Effort, B. E. (2017). Agricultural Research for Ethiopian Renaissance : Challenges , Opportunities and Directions.

Aloo, L. A., Kihato, P. K., & Kamau, S. I. (2016). DC Servomotor-based Antenna Positioning Control System Design using Hybrid PID-LQR Controller. 5(2), 17–31.

Awulachew, S. B. (2010). Irrigation potential in Ethiopia. *International Journal of Agricultural Policy and Research*, (July).

Banzi, M., & Shiloh, M. (2009). Make : Getting Started with Arduino. In Make : Getting Started with Arduino. Retrieved from makezine.com

Barua, A., Hoque, M. M., & Akter, R. (2014). Embedded Systems: Security Threats and Solutions. American Journal of Engineering Research (AJER), 03(12), 119–123. Retrieved from www.ajer.org

Branan, C. (2007). Pumps and Motors. Pocket Guide to Chemical Engineering, 42–46. https://doi.org/10.1016/b978-088415311-5/50002-1

Choudhary, S. K., Kumar, V., Dwivedi, N. K., & Tiwary, A. (2017). Smart Water Sprinkler System Based on Arduino Microcontroller. *International Journal of Engineering Science and Computing*, (4), 10033–10035. Retrieved from http://ijesc.org/

Dhabi, A., & Derbew, B. D. (2013). Brief Facts about Ethiopia.

Dorf, R. C., Bishop, R. H., & Hall, P. (2010). MODERN CONTROL SYSTEMS SOLUTION MANUAL MODERN CONTROL SYSTEMS TWELFTH EDITION Instructor's Solutions Manual.

Dukes, M. D., Shedd, M., & Cardenas-Lailhacar, B. (2012). Smart Irrigation Controllers: How Do Soil Moisture Sensor (SMS) Irrigation Controllers Work? 3. Retrieved from http://edis.ifas.ufl.edu/ae437

Dumic, D. (2017). Automatic Plant Watering System via Soil Moisture Sensing by means of Suitable Electronics and its Applications for Anthropological and Medical Purposes Nermin Đuzić and Dalibor Đumić Abstract Conclusion and Future. (July 2018), 0–4. https://doi.org/10.13140/RG.2.2.27022.87369

Girma, M. M., & Awulachew, S. B. (2007). Irrigation practices in Ethiopia: Characteristics of selected irrigation schemes. In IWMI Working Paper 124.

Guta, F., Damte, A., & Rede, T. F. (2015). The Residential Demand for Electricity in Ethiopia, Environment for Development (EfD): Discussion Paper Series. (April), 38.

Haile, G.G., Kasa, A. K. (2015). Irrigation in Ethiopia: A review. *Academia Journal of Agricultural Research*, 3 (10)(10), 264–269. https://doi.org/10.15413/ajar.2015.0141

Haile G.G, & Kasa. (2015). Review Paper Irrigation in Ethiopia : A review. *Academia Journal of Agricultural Research* 3(10): 264-269, 3(October), 264–269. https://doi.org/10.15413/ajar.2015.0141

Hayter, A. (n.d.). Instructor Solution Manual Probability and Statistics for Engineers and Scientists (3rd Edition) (International Student Edition). Statistics.

Kizito, F., Campbell, C. S., Campbell, G. S., Cobos, D. R., Teare, B. L., Carter, B., & Hopmans, J. W. (2008). Frequency, electrical conductivity and temperature analysis of a low-cost capacitance soil moisture sensor. *Journal of Hydrology*, 352(3–4), 367–378. https://doi.org/10.1016/j.jhydrol.2008.01.021

Kumar, A., & Magesh, S. (2017). Automated Irrigation System Based on Soil Moisture Using Arduino. *International Journal of Pure and Applied Mathematics*, 116(21), 319–323.

Kumbhar, S. R., & Ghatule, A. P. (2013). Microcontroller based Controlled Irrigation System for Plantation. II, 13–16.

Liu, Z., & Xu, Q. (2018). An automatic irrigation control system for soilless culture of lettuce. Water (Switzerland), 10(11), 1–9. https://doi.org/10.3390/w10111692

Long-term Agro-climatic and Hydro-sediment Observatory Report Long-term Agro-climatic and Hydro-sediment Observatory Report. (2017).

Lozoya, C., Mendoza, C., Aguilar, A., Román, A., & Castelló, R. (2016). Sensor-Based Model Driven Control Strategy for Precision Irrigation. *Journal of Sensors*, 2016, 1–12. https://doi.org/10.1155/2016/9784071

Mahzabin, A., Taziz, C. A., Amina, M. H., Gloria, M., & Zishan, M. S. R. (2016a). Design and Implementation of an Automatic Irrigation System. Iarjset, 3(10), 159–162. https://doi.org/10.17148/IARJSET.2016.31030

Mahzabin, A., Taziz, C. A., Amina, M. H., Gloria, M., & Zishan, M. S. R. (2016b). Design and Implementation of an Automatic Irrigation System. Iarjset, 3(10), 159–162. https://doi.org/10.17148/IARJSET.2016.31030

Mandloi, R., & Shah, P. (2015). Methods for closed loop system identification in industry. Available Online Www.Jocpr.Com *Journal of Chemical and Pharmaceutical Research*, 7(1), 892–896. Retrieved from www.jocpr.com

Masters, G. M. (2013). Renewable and efficient electric power systems. In Choice Reviews Online (Vol. 42). https://doi.org/10.5860/choice.42-3448

Matthew Milnes. (n.d.). The Mathematics of Pumping Water AECOM Design Build Civil, Mechanical Engineering. The Royal Academy of Engineering. Retrieved from http://www.raeng.org.uk/publications/other/17-pumping-water

MoFED. (2015). Growth and Tranformation Plan II (GTP II). I(Gtp Ii).

Ogata, K. (2002). Modern Contro Engineering a Fourth Edition Pearson Education International.

Osman, M., & Sauerborn, P. (2001). Soil and water conservation in ethiopia. In *Journal of Soils and Sediments* (Vol. 1). https://doi.org/10.1007/bf02987717

Salem, F. A., Mahfouz, A. A., & Aly, A. A. (2015). Systems Dynamics and Control , Proposed Course Overview and Education Oriented Approach for Mechatronics Engineering Curricula; Case Study. *American Journal of Educational Science*, 1(4), 135–151.

Shebani, M. M., & Iqbal, T. (2017). Dynamic Modeling, Control, and Analysis of a Solar Water Pumping System for Libya. *Journal of Renewable Energy*, 2017, 1–13.

https://doi.org/10.1155/2017/8504283

Shifa, T. K. (2018). Moisture Sensing Automatic Plant Watering System Using Arduino Uno Tasneem Khan Shifa American Journal of Engineering Research (AJER). *Americal Journal of Engineering Research* (AJER), 7(7), 326–330.

Soria, A., Garrido, R., & Concha, A. (2010). Low cost closed loop identification of a DC motor. Program and Abstract Book - 2010 7th *International Conference on Electrical Engineering, Computing Science and Automatic Control*, CCE 2010, (July 2014), 40–45. https://doi.org/10.1109/ICEEE.2010.5608594

Taddese, G., Sonder, K., & Peden, D. (2004). The water of the Awash River Basin: A Future Challenge to Ethiopia. 13.

Tajebe, L. (2017). Status , Challenges and Opportunities of Environmental Management in Ethiopia. 8(3), 107–114.

Tilahun, H., Teklu, E., Michael, M., Fitsum, H., & Awulachew, S. B. (2011). Comparative performance of irrigated and rainfed agriculture in Ethiopia. *World Applied Sciences Journal*, 14(2), 235–244.

U.S. Environmental Protection Agency. (2013). Moisture Control Guidance for Building Design , Construction and Maintenance. (December), 144.

Yavuz, D., Kara, M., & Suheri, S. (2012). Comparison of different irrigation methods in terms of water use and yield in potato farming. *Journal of Selcuk University Natural and Applied Science,* 1(2), 1–12.

Zaragoza, M. G., & Kim, H.-K. (2017). Comparative Study of PLC and Arduino in Automated Irrigation System. *International Journal of Control and Automation*, 10(6), 207–218. https://doi.org/10.14257/ijca.2017.10.6.20

APPENDICES

Appendix 1: Common z-transform pairs

2	$\delta[n-n_0]$	$\frac{1}{z^{n_0}}$	$\lvert z\rvert > 0$
3	$u[n]$	$\frac{z}{z-1}$	$\lvert z\rvert > 1$
4	$a^n u[n]$	$\frac{1}{1-az^{-1}}$	$\lvert z\rvert > \lvert a\rvert$
5	$na^n u[n]$	$\frac{az^{-1}}{(1-az^{-1})^2}$	$\lvert z\rvert > \lvert a\rvert$
6	$-a^n u[-n-1]$	$\frac{1}{1-az^{-1}}$	$\lvert z\rvert < \lvert a\rvert$
7	$-na^n u[-n-1]$	$\frac{az^{-1}}{(1-az^{-1})^2}$	$\lvert z\rvert < \lvert a\rvert$
8	$\cos(\omega_0 n)u[n]$	$\frac{1-z^{-1}\cos(\omega_0)}{1-2z^{-1}\cos(\omega_0)+z^{-2}}$	$\lvert z\rvert > 1$
9	$\sin(\omega_0 n)u[n]$	$\frac{z^{-1}\sin(\omega_0)}{1-2z^{-1}\cos(\omega_0)+z^{-2}}$	$\lvert z\rvert > 1$
10	$a^n\cos(\omega_0 n)u[n]$	$\frac{1-az^{-1}\cos(\omega_0)}{1-2az^{-1}\cos(\omega_0)+a^2z^{-2}}$	$\lvert z\rvert > \lvert a\rvert$
11	$a^n\sin(\omega_0 n)u[n]$	$\frac{az^{-1}\sin(\omega_0)}{1-2az^{-1}\cos(\omega_0)+a^2z^{-2}}$	$\lvert z\rvert > \lvert a\rvert$

Appendix 2: Common S-transform pairs

Table of Laplace Transforms

	$f(t)=\mathcal{L}^{-1}\{F(s)\}$	$F(s)=\mathcal{L}\{f(t)\}$		$f(t)=\mathcal{L}^{-1}\{F(s)\}$	$F(s)=\mathcal{L}\{f(t)\}$
1.	1	$\frac{1}{s}$	2.	e^{at}	$\frac{1}{s-a}$
3.	$t^n,\quad n=1,2,3,\ldots$	$\frac{n!}{s^{n+1}}$	4.	$t^p,\ p>-1$	$\frac{\Gamma(p+1)}{s^{p+1}}$
5.	$\sqrt{t}$	$\frac{\sqrt{\pi}}{2s^{\frac{3}{2}}}$	6.	$t^{n+\frac{1}{2}},\quad n=1,2,3,\ldots$	$\frac{1\cdot3\cdot5\cdots(2n-1)\sqrt{\pi}}{2^n s^{n+\frac{1}{2}}}$
7.	$\sin(at)$	$\frac{a}{s^2+a^2}$	8.	$\cos(at)$	$\frac{s}{s^2+a^2}$
9.	$t\sin(at)$	$\frac{2as}{(s^2+a^2)^2}$	10.	$t\cos(at)$	$\frac{s^2-a^2}{(s^2+a^2)^2}$
11.	$\sin(at)-at\cos(at)$	$\frac{2a^3}{(s^2+a^2)^2}$	12.	$\sin(at)+at\cos(at)$	$\frac{2as^2}{(s^2+a^2)^2}$
13.	$\cos(at)-at\sin(at)$	$\frac{s(s^2-a^2)}{(s^2+a^2)^2}$	14.	$\cos(at)+at\sin(at)$	$\frac{s(s^2+3a^2)}{(s^2+a^2)^2}$
15.	$\sin(at+b)$	$\frac{s\sin(b)+a\cos(b)}{s^2+a^2}$	16.	$\cos(at+b)$	$\frac{s\cos(b)-a\sin(b)}{s^2+a^2}$
17.	$\sinh(at)$	$\frac{a}{s^2-a^2}$	18.	$\cosh(at)$	$\frac{s}{s^2-a^2}$
19.	$e^{at}\sin(bt)$	$\frac{b}{(s-a)^2+b^2}$	20.	$e^{at}\cos(bt)$	$\frac{s-a}{(s-a)^2+b^2}$
21.	$e^{at}\sinh(bt)$	$\frac{b}{(s-a)^2-b^2}$	22.	$e^{at}\cosh(bt)$	$\frac{s-a}{(s-a)^2-b^2}$
23.	$t^n e^{at},\quad n=1,2,3,\ldots$	$\frac{n!}{(s-a)^{n+1}}$	24.	$f(ct)$	$\frac{1}{c}F\left(\frac{s}{c}\right)$
25.	$u_c(t)=u(t-c)$ Heaviside Function	$\frac{e^{-cs}}{s}$	26.	$\delta(t-c)$ Dirac Delta Function	e^{-cs}
27.	$u_c(t)f(t-c)$	$e^{-cs}F(s)$	28.	$u_c(t)g(t)$	$e^{-cs}\mathcal{L}\{g(t+c)\}$
29.	$e^{ct}f(t)$	$F(s-c)$	30.	$t^n f(t),\quad n=1,2,3,\ldots$	$(-1)^n F^{(n)}(s)$
31.	$\frac{1}{t}f(t)$	$\int_s^\infty F(u)\,du$	32.	$\int_0^t f(v)\,dv$	$\frac{F(s)}{s}$
33.	$\int_0^t f(t-\tau)g(\tau)\,d\tau$	$F(s)G(s)$	34.	$f(t+T)=f(t)$	$\frac{\int_0^T e^{-st}f(t)\,dt}{1-e^{-sT}}$
35.	$f'(t)$	$sF(s)-f(0)$	36.	$f''(t)$	$s^2F(s)-sf(0)-f'(0)$
37.	$f^{(n)}(t)$	$s^nF(s)-s^{n-1}f(0)-s^{n-2}f'(0)\cdots-sf^{(n-2)}(0)-f^{(n-1)}(0)$			

Appendix 3: LCD Pins Interconnection and Functions

Liquid Crystal Display		**Connected to**				**Extra Description**
Pin no.	Pin name	Arduino	Pin	ground	Power	
1.	VSS	Pin no.	Pin symbol	ground		
2.	VDD/VCC				+5V	
3.	VEE			ground		Provides better maximum contrasting
4.	Register Selection (RS)	12	PB4/MISO			Command register (rs=0) & data register(rs=1)
5.	Read/Write (RW)			ground		Write-Read mode R/W=1 read while R/W=0,Write
6.	Enable(E)	11	PB3/MOSI/OC2A			Enabling the LCD module
7.	D0					
8.	D1					
9.	D2					
10.	D3					
11.	D4	5	PD5/T1			
12.	D5	4	PD4/T0/XCK			
13.	D6	3	PD3/INT1			
14.	D7	2	PD2/INT0			